

**ALKYLATION OF BENZENE WITH HIGHER OLEFINS
OVER ZEOLITES: A GREEN ROUTE FOR LAB
SYNTHESIS**

Bejoy Thomas

DEPARTMENT OF APPLIED CHEMISTRY
COCHIN UNIVERSITY OF SCIENCE AND TECHNOLOGY
KOCHI-682 022

Ph. D Thesis submitted to Cochin University of Science and
Technology in partial fulfilment of the requirements for the degree of
Doctor of Philosophy in Chemistry in the Faculty of Science

SEPTEMBER – 2004

Alkylation of Benzene with higher olefins over zeolites: A green route for lab synthesis.

Ph. D thesis in the field of surface science and catalysis.

Author:

Bejoy Thomas

Research Fellow, Department of Applied Chemistry,
Cochin University of Science and Technology,
Kochi-682 022, Kerala INDIA.

E-mail: bjoy@cusat.ac.in bjoy_999@yahoo.co.in

Research Guide:

Professor Dr. S. Sugunan

Department of Applied Chemistry
Cochin University of Science and Technology
Kochi-682 022 Kerala, INDIA.

E-mail: ssg@cusat.ac.in

Department of Applied Chemistry
Cochin University of Science and Technology
Kochi-682 022.

URL: www.cusat.ac.in/dac

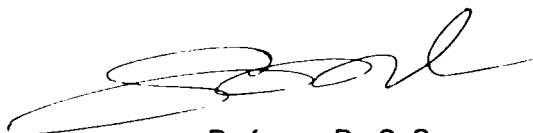
September 2004

Front cover: "*Structure of HFAU-Y Zeolite*" Painting in the digital art medium.

...To My Parents, Brother and Sisters

CERTIFICATE

Certified that the present work entitled “**ALKYLATION OF BENZENE WITH HIGHER OLEFINS OVER ZEOLITES: A GREEN ROUTE FOR LAB SYNTHESIS**” submitted by Mr. Bejoy Thomas is an authentic record of research work carried out by him under my supervision at the Department of Applied Chemistry in partial fulfilment of the requirements for the degree of Doctor of Philosophy in Chemistry of the Cochin University of Science & Technology and has not been included in any other thesis previously for the award of any degree.



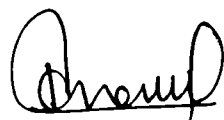
Professor Dr. S. Sugunan
(Supervising Guide)

Kochi-22
22-09-2004

Department of Applied Chemistry
Cochin University of Science and Technology
Kochi-682 022.

DECLARATION

I hereby declare that the present work entitled “**ALKYLATION OF BENZENE WITH HIGHER OLEFINS OVER ZEOLITES: A GREEN ROUTE FOR LAB SYNTHESIS**” which will be submitted is based on the original work done by me under the guidance of Dr. S. Sugunan, Professor in Physical Chemistry, Department of Applied Chemistry, Cochin University of Science & Technology and has not been included in any other thesis submitted previously for the award of any other degree.



BEJOY THOMAS

Kochi-682 022

22-09-2004

Preface

Surface science and catalysis is often presented as a perfect blend between many branches of chemistry including inorganic chemistry, colloidal chemistry, cluster chemistry, physical chemistry, materials chemistry, and organic chemistry. Knowledge of surface science and catalysis continues to move ahead of many fronts. The enormous developments in the field during the last couple of decades have been mandated by the considerations related to the abatement and prevention of pollution, conservation of raw materials, production of new and more competent drugs, and *Green synthesis* of many industrially imperative speciality chemicals.

Responsible care and sustainable development have become the paradigms of industrial production. It is therefore required that all processes are optimized with respect to energy efficiency, chemical utilization, and waste minimization. The need for more environmentally friendly production technology in the chemical industry is universally acknowledged and much progress has already been made. In the past, the need to reduce costs has provided the driver for improvements in process efficiency, since wasteful processes are also uneconomic. However, recent public concern about the environment, leading to regulatory activity by governments, has accelerated this tendency to the so-called *cleaner-technology*. Legislation enacted to control the discharge of waste products into the environment, and restrict the manufacture, transport, storage and use of certain hazardous chemicals, has acted as a spur to the introduction of so called *cleaner technology*.

Industrial processes employing acids and bases requiring neutralization, or stoichiometric redox reagents, represent the major sources of waste production in the form of salts and heavy metals and have high *E-factors* and low *atom utilization*. Reactions of this type, employed in the fine-chemicals industry particularly, include *Friedel–Crafts alkylation* mediated by Lewis acids such as aluminium chloride, reductions with metal hydrides or dissolving metals such as

zinc or iron, and stoichiometric oxidations with dichromate or permanganate, all of which generate prohibitive amounts of metal-containing wastes. The work-up of products from nitrations, sulphonations and many other acid-catalyzed reactions involves neutralization and the concomitant generation of salts such as NaCl, Na₂SO₄ and (NH₄)₂SO₄. The increasing demands of environmental legislation have been prompting the chemical industries to minimise, or preferably eliminate, waste production in chemical manufacture. The global demand of solid acid and solid base catalyst has increased considerably in recent years since such systems often give value added products with much improved yield without creating major burden on the environment. The DETAL™ process for the synthesis of LABs is one example of how a more environmentally friendly process can replace the existing conventional technology.

The objective of the present work is to improve the textural and structural properties of zeolite-Y through ion exchange with rare earth metals. We meant to obtain a comparative evaluation of the physicochemical properties and catalytic activity of rare earth modified H-Y, Na-Y, K-Y, and Mg-Y zeolites. Friedel-Crafts alkylations of benzene with higher 1-olefins such as 1-octene, 1-decene, and 1-dodecene for the synthesis of linear alkylbenzene (LAB) have been selected for the present study. An attempt has also been directed towards the correlation of the enhancement in 2-phenylalkane formation to the improvement in the textural and structural properties upon rare earth modification for the zeolite-Y. The present method for LAB synthesis stands as an effective *Green* alternative for the existing hydrofluoric acid technology.

ACKNOWLEDGEMENTS

"A hundred times a day I remind myself that my inner and outer life are based on the labours of others"

Albert Einstein

My fascination with Materials Chemistry and Catalysis started during the last three years of stay in the laboratory of Professor Dr. S. Sugunan. It gives me great pleasure to record my sincere gratitude to him for his constant support, encouragement and inspiring guidance throughout the period of work.

I am greatly indebted to Professor Prathapachandra Kurup, Head, Department of Applied Chemistry, CUSAT for the opportunity to carry out my doctoral work in this department. His always calm and friendly nature was much a relaxation during hectic and complicated working days.

My understanding of the subject became sharpened through many informal discussions with Dr. S. Prathapan, at CUSAT. He taught me Organic Chemistry from preliminary notes, which gave me a great deal of encouragement. The valuable suggestions offered in proposing the mechanisms of many reactions are remembered with lot of gratitude. I record my gratefulness to Professor K. K. Muhammad Yussuf, former Head, Department of Applied Chemistry, for timely help and constant support extended. His active interest in the work did much to restore my sagging enthusiasm. Dr. Sree Kumar, Dr. Giresh Kumar, Dr. Unnikrishnan and many other faculties at CUSAT supported me during the entire period of research. I extend my sincere thanks to all non-teaching staff, especially Manoj Kumar of Department of Applied Chemistry for their timely help and assistance.

My major source of inspiration to learn basic NMR spectroscopy and solid state chemistry was Professor N. M. Nanje Gowda and Dr. Vishnu Kamath, Department of Chemistry, Bangalore University. They supported me during my post graduation and entire period of doctoral work by providing helpful advice and critical comments. I remember with gratitude the help extended by Professor Mahendra, Professor K.R. Nagasundara, Professor Farooq Ahamad, Dr. V. Gayathri, Dr. Leelamani, Department of Chemistry, Bangalore University. I am happy to acknowledge the assistance of Patric Chacko who was kind enough to read the entire thesis with patience and send me his exceeding comments. The essential part of the thesis is provided by Sophisticated

Instruments Facility, IISc, Bangalore. I thank Dr. N Suriaprakash for fruitful discussions and providing NMR results. I thank Dr. Asokan, Reader, School of Chemical Sciences, M. G. University, Kottayam for providing GC-MS results.

I am greatly indebted to my dear lab-mates for their timely help and helpful suggestions. The lively and highly vibrant atmosphere created by them was much a relaxation during the stressful hours of lab work. I learn by heart the company of Dr. Ramankutty, Dr. Rehna, Dr. Sreejarani, Dr. Nisha, Dr. Suja, and Dr. Deepa. I extend my whole hearted thanks to Sanjay, Sunaja, Smitha, Maya, Radhika, Shali, Binitha, Ramanathan, Kochurani, Ajitha, Shalini. My heart-felt thanks to Manju and Fincy for their sincere, loving, and creative assistance, helpful suggestions during the whole period of project work and stay at CUSAT. I acknowledge the help offered other colleagues of the department. I remember with lot of gratitude the company and help offered by my dear friends Dr. Jacob Samuel, Dr. Rohith John, Sunilkumar, and Sreekanth. Their company was a great relief in the midst of hectic daily business. I remember with love my friends Joby, Shijo, Jigo, Ravindra, Anil, Vasanthakumar, Uday, Deepak, Fr. Sibi John, Rajech, Bino, Wilson, Anwar, Jijo, Aneesh, Rakesh, Alex, Vinukrishnan, and Biju for their love, constant support and care. I acknowledge the love and support offered by Vinod and Benny during last three years.

The technical support offered by Mr. Gopi Menon, Mr. Joshi, and Mr. Kasmeri, Department of USIC, is acknowledged with gratitude. At this point, I extend my gratefulness to Mr. Suresh, service engineer, Chemito for his help during technical problems to Gas Chromatograph.

Words fail to express my appreciation to my dear Ammachi, Chachan, brother, and sisters for their love, immense patience and excellent backing throughout my life. My brother and little sister were my source of strength and gave me great deal of encouragement. I apologise to my elder sister for her hard work during my M. Sc. period and project. The financial supports from UGC and CSIR, Govt. of India is gratefully acknowledged. Above all, I submit myself before the supreme power of GOD ALMIGHTY for guiding me through the critical stages of my life, Thank GOD.

BEJOY THOMAS

Contents

1. Introduction and literature survey

Abstract	
1.1 General introduction	2
1.2 Structure and classification	5
1.3 The Faujasite-Y Zeolite	9
1.4 The rare earth exchanged Y zeolites	11
1.5 Nature of active sites in zeolites	13
1.6 Applications of zeolites	16
1.7 Linear Alkyl Benzenes (LABs)	17
1.8 Main objectives of the present work	25
References	27

2. Materials and Methods

Abstract	
2.1 Preparation of the catalyst	33
2.2 Preparation of MFAU-Y (M= Na, K, Mg)	34
2.3 Preparation of rare earth FAU-Y (RE= Ce ³⁺ , La ³⁺ , RE ³⁺ , Sm ³⁺)	34
2.4 Zeolite characterization	35
2.5 Characterization of acid sites on zeolites	48
2.6 Alkylation of benzene with higher olefins (C ₈ , C ₁₀ , and C ₁₂ olefins)	52
References	54

3. Zeolite Characterization

Abstract	
3.1 Chemical composition (EDX)	57
3.2 Surface morphology (SEM)	58
3.3 Powder X-ray diffraction (PXRD)	60
3.4 Vibrational spectral studies (IR)	63
3.5 UV-vis- diffuse reflectance spectroscopy (UV-vis DRS)	67
3.6 MAS Nuclear magnetic resonance studies (MAS NMR)	69
3.7 Surface area and pore volume measurements	85
3.8 Characterization of acid sites in zeolites	87
3.9 Conclusions	98
References	100

4. Friedel-Crafts Alkylation 1

Abstract	
4.1 Alkylation of Aromatics	107
4.2 Alkylation of Benzene with 1-Octene	111
4.3 Optimization of reaction conditions	113
4.4 Activity of different systems	128
4.5 Deactivation studies	128
4.6 Nature of carbonaceous compounds blocked inside the zeolite pores	133
4.7 Conclusions	136

References	139
5. Friedel-Crafts Alkylation 2	
Abstract	
5.1 General introduction	144
5.2 Alkylation with C ₁₀ and C ₁₂ olefins	148
5.3 Effect of Reaction Variables	149
5.4 Performance of different zeolite systems	154
5.5 Deactivation studies	162
5.6 Conclusions	172
References	175
6. Summary and Conclusions	
Abstract	
6.1 Summary of the work	180
6.2 Future perspectives and conclusions	182

Chapter 1

Introduction and Literature Survey

"Fortunately, science, like nature to which it belongs, is neither limited by time nor by space. It belongs to the world, and is of no country and no age. The more we know, the more we feel our ignorance, the more we feel how much remains unknown, and in philosophy, the sentiment of the Macedonian hero can never apply –there are always new fields to conquer."

Sir Humphry Davy

Traditionally heterogeneous catalysts have been based primarily on inorganic based metal oxide materials, and attempt to construct molecularly well defined metal complex centers are few in numbers. The drive to develop increasingly active and selective heterogeneous catalysts continues with considerable vigour. The use of catalysts in the chemical and process industries is currently widespread. The nature of catalytic process whereby a given reaction may be accomplished at a lower temperature than that required for the homogeneous reaction is likely to lead to the application of catalytic methods to even more processes as the fuel costs continue to rise. However, in the case of large and medium scale production processes the stimulation remains the need to increase profitability and to improve process environmental acceptability. Zeolites and zeo-types constitute a novel class of microporous solid acid materials with good thermal stability, high surface area, and pronounced Brønsted and Lewis acid amount, which are highly tunable. There are many methods to improve the textural and structural properties these materials. Exchange of counter cations with rare earth metal ions is one of such methods. A brief introduction on zeolites and rare earth exchanged zeolites as well as Friedel-Crafts alkylations in the production of linear alkylbenzenes are presented.

1.1 General introduction

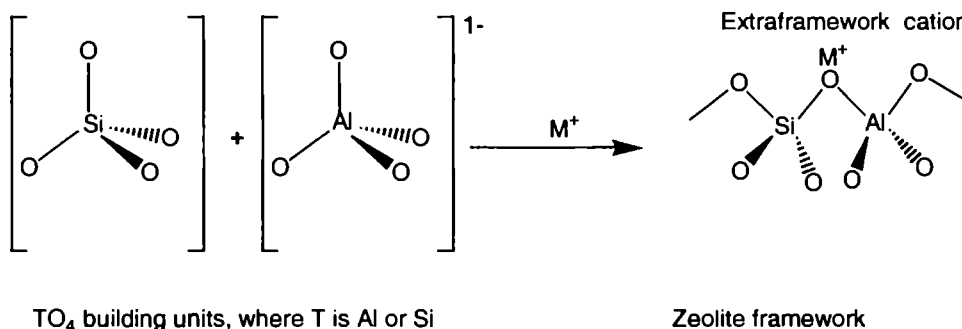
Rarely in our technical society does the discovery of a new material result in such a wide interest and kaleidoscopic developmental application as happened with zeolites and molecular sieves. The properties and uses of zeolites are being explored in many scientific disciplines; contemporary inorganic and organic chemistry, physical chemistry, colloidal chemistry, biochemistry, mineralogy, geology, surface chemistry, oceanography, crystallography, catalysis and all types of chemical engineering process technology¹.

Zeolite was originally discovered by Swedish mineralogist, A. F. Cronstedt way back in 1756. The name is derived from its ability to hold a lot of water within and release it upon heating. The water comes out well beyond 100 degrees, so that as the stone is heated, it seems to expand and boil. Hence the name derived from the Greek words 'zein' to boil and 'lithos' for stone- boiling stone. The wide range of applicability of zeolite becomes understood once its structural architecture becomes known.

Zeolites are tecto-aluminosilicates which can be described by the general formula $M^{n+}_{x/n} [(AlO_2)_x (SiO_2)_y]^x \cdot zH_2O$, where M can be a metal cation or a proton.¹⁻² The Si/Al ratio in synthetic zeolites varies considerably; limiting extreme being 1:1 (Lower ratio for zeolite-X) to near infinity; (in silicalites). This provides a means to modulate the ionicity of the material, which increases with decreasing Si/Al ratio.

The framework of every zeolite is constructed from tetrahedral building blocks, TO_4 , where T is the building tetrahedrally coordinated atom (i.e. Si and Al) as seen in Figure 1.1.

Figure 1.1. The framework of a zeolite constructed from tetrahedral building blocks, TO_4 , where T is a tetrahedrally coordinated atom; Si or Al.



Zeolites represent a large class of minerals found in the earth, and can also be made synthetically, e.g. ZSM-5, which was synthesized at the Mobil Oil Company.³⁻⁴ They are made up of $[AlO_4]^{5-}$ and $[SiO_4]^{4-}$ tetrahedra which are corner linked by oxygen bridges to form cages, which in turn form a super cage when linked together. These have pores and channels, and typical pore sizes are between 4 to 10 angstroms. Substitution of Si (IV) by Al (III) leaves a net negative charge, which is compensated by the exchangeable cations, such as Na^+ , Li^+ , K^+ i.e. every $[AlO_4]^{5-}$ tetrahedra needs a cation to balance the charge. The cations are held in the framework electrostatically.^{1-2, 5}

An isolated SiO_4 group carry a formal charge of -4 , but in a solid having O/T ratio of 2 (as found in zeolites) the SiO_4 unit is neutral, because each oxygen atom is part of a bridge between two 'T' atoms.²⁻³ However, the net formal charge of AlO_4 units is -1 , so that the zeolite framework is negatively charged and is balanced by M^{n+} cation or by protons in the acidic zeolites. However, these ions are not part of the zeolitic framework. Under right conditions these ions can be exchanged by other cations and such an exchange has very little influence on the crystal structure, which depends on the way in which the TO_4

units arrange themselves. But, it does affect other relevant properties of zeolites such as acid structural properties and internal electric fields. Brønsted acidity arises from bridging Si(OH) Al groups in the protonic form of zeolites. Extra framework (charge balancing) cations act as Lewis acid centres in a broad sense, since they are electron acceptors. A different (and of course more important) source of Lewis acidity comes from the concerned structural defects and extra framework aggregates.^{1-2, 5} Charge-balancing cations are also the main source of intra-zeolite electric fields, which have strength of several V nm^{-1} , the actual value depends on cation charge and radius.

A characteristic feature of zeolites is their structural porosity. The framework of all zeolites defines regular system of intracrystalline voids and channels of discrete size, usually in the nanometer range, accessible through apertures of well-defined molecular dimensions. This is a striking feature that differentiates zeolites from other microporous materials, like amorphous carbon or silica gel (which have irregular pore system) and which places them in the same class as other molecular sieves ^{1-2, 5}. Their microporous framework structure, wide range of chemical composition, surface acidity, and the possibility of tuning internal electric fields by appropriate choice of extra-framework cations are key factors which render zeolites (and of course zeotypes) versatile materials for an increasing number of technological applications. Paramount among these is the use of zeolites as catalysts for petroleum industry, pollution control and in the synthesis of a large number of speciality chemicals.⁶⁻⁸

Zeolites and zeo-types cavities can be considered as nano-reactors where adsorbed molecules are guided to react following specific paths dictated by: (I) the electrostatic forces acting inside the cavities, (ii) the distribution of sites on the internal surface, (iii) the spatial restrictions imposed by the dimension and shape of the void space, and (iv) limitation on the diffusion

paths imposed by the regular organization of (intersecting) channels. All these points can be summed up under the synthesizing concept of host-guest interactions, so fruitfully used to understand many properties of supramolecular and enzyme-substrate systems. More specifically, electrostatic fields operating inside the cavities and channels can lead to the formation of internal adducts characterized by a profound deformation of electron distribution of perturbed molecules with simultaneous polarization, and appearance of new nucleophilic and electrophilic regions and ultimately of new chemical properties. In the case of proton-exchanged zeolites the internal adducts can be more properly classified as hydrogen-bonded complexes, which under suitable conditions can evolve towards protonated species and initiate the chain of Brønsted acid – catalyzed reactions that (together with shape selectivity) make acidic zeolites so important in petrochemistry.⁹⁻¹⁰

1.2 Structure and classification

The zeolite comprise the largest group of aluminosilicates with framework structures since there are over 35 known, different framework topologies and an infinite number possible arrangements.¹⁻² Early interpretations of the physical properties of zeolites were based upon fragmentary structural information. As a result of investigation during the last ten years, there is extensive information on the crystal structure of over 35 zeolites. Nearly 100 synthetic zeolites have also been reported. In general, zeolites are classified into groups according to common features of aluminosilicate framework structures. The properties which are structure-related include;

1. High degree of dehydration and the behavior of “zeolitic” water.
2. Low density and large void volume when dehydrated.

3. Stability of the crystal structure of many zeolites when dehydrated and when as much as 50 vol% of the dehydrated crystal is void.
4. *Cation exchange properties.*
5. Uniform molecular –sized channels in the dehydrated crystals.
6. Various physical properties such as electrical conductivity.
7. Adsorption of gases and vapors
8. *Catalytic properties.*

In order to understand and relate these properties, new concepts are needed concerning the spatial arrangement of the basic structural components, i.e. the tetrahedra, cations (both residual and counter), and water molecules. Structural classifications of zeolites have been proposed by Smith, Fischer and Meier and Beck.¹¹⁻¹⁴ Earlier classifications were based on morphological properties.

Most zeolite structures obey *Loewenstein rule* that govern the linking together of silica tetrahedra and tetrahedra and octahedra of alumina.¹⁵ The distribution of tetrahedra in a crystal is not entirely random in amorphous and crystalline aluminosilicates.

1. Whenever two tetrahedra are linked by one oxygen bridge, the center of only one of them can be occupied by aluminium; the other center must be occupied by silicon or another small ion of electrovalence 4 or more such as phosphorous.
2. Whenever two aluminium ions are neighbors to the same oxygen anion, at least one of them must have a coordination number larger than 4 that is, 5 or 6 towards oxygen.

These rules explain the maximum substitution of 50% of the silicon in three-dimensional framework networks of tetrahedra by aluminium. For 50 percent substitution, rigorous alternation between silicon and aluminium

tetrahedra becomes necessary. To date no deviation from these rules has been observed in zeolite system, the aluminophosphates, or metasilicates studied.¹⁻²

The most important classification is based on the framework topology of the zeolites. The classification consists of seven groups; within each groups, zeolites have a common subunit of structure which is a specific array of (Al, Si) O_4 tetrahedra. In this classification the cation distribution is neglected. For example, the two simplest units are the ring of four tetrahedra (4 ring) and six tetrahedra (six ring) as found in many other framework aluminosilicates. These subunits have been called as *secondary building units* (SBU) by Meier.¹³ It is to be noted that the primary building units are of course the SiO_4 and AlO_4 tetrahedra. In some cases, the zeolite framework can be considered in terms of polyhedral units, such as the truncated octahedron. Some of the SBU are probably involved in crystal growth processes. The polyhedra are cage-like units designated by Greek letters; α , β , γ , δ etc. The α -cage refers to the largest unit- the truncated cuboctahedron.

The classification which follows is based on seven groups. Although, in other classifications, each group has been named after representative member, an arbitrary designation by number is preferable since no single member is more representative than any other. The seven groups are as follows:

Table 1.1. Plausible classification, corresponding secondary building units, and examples of zeolites.

Group	Secondary building unit (SBU)	Example
1	Single 4- ring, S4R	Analcime, Zeolite P ¹⁶
2	Single 6- ring, S6R	Erionite, Offretite ¹⁷
3	Double 4- ring, D4R	Zeolite A, Zeolite ZK-4 ¹⁸⁻¹⁹
4	Double 6- ring, D6R	Faujasite- X and Y, Zeolite- L ²⁰⁻²⁴
5	Complex 4-1, T ₅ O ₁₀ unit	Natrolite, Mesolite ^{16, 26}
6	Complex 5-1, T ₈ O ₁₆ unit	Mordenite, Ferrierite ²⁷⁻³⁰
7	Complex 4-4-1, T ₁₀ O ₂₀ unit	Heulandite, Stilbite ^{13, 31-32}

The simplest level of zeolite classification is pore size. For most zeolite applications, this simplest level for classification of zeolites should be adequate. All zeolites that are significant for catalytic and adsorbent applications can be classified by number of T atoms, where T is Al or Si, which defines the pore opening. There are, however only three pore openings known to date in the aluminosilicate zeolite system that are practical interest for catalytic applications, and are referred to as 8, 10, and 12 ring openings. Zeolite containing these pore openings may also be referred to as small (8-membered ring), medium (10-membered ring), and large (12-membered ring) pore zeolites.^{1-2, 4-5, 18-19, 22, 28-29} In this simplified classification system, no identification is given as to the exact dimension of the pore opening or whether the zeolite contains a one-, two-, or three- dimensional pore system

Now, we shall consider some examples for each of the above classes. Zeolite-A is the most well-known small pore material, while ZSM-5^{3, 33}, ZSM-11³⁴⁻³⁵ etc of MFI family makes the medium pore zeolite class. Zeolite FAU-Y and FAU-X (FAU family),²⁸⁻²⁹ Beta (BEA family),³⁶⁻³⁷ Mordenite (MOR family)

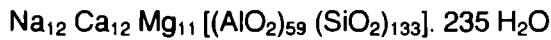
etc fill the large pore zeolite class.²⁸⁻³⁰ The corresponding pore openings are about 0.4, 0.55 and 0.74 nm respectively. However, other materials having extra large pore opening have been synthesized; among them are Gallo silicates molecular sieve³⁸, AIPO-15³⁹, VPI-5⁴⁰ with pore opening up to 1.2 to 1.4 nm in diameter. These materials are zeo-types and are structurally very much like zeolites. In these materials Si or Al atom have been replaced with other atoms like Ga for Al or P for Si.

Perhaps, molecular sieve action has been reported in other solids, crystalline and non-crystalline. These include coal, special active carbon, porous glass, microporous beryllium oxide powders, and layer silicates modified by exchange with organic cations.¹⁻² The controlled thermal decomposition of beryllium hydroxide *in vacuo* produces BeO consisting of porous aggregates of 30 Å crystallites. However, the micropore size depends strongly on whether the hydroxide is decomposed *in vacuo* or in presence of steam.^{1-2, 41} Many studies show that coals found to have pore diameter approaching molecular sieves.¹

1.3 The Faujasite-Y Zeolite

Although there are 34 species of zeolite minerals and about 100 types of synthetic zeolites, only a few have practical significance at present. Many of the zeolites after dehydration are permeated to very small channels systems which are not interpenetrating and which may contain serious diffusion blocks. In some other cases dehydration irreversibly disturbs the framework structure and the position of the metal cations, so that the structure partially collapses and dehydration is not completely reversible. To be used as a molecular sieve, the structure of the zeolites after dehydration must remain intact. Zeolite-Y is one of the most widely used zeolite in industrial applications.⁴²⁻⁴³

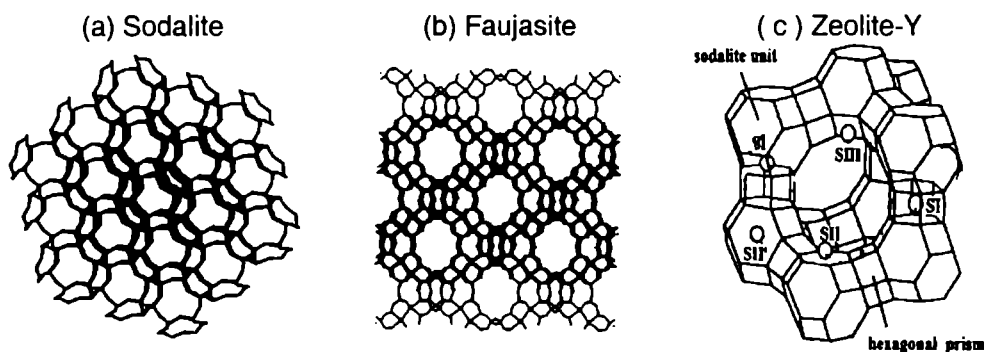
FAU-Y and X are examples of group 4 zeolites, which are characterized by the double 6-ring, D6R, as the secondary building unit in their structural frameworks. They belong to the faujasite family. The space group is F3dm and unit cell volume is 15.014 Å³. The unit cell is cubic with a large cell dimension of nearly 25 Å and contain 192 (Si, Al)O₄ tetrahedra.^{22-23,44-45} The remarkably stable and rigid framework contains the largest void space of any known zeolite and amounts to about 50 vol% of the dehydrated crystal. The typical chemical composition (unit cell content) is;



The structure of zeolite Y contains truncated octahedral or β-cages (sodalite unit), linked tetrahedrally through D6R's (double ring) in arrangement like the carbon atoms in diamond. It contains eight cavities ~ 13 Å in diameter in each unit cell. FAU-Y has a 3-D interconnecting pore systems with super cages of 1.18 nm connected by circular 12-ring 0.74 nm windows.²² Figure 1.2 shows the open structure of sodalite, and faujasite, which is made up of sodalite (or β cages) units linked together by double six rings (D6R).¹⁻² This type of structure creates cages (designated as super cages and small cages) and cavities inside zeolite structure. Thus cations (both residual as well as counter cations) can be located in different cation locations. The cation positions in Y zeolite are SI (site I) in hexagonal prism, SII and SIII in super cages (see structure c in Figure-1.2), and I' and SII' in small cages. Thus the determination of cation location is of prime importance in zeolite characterization.⁴⁶⁻⁴⁸

The cation distribution is highly dependent on the extent of hydration of the zeolite. The cations move upon dehydration from position where they are coordinated with water molecules near framework oxygen. Thus, the cation distribution will be totally different for a hydrated and a dehydrated zeolite. For example the Na⁺ ions in dehydrated zeolite Na-Y occupy three sites.

Figure 1.2 The structure of Sodalite (a), Faujasite unit (b), and Zeolite-Y with different cation locations (c).



On an average, 7.5 ions were found in SI, 30 ions in SII, and 20 ions in SI'. Similar site occupancies in K exchanged and Ag exchanged zeolite-Y were found. X-ray diffraction studies on dehydrated Ca-Y and La-Y zeolites have shown that the Ca^{2+} ions occupy SI in preference to SII and La^{3+} ions in SI at ambient temperatures move to SII at 973 K.⁴⁹⁻⁵⁰

1.4 The rare earth exchanged Y zeolites

The zeolites in the as-synthesized form usually contain quaternary amine cations along with residual inorganic cations such as alkali cations, most typically sodium. The reactivity and the selectivity of molecular sieve zeolites as catalysts are determined by active sites provided by an imbalance in charge between silicon and aluminium ions in the framework. To produce the zeolite acid catalysts, it is necessary to replace the cations present in the freshly synthesized material with other cations. Zeolites can be modified suitably by any of the following methods.

- (1) *Isomorphous substitution* of lattice aluminium and or silicon by other elements can performed at the time of hydrothermal synthesis or by post synthesis methods. The substitution of other ions for Al or Si in the

framework change the zeolite properties, perhaps they still have the same topology and channels system.⁵¹

- 1) Most of the zeolites are synthesized in a cationic form in which the positively charged cations balance the negatively charged framework system. These extra-framework cations can be replaced by other cations. Usually metal ion exchange is for improving the acid structural properties as well as their thermal stabilities. The possibility of metal substitution into the framework has been reviewed in many articles.⁵² The unique structure and the ability of zeolites to be ion-exchanged with metal ions promise the development of inorganic mimics of various enzymes. Herron prepared a mimic of cytochrome-P.450 by exchanging Pd^{II} and Fe^{II} ions into different zeolite structures.⁵³
- 2) For many industrial reactions, for example, those involving hydrogenation or oxidation, it is necessary to have additional components in the catalysts to perform the total or partial catalytic function. Such components are frequently metals, their oxides, or sulphides similar to those used in non-zeolite or amorphous catalyst systems. Metals usually introduced include Ni, Pt, Pd etc.^{2, 42}

The modifications of zeolites by ion exchange of exchangeable cations provide a useful means of tailoring their properties to particular applications. Thus the introduction of rare earth elements, in particular into Y zeolite, has been an important means of enhancing the performance of, for example, FCC catalysts, and they are also known to increase the activity of the zeolite in a variety of reactions due to the increased acid amount.⁵⁴ Lanthanum exchanged zeolite Na-Y plays an important role in the preparation of catalysts for fluid catalytic cracking, one of the most widely applied petroleum refinery processes that make use of zeolites as catalyst components.^{1-2, 9, 54} A number of investigations were published in the last decade using solid-state MAS NMR

spectroscopy to study the cation location and migration in hydrated and dehydrated rare earth zeolites.

In addition to the important modification of the catalytic properties of the zeolite, the detailed changes in the state and location of rare earth cations during thermal treatment have also been attracted considerable interest. As has been documented by a variety of studies, the initially hydrated rare earth cation (mainly $\text{La}(\text{H}_2\text{O})^{3+}$ in the hydrated zeolite before thermal treatment is located within the large super cages of zeolite Y at the SI and SII cation sites.¹ Subsequent thermal treatment at temperatures as low as 353 K initiates a process of dehydration/dehydroxylation of cations, which allows it to migrate through the six-ring opening of the sodalite cage and the residue in the SI and SI' sites.^{1-2, 55} Early structural studies and recent modeling calculations point to SI' site as favourable site for the dehydrated rare earth cation, despite the greater opportunity for six-fold coordination within the double ring.¹

1.5 Nature of active sites in zeolites

The activity of zeolites in acid catalyzed reactions originates from the tetrahedral framework aluminium atoms. There are two types of acid catalytic activity associated with zeolites namely; Brønsted acidity (H^+) and Lewis acidity.^{1-2, 5} These acid centres are created by imbalance in the charge between silicon and aluminium ions in the framework of zeolites. Each aluminium atom of the framework induces potentially active acid site. Silicates never have acidity. Brønsted acid sites (BAS) in zeolites arises when cations (often Na, K or Cs) are replaced by proton, rare earth metal ions (H^+ , from ammonium ion exchange followed by the thermal decomposition of the ammonium form to H^+ form of the zeolites). The strength of these acid sites is found to vary with (i) zeolite structure (ii) Si/Al ratio and (iii) isomorphously substituted metal ions in the zeolite framework. Brønsted acidity is normally

associated with trivalent metal ions such as rare earth metal ions. Lewis acid sites (LAS) arise at the defect sites where trigonal Al is present either in the framework or at charge compensating ions.²⁻³ The Lewis acid amount can also be formed by high temperature (> 773 K) dehydroxylation of Si(OH)Al (i.e. Brønsted) sites. Several methods have been developed to determine the number and strength of both types of acid sites ranging from Temperature Programmed Desorption of ammonia (NH₃-TPD), thermodesorption of amines, IR spectroscopy, and catalytic probe reactions.

All the pre-treatment conditions as well as synthesis and post synthesis treatments (hydrothermal, thermal, and chemical) affect the ultimate acid amount and activity observed in the zeolite molecular sieves.⁵¹⁻⁵⁵ Both BAS and LAS are claimed in these materials; with assertions by various investigators that: (1) BAS are the active centers. (2) LAS are active centers. (3) BAS and LAS together act as the active site. (4) Cations or other types of sites in small concentrations act in conjunction with the B/L-AS to function as the active centers.² Figure 1.3 depicts a zeolite surface, showing possible types of structures expected to be present at various stages of treatment of a silica rich zeolite.

Figure 1.4 depicts the probable influence of rare earth cations on the framework of zeolite-Y. IR spectra and X-ray diffraction studies revealed the existence of [RE-OH²⁺] species and [H⁺---O⁻---Zeolite] species after thermal treatment. The acidic hydroxyl groups are perturbed by the polarization effects of RE cations in such a way as to enhance the acid strength of the catalyst.⁵⁶⁻⁵⁷ The IR spectra of pyridine selectively adsorbed in the acid sites of the zeolite revealed the presence of BAS (1549 cm⁻¹) and LAS (1443 cm⁻¹).⁵⁷

Figure 1.3. Diagram of the “surface” of a zeolite framework. (a) In the as-synthesized form, M^+ is either an organic cation or an alkali metal cation. (b) Ammonium ion exchange produces the NH_4^+ exchanged form. (c) Thermal treatment is used to remove ammonia, producing the H^+ acid form. (d) The acid form in (c) is in equilibrium with the form in (d), where there is a silanol group adjacent to a tri-coordinate aluminium.

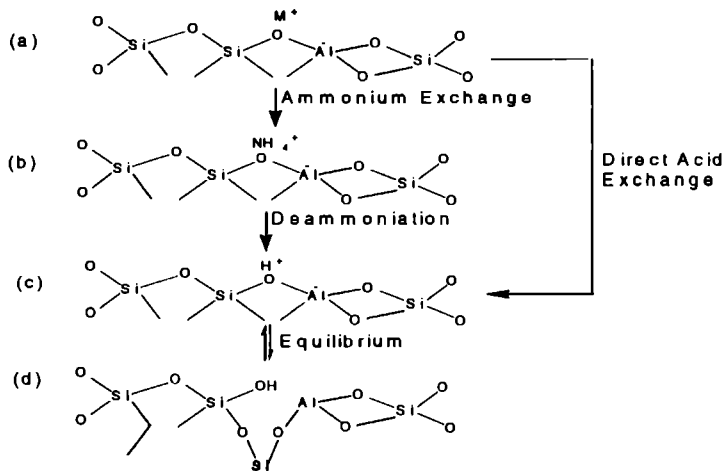
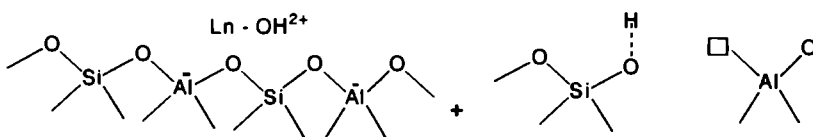


Figure 1.4. A presentation of the possible acid centers in rare earth exchanged- Y zeolites.



There are several methods to study acid structural properties RE-Y zeolites (of course of others too) such as n-butylamine desorption and thermal decomposition using thermoanalytical methods.² From TG too the total acid amount could be calculated. The values corresponding to the acid properties invariably show enhanced acid structural properties.

6 Applications of zeolites

Zeolites are widely used in industry for various purposes. Their ability to act as solid acids and bases makes them suitable for applications such as catalysis. One area of this is in the petrochemical industry, where zeolites are used for cracking of hydrocarbons to produce higher octane molecules. Lanthanum exchanged zeolite Na-Y plays an important role in the preparation of catalysts for fluid catalytic cracking, one of the most widely applied petroleum refinery processes that makes use of zeolites as catalyst components.^{1-2, 9-10 54} They can also be used as shape selective catalysts, e.g. in the preparation of p-xylene.² Zeolites are also used for water softening and for the separation and storage of nuclear waste.

A more recent perspective is the proposed use of zeolites as host materials for host-guest composites. These are a kind of advanced materials where zeolites (of course zeo-types too) act as hosts for encapsulating and organizing guest molecules, crystalline nano-phases and supramolecular entities inside their pores. Space confinement and host-guest (electrostatic) interaction result in a type of materials with novel properties.^{1-2, 5} Potential applications are expected in number of technological fields, such as photochemistry, optoelectronics, semi-conducting devices, and chemical sensors.

Another use for zeolites lies in the area of gas separation, making use of the zeolite as a molecular sieve. Work has been conducted in studying the sorption of various gases such as CO₂, O₂, N₂ and other gases such as CFCs. Some of the other applications of zeolites involve (1) separation and recovery of natural paraffin hydrocarbons, (2) catalysis of hydrocarbon reactions, (3) drying of refrigerants, (4) drying of air components, (5) carrying catalysts in the drying of plastics and rubber, (6) recovering radioactive ions from radioactive waste solution, (7) removing carbon dioxide and sulphur compounds from

natural gas, (8) solubilising enzymes, (9) separating hydrogen isotopes and (10) removing atmospheric pollutant such as sulphur dioxide.^{1-2, 5-7}

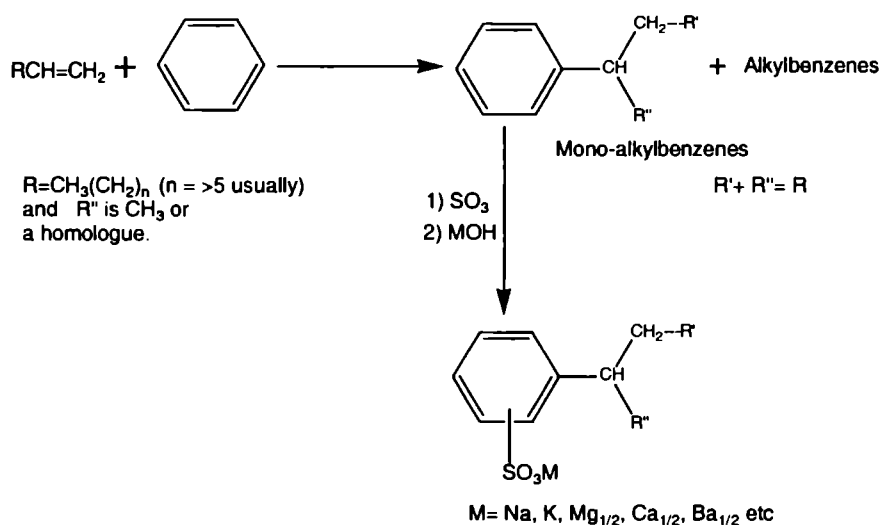
1.7 Linear Alkyl Benzenes (LABs)

Linear alkylbenzene sulphonates (LAS) are widely used in the manufacture of soft anion- active detergents. They are prepared by sulphonating the alkylbenzene obtained by alkylation of benzene with olefins, alcohols, alkyl halides etc in presence of Friedel-Crafts catalysts. However alkenes are the preferred alkylating agents as they are cheap and are freely available. Studies on the solubility, form stability, and most importantly the surface-active properties of these products have shown that the length of their alkyl chain and the position of the phenyl group on it are important factors in determining their performance characteristics.⁵⁸⁻⁶⁰ Certain constant synergistic effects have also been observed for various combinations of phenylalkanes.⁶¹ In general, the 2-phenylalkane isomer differs in its performance characteristics, which makes the control of its amount in the product, a matter of considerable importance.

The interaction of benzene with a straight-chain olefin in presence of Friedel-Crafts catalysts affords all the possible secondary phenylalkanes.⁶² The isomerization of the alkylating agent and under certain conditions of product alkylbenzene is well established.⁶³ The extent of these two isomerizations which determine the final isomer distribution of the product has found to depend on the strength and amount of the catalyst, the solvent, and the position of the double bond (in case of alkene alkylating agent) in the starting alkene.⁶⁴⁻⁶⁷ This is contrary to earlier reports of no isomerization and formation of only 2-arylalkane, and partial isomerization to give mainly the 2-phenyl and 3-phenyl isomers.⁶⁸⁻⁷⁰

Traditionally, the production of linear alkyl benzenes; LABs from detergent range olefins plus benzene has been practiced commercially using either Lewis acid catalysts, or liquid acid catalysts such as HF acid.⁷⁰⁻⁷¹ The HF catalyst typically gives 2-phenylalkane selectivities of only 17-18%. The selectivity is really low because the 2- isomers are preferred amongst the possible phenylalkane sulphonate (LAS) isomer derivatives (Scheme 1), since the 2-phenyl LAS have the most favorable biodegradation and solubility characteristics. The most commonly used Friedel-Crafts catalysts for the

Figure 1.5. Scheme showing the general pathway for the production of detergents. Benzene on alkylation with 1-alkene produces linear alkylbenzenes having all possible positional isomers from 1-isomer to 2-isomer. LAB on sulphonation in presence of metal hydroxide produces linear alkylbenzene sulphonates or LAS.¹⁵⁻¹⁶



Reaction conditions are HF, AlCl_3 , FeCl_3 , BF_3 , and H_2SO_4 .⁷⁰⁻⁷³ The corrosive nature and potential environmental hazards in case of these catalysts are major

concerns.⁷⁴ Hence we need to have some alternative process for producing maximum 2-phenylalkane in an environmentally friendly way.

I. Introduction: environmental impact

Responsible care and sustainable development have become paradigms of industrial production. It is therefore required that all processes are to be optimized with respect to energy efficiency, chemical utilization, and waste minimization.⁷⁵⁻⁷⁹

The need for more environmentally friendly production technology in the chemical industry is universally acknowledged and much progress has already been made. In the past, the need to reduce costs has provided the driver for improvements in process efficiency, since wasteful processes are also uneconomic. However, recent public concern about the environment, leading to regulatory activity by governments, has accelerated this tendency to the so-called *cleaner-technology*. Legislation enacted to control the discharge of waste products into the environment, and restrict the manufacture, transport, storage and use of certain hazardous chemicals, has acted as a spur to the introduction of *cleaner technology*.

Two useful measures of the environmental impact of chemical processes are the *E-factor*, defined by the mass ratio of waste to desired product, and the *atom utilization*, calculated by dividing the molecular weight of the desired product by the sum of the molecular weights of all substances produced in the stoichiometric equation. Processes employing acids and bases requiring neutralization, or stoichiometric redox reagents, represent the major sources of waste production in the form of salts and heavy metals and have high E-factors and low atom utilization. Reactions of this type, employed in the fine-chemicals industry particularly, include Friedel–Crafts acylations mediated by Lewis acids

Such as aluminium chloride, reductions with metal hydrides or dissolving metals such as zinc or iron, and stoichiometric oxidations with dichromate or permanganate, all of which generate prohibitive amounts of metal-containing wastes. The work-up of products from nitrations, sulphonations and many other acid-catalyzed reactions involves neutralization and the concomitant generation of salt such as NaCl, Na₂SO₄ and (NH₄)₂SO₄. Processes which proceed via chlorine-containing intermediates, but in which chlorine does not appear in the product, generate chloride-containing waste. The elimination of such wastes forms the first goal of environmentally friendly processing; the second is the reduction of dependence on the use of hazardous chemicals such as phosgene, dimethyl sulphate, peracids, sodium azide, halogens and HF.^{76, 79-80}

Typical Friedel-Crafts are liquid acids HF and AlCl₃.⁷⁰⁻⁷¹ Both possess very good activity towards alkylation, but the selectivity for the most desired 2-isomer is only around 20%. And these strongly acidic catalysts in commercial process are extremely corrosive in nature, thus requiring special handling equipments. Furthermore, the use of these acidic catalysts might induce some very serious environmental problems.⁷⁸ With increasing environmental concern, it is very much important to find a substitution equal or superior to these acids in all respect. Therefore it would be desirable to utilize a safer and simpler catalyst, preferentially in the solid state, to produce the desired products. Hence there is a real need for a solid acid that offers the activity of HF coupled with increased selectivity and stability to the process. HF acid and anhydrous AlCl₃ have problem with recovery of the catalyst and reusability.⁷⁴⁻⁸⁰ This makes the process involving them economically very costly. However, hydrogenation followed by HF accounts for round about 88% of world production.^{7, 74} This is done by taking maximum safety measures at modern HF alkylation plants thereby potential release of harmful effluents is minimal.

The manufacture of fine and speciality chemicals in traditional processes has commonly been associated with the large quantities of toxic waste.^{75-76, 78-79} Use of traditional catalysts such as mineral acids, strong bases, and toxic metal reagents is widespread and has many drawbacks including handling difficulties, inorganic contamination of the organic products, sublimation at high temperatures, poor solubility in organic reagents, formation of large volumes of toxic waste and very poor reaction selectivity leading to unwanted isomers and other side-reaction products. Again, the normal work-up procedure for the reaction employing these catalysts involves a water quench that prevents the acid being used. In addition, since the catalysts are irreversibly lost, the overall atom efficiency is very low and hence is not cost effective. Thus, these traditional catalysts are marked by high *E-factor* and low *atom efficiency*.⁷⁹⁻⁸⁰ Consequently, a judicious choice for a safe, acid catalyst for the alkylation reaction attains significance. *Green chemistry* demands the replacement of these highly corrosive, hazardous and polluting acid catalysts with eco-friendly solid acid catalysts.⁷⁵⁻⁷⁶

These problems can be largely overcome if genuinely catalytic, heterogeneous alternatives to environmentally unacceptable catalytic systems can be developed. An alkylation process that employs a fixed bed of stable, non-sludging solid catalyst has advantages. Sebalsky et al. reported the use of supported silicotungstic acid in the alkylation of benzene with 1-dodecene back in 1971.⁸¹ Solid acid catalysts are the best alternatives. Recently many new solid acids emerged as better substitutes for HF, AlCl₃, and BF₃. Solid acids possessing strong acid sites have been reported to have activities comparable to that of HF or AlCl₃. There are number of papers and a handful of patents describing the LAB synthesis using a range of solid acid catalysts including acidic clays and pillared clays,⁸²⁻⁸³ metal oxides, sulphated oxides, and heteropoly acids,^{80, 84-89} mesoporous materials,⁹⁰⁻⁹⁴ cation exchange resins,⁹⁴⁻¹⁰⁰

and a variety of acidic zeolites.^{74, 77, 79,101-124} Many of these materials provide activity comparable to HF and an improved selectivity for the most desired 2-henylalkane. High chemical and thermal stability of the systems, high activity, reusability and resistance to deactivation coupled with its eco-friendly nature makes rare earth exchanged zeolites a superior choice of catalyst for the synthesis of LABs over the conventional catalysts such as HF or $AlCl_3$.

. LABs Technology- an overview

Several routes have been used for the production of linear alkylbenzenes. The various technologies developed include,

Chlorination of linear paraffin to form monochloroparaffin. Aluminium chloride is used to alkylate benzene with monochloroparaffin. ARCO Technology Inc.¹²⁵ has developed and commercialized this route.

Chlorination of linear paraffins followed by dehydrochlorination to form olefins. HF is used as the alkylation catalyst for benzene alkylation with these linear olefins. Shell's CDC process is an example.

Wax cracking, alpha olefins from ethylene oligomerization, or linear internal olefins from olefin disproportionation can produce olefins. Alkylation of benzene with these olefins is conducted using HF. Companies that use this technology include Albermark, Chevron and Shell.

Dehydrogenation of linear paraffin to a mixture of linear olefins is another route to paraffin activation. The olefin-containing stream is used to alkylate benzene using HF acid catalyst. Here the unconverted paraffins are recycled back to dehydrogenation after separation by distillation. UOPs PacolTM process and UOPs Detergent AlkylateTM process are examples of this approach.⁷²⁻⁷³

5. Most recently, a new process using a solid acid catalyst was developed. The Detai™ process that uses a non-corrosive solid acid catalyst was commercialized in 1995.

Table 1.2. World LAB production by technology route (in metric tons).¹

Process	Year			
	1970	1980	1990	2000
Chlorination+ alkylation.	400	400	240	180
High purity olefins for alkylation.	0	100	280	120
Dehydrogenation + HF alkylation.	260	600	1280	1850
Dehydrogenation+ solid acid bed alkylation.	0	0	0	260
Total	660	1100	1800	2410

Note: ¹ Based on available literature till 2001)

III. Advances in LAB alkylation catalysts

Hydrofluoric acid was the alkylation catalyst of choice for the production of branched chain alkylbenzenes since 1960, when the first UOP detergent alkylation plant came on stream. The same flow scheme with mild modification has been used for the production of linear alkyl benzenes using olefins derived from Pacol unit since 1968. High efficiency, superior product quality and ease of use relative to aluminium chloride technology lead to its dominance in alkylation complexes. However, the handling of corrosive HF acid or $AlCl_3$ had negative implications in terms of increased capital cost for the commercial plant as well as the disposal of huge amounts of waste products generated in the production process. In addition to being environmentally friendly and safe, the heterogeneous catalyst is advantageous for enabling the use of ordinary metallurgy for construction, easy separation of product and elimination of HF waste by-product.

Many solid acid involving clays, zeolites, metal oxides, metal sulphides, mesoporous materials, cation exchanged resins etc have been widely used in the production of linear alkylbenzenes which have been already discussed in the previous sections.⁸¹⁻¹²⁵ Although many of them are active, they generally lack the required selectivity towards the linear alkylbenzenes and stability for process time. Many of them have high initial activity and undergo slow deactivation with time due to deposition of heavy molecules inside the pores. A successful solid acid catalyst demands high activity, selectivity, stability for prolonged periods of operation, and regenerability, to be economical compared to HF or AlCl_3 . A most recent approach to improve the catalytic stability with solid acid catalysts involves supporting AlCl_3 on mesoporous silica.⁹⁰ The researchers are able to produce a reusable catalyst that is prepared by chemically supporting AlCl_3 on mesoporous MCM-41 type silica (heterogenized homogeneous catalyst).⁹³ Selectivity to the desired (of course the product of interest is the 2-phenyl isomer) product was further improved by poisoning the external surface acid sites with bulky triphenylchlorosilane or triphenylamine. Up to 90% selectivity to phenyldodecane was observed by using this modification. However, it should be remembered that mordenite zeolite can produce almost the same phenyl isomer. This very high selectivity is explained in terms of an effective uni-directional pore system.¹¹⁰ However, unfortunately it undergoes very fast deactivation and hence not implemented in any industrial process.

7. Current commercial linear alkylbenzene technology

Current technologies for linear alkylbenzene production are based on either HF acid or a solid acid. To date there is only one known technology using solid acid catalyst that has been demonstrated commercially. A second technology is under test in India. There is little known about this technology other than it is based on zeolite. To date this system has not been fully

demonstrated or commercialized (the data are based on available literature till 2001). The only commercialized technology is Detal™ process offered by UOP. The technology has two commercial units in operation to date.⁷⁴

V. Product quality

Bromine index and sulfonatability are key measures of product quality because they affect the final product cost. Both these parameters are related to the improved rate of biodegradation of the ultimate product. The Detal™ linear alkylbenzene product is produced in higher yield with higher linearity, improved sulphonate color, and less tetralin by-product. It also has greater 2-phenylalkane content that adds improved solubility in many formulations. All of these properties demonstrate that the current Detal technology produces a superior product than HF acid technology.

VI. Economics

Economics of the current Detal and HF acid technology have been compared. For 80,000 MTA linear alkylbenzene unit, the estimated cost for Detal and HF systems are US\$ 67 and 72 million, respectively. The fixed plant deposit has been reduced by approximately 15%. The absence of HF acid and required neutralization facilities for the acid wastes is reflected in lower operating costs (based on available literature till 2001).

1.8 Main objectives of the present work

The major objectives of the present work include;

1. Exchange of pure H-Y zeolite with sodium, potassium, and magnesium to make it into Na-Y, K-Y, and Mg-Y zeolite (represented as M-Y).
2. To prepare rare earth exchanged (Ce^{3+} , La^{3+} , RE^{3+} , and Sm^{3+}) M-Y zeolites.

Investigate the chemical composition of the prepared zeolite systems using EDX.

To prove the intact nature of zeolite-Y framework even after exchange at moderately high temperature using XRD and IR spectral studies.

Electronic transitions has to be monitored by UV-vis DRS analysis of the zeolites.

To locate the residual cations (H^+ , Na^+ , K^+ , and Mg^{2+}) using ^{23}Na MAS NMR studies (for sodium exchanged zeolites only) and a proper comparison in case of other systems.

Nature of alumina tetrahedra has to be followed by ^{27}Al MAS NMR studies. Different kinds of aluminium coordinations have to be proved using the technique. A predominant broadening of the tetrahedral peak, which is common in ^{27}Al NMR also, has to be investigated.

The nature of silicon atom and its coordination ion the zeolite framework has to be followed using ^{29}Si MAS NMR spectra. The possible influence of the bulky extra-framework cations on the framework tetrahedra also has to be proved.

To study the acid structural properties of the rare earth zeolites using NH_3 -TPD studies, 1H MAS NMR has to be taken to get an idea about the strength of BAS. The results from these studies shall be compared with the results from cumene cracking test reaction.

0. The prepared systems are to be employed for the vapour phase Friedel-Crafts alkylation of benzene with higher olefins. The enhancement in the 2-phenylalkane content in the product mixture is the main objective of the present work. A comparison of the amount of deactivation for the pure H-Y and various rare earth exchanged zeolites has to be done. The nature of

carbonaceous compounds blocked inside the zeolite pores are to be studied to know the possible cause of deactivation of different zeolites.

References

1. D. W. Breck, "Zeolites molecular sieves; structure characterization and uses", Wiley Inter-science Pub. Inc., 1973
2. R. Szostak, "Molecular sieves-principles of synthesis and identification", Van Nostrand Reinhold catalysis Series, New York, 1989.
3. G. T. Kokotailo, S. L. Lowton, D. H. Olson, W. M. Meier, *Nature*, 272 (1978) 437.
4. D. H. Olson, G. T. Kokotailo, S. L. Lowton, W. M. Meier, *J. Phy. Chem. B.* 85 (1981) 2238.
5. A. Zecchina, C. O. Arean, *J. Chem. Soc. Chem. Soc. Reviews* (1996) p. 187.
6. J. A. Rabo, M. W. Schoonover, *Appl. Catal. A. Gen.* 222 (2001) 261.
7. K. Tanabe, W. F. Holderich, *Appl. Catal. A. Gen.* 181 (1999) 299.
8. M. J. Climent, A. Velty, A. Corma, *Green Chem.* 4 (2002) 565.
9. M. L. Ocelli (Ed.), "Fluid Catalytic Cracking", Am. Chem. Society, Washington DC, 1988.
10. H.G. Karge, K. Hatada, Y. Zhang, R. Fiederow, *Zeolites*, 3 (1983) 13
11. J. V. Smith, *Mineral. Soc. Amer. Spec. Pap. No. 1*, 1963.
12. K. F. Fisher, W. M. Meier, *Fortschr. Mineral.* 42 (1965) 641.
13. W. M. Meier, "Molecular Sieves", Society of Chem. Industry, London, 1968, p. 10.
14. D. W. Breck, "Molecular Sieve Zeolites", *Adv. Chem. Ser.* 101, Am. Chem. Soc. Washington, DC, 1971, p. 1.
15. W. Loewenstein, *Am. Minerl.* 39 (1954) 92.
16. W. H. Taylor, *Z. Krystallogr.* 99 (1938) 283.
17. J. M. Bennet, J. A. Gard, *Nature*, 214 (1967) 1005.
18. T. B. Reed, D. W. Breck, *J. Am. Chem. Soc.* 78 (1956) 5972.
19. J. V. Smith, L. G. Dowell, *Z. Kristallogr.* 133 (1971) 134
20. R. M. Barrer, H. Villiger, *Z. Kristallogr.* 128 (1969) 1089.
21. E. Dempsey, G. H. Kuehl, D. H. Olson, *J. Phys. Chem.* 73 (1969) 387.
22. W. H. Baur, *Am. Mineral.* 49 (1964) 697.
23. P. Y. Feng, X. H. Bu, G. D. Stucky, *Nature*, 388 (1997) 735.
24. T. E. Gier, G. D. Stucky, *Zeolites*, 12 (1992) 770.

5. L. Pauling, *Proc. Nat. Acad. Sci.* 16 (1930) 453.
6. P. A. Vaughan, *Acta Crystallorg.* 21 (1966) 983.
7. I. S. Kerr, *Nature*, 202 (1964) 589.
8. W. M. Meier, *Z. Kristallogr.* 115 (1961) 439.
9. M. J. Eapen, K. S. N. Reddy, P. N. Joshi, V. P. Shiralkar, *J. Incl. Phenom.* 14 (1992) 119.
0. R. C. Rouse, D. R. Peacor, *Am. Mineral.* 79 (1994) 175.
1. A. B. Merkle, M. Slaughter, *Am. Mineral.* 53 (1968) 1120.
2. M. Slaughter, *Am. Mineral.* 55 (1970) 387.
3. G. T. Kokotailo, S. L. Lawton, D. H. Olson, W. M. Meier, *Nature*, 272 (1978) 437.
4. G. T. Kokotailo, P. Chu, S. L. Lawton, W. M. Meier, *Nature*, 275 (1978) 119.
5. J. M. Thomas, G. R. Millward, *J. Chem. Soc. Chem. Commun.* (1982) 1380.
6. J. B. Higgins, R. B. LaPierre, J. L. Schlenker, A. C. Rohman, G. T. Kerr, W. J. Rohrbaugh, *Zeolites*, 8 (1988) 446.
7. K. S. N. Reddy, M. J. Eapen, P. N. Joshi, S. P. Mirajkar, V. P. Shiralkar, *J. Incl. Phenom. Mol. Recogn. Chem.* 20 (1994) 197.
8. R. M. Barrer, L. W. R. Dicks, *J. Chem. Soc. A.* (1966) 1379.
9. J. J. Pluth, J. V. Smith, J. M. Bennett, *Acta Crystallorg.* C42 (1986) 283
0. J. V. Smith, W. J. Derrych, *Nature (London)*, 309 (1984) 607.
1. R. F. Horlock, P. J. Anderson, *Trans. Faraday Soc.* 63 (1967) 717.
2. N. Najiri, M. Misono, *Appl. Catal. A. Gen.* 93 (1993) 103.
3. E. Min, P. Zhou, "Progress in Catalytic Technology in the People's Republic of China during 1980s", *Appl. Catal. A. Gen.* 95 (1993) 1.
4. D. H. Olson, *J. Phys. Chem. B.* 74 (1970) 2758.
5. G. T. kokotailo, J. Ciric, *Adv. Chem. Ser.* 101 (1971) 109.
6. P. Gallezot, Y. B. Taarit, B. Imelik, *J. Catal.* 26 (1970) 481.
7. G. R. Eulenberger, D. P. Shoemaker, J. G. Keil, *J. Phys. Chem. B.* 71 (1967) 1812.
8. D. W. Breck, U.S. Patent, 3, 130, 007 (1964).
9. J. J. V. Dun, K. Dhaeze, W. J. Mortier, *J. Phys. Chem. B.* 92, No. 22 (1988) 6747.
0. J. J. V. Dun, W. J. Mortier, B. Uytterhoeven, *J. Phys. Chem. B.* 88 (1988) 6747.
1. H. Hamden, J. Klinowski, "Zeolite Synthesis", *ACS Symp. Ser.* 398 (1988) 449.
2. R. Carvajal, P.-J. Chu, J. H. Lunsford, *J. Catal.* 125 (1990) 123.
3. N. Herron, *New J. Chem.* 13 (1989) 761.

54. J. Biswas, I. E. Maxwell, *Appl. Catal. A. Gen.* 63 (1990) 197.
55. K. Gaare, D. Akporiaye, *J. Phys. Chem. B.* 101 (1997) 48.
56. J. Datka, E. Tuznick, *J. Catal.* 102 (1986) 43.
57. E. M. Flanigen, L. B. Sand, *Molecular Sieve Zeolites*, American Chemical Society, New York, 1971, p. 201.
58. R. M. Anstett, P. A. Munger, J. Rubinfeld, *J. Am. Oil Chemists Soc.* 43 (1966) 25.
59. J. Rubinfeld, E. M. Emery, H. D. Cross, *Ind. Eng. Chem. Prod. Res. Develop.* 4 (1965) 33.
60. J. Rubinfeld, E. M. Emery, H. D. Cross, *J. Am. Oil Chemists Soc.* 41 (1964) 822.
61. W. A. Sweeny, A. C. Olson, *J. Am. Oil Chemists Soc.* 41 (1964) 815.
62. A. C. Olson, *Ind. Eng. Chem.* 52 (1960) 833.
63. R. D. Swisher, E. F. Kaelble, S. K. Liu, *J. Org. Chem.* 26 (1961) 4066.
64. R. H. Allen, D. Yats, *J. Am. Chem. Soc.* 83 (1961) 2799.
65. H. R. Alul, G. J. McEwan, *J. Org. Chem.* 32 (1967) 3365.
66. D. A. McCaulay, "Friedel-Crafts and Related Reactions" G. Olah, Ed. Vol. II, Chapter 24, Interscience, New York, 1964.
67. H. C. Brown, C. R. Smoot, *J. Am. Chem. Soc.* 78 (1956) 6255.
68. F. N. Baumgartner, *Ind. Eng. Chem.* 46 (1954) 1349.
69. F. W. Gray, J. F. Gerecht, I. J. Krems, *J. Org. Chem.* 20 (1955) 511.
70. G. Olah, "Friedel-Crafts and Related Reactions", Vol. 1, Wiley-Interscience, New York, 1963.
71. J. F. Roth, A. R. Schacfer, US Patent, 3, 356, 757.
72. R. E. Berg, B. V. Vora, *Encyclopedia of Chemical Processing and Design*, Vol. 15. Marcel Dekker, New York, 1982, p. 266.
73. P. R. Pujado, *Linear Alkylbenzene Manufacture: "Handbook of Petroleum Refining Process"*, 1997, p. 1.53.
74. J.A. Kocal, P.V. Vora, T. Imai. *Appl. Catal. A: Gen.* 221 (2001) 295.
75. J. H. Clark, (ed.), "Chemistry of Waste Minimization", Chapman and Hall, London 1995.
76. J. H. Clark, *Green Chem.* 1 (1999) 1.
77. K. Smith, G. M. Pollaud, I. Mathews, *Green Chem.* 1 (1999) 75.
78. J. H. Clark, A. J. Butterworth And S. T. Tavener, A. J. Teasdale, S. J. Barlow, T. W. Bastok, K. Martin, *J. Chem. Tech. Biotechnol.* 68 (1997) 367.
79. R.A. Sheldon, R. S. Dowling, *Appl. Catal. A. Gen.* 189 (1999) 163.

0. Arumugamangalam, V. Ramaswamy, *Chimica & Industria- Science and Tech.* (2000) p. 1.
1. R. T. Sebulsky, A. M. Henke. *Ind. Eng. Chem. Process. Des. Develop.* Vol. 10, No.2, 272 (1971).
2. H. M.- Yuan, L. Zhonghui, M. Enze, *Catal. Today* 2 (1988) 321.
3. L. Zhonghui, S. Guida, in *Stud. Surf. Sci. Catal.* 24, "Zeolites", Eds. B. Drazoj, S. Hoescevar, S. Pejovnik, Elsevier, Amsterdam, Oxford, New York, Tokyo, 1985, p. 493.
4. J. H. Clark, G. L. Monks, D. J. Nightingale, P. M. Price, J. F. White, *J. Catal.* 193 (2000) 348.
5. C. Hu, Y. Zhang, L. Xu, G. Peng, *Appl. Catal. A: Gen.* 177 (1999) 237
6. T. Okuhara, N. Mizuno, M. Misono, *Adv. Catal.* 41 (1996) 113.
7. Y. Inzumi, N. Natsume, H. Tamamine, K. Urabe, *Bull. Chem. Soc. Jpn.* 62 (1989) 2159.
8. A. Corma, *Chem. Rev.* 95 (1995) 559.
9. P. M. Price, J. H. Clark, K. Martin, D. J. Macquarrie, T. W. Bastock, *Org. Process. Res. Dev.* 2 (1998) 221.
0. X. Hu, M. L. Foo, G. K. Chuah, S. Jaenicke, *J. Catal.* 195 (2000) 412.
1. X. Lin, G. K. Chuah, S. Jaenicke, *J. Mol. Catal. A. Chem.* 150 (1999) 287.
2. E. E. Getty, R. S. Drago, *Inorg. Chem.* 29 (1990) 1186.
3. J. S. Beck, J. C. Vartuli, W. J. Roth, M. E. Leonowicz, C. T. Kresge, K. D. Schmitt, C. T. W. Chu, D. H. Olson, E. W. Sheppard, S. B. McCullen, J. B. Higgins, J. L. Schlenker, *J. Am. Chem. Soc.* 114 (1992) 10834.
4. E. R. Lachter, R. A. da S. S. Gil, D. Tabak, V. G. Costa, C. P. S. Chaves, J. A. dos Santos, *React. Funct. Polym.* 44 (2000) 1.
5. J. Klein, H. Widdeke, *Chem. Ing. Tech.* 51 (1979) 560.
6. C. Buttersack, H. Widdeke, J. Klein, *J. Mol. Catal. A. Chem.* 35 (1986) 77.
7. C. Buttersack, H. Widdeke, J. Klein, *J. Mol. Catal. A. Chem.* 35 (1986) 365.
8. C. Buttersack, J. Klein, H. Widdeke, *React. Polym.* 5 (1987) 181.
9. A. Chakrabarti, M. M. Sharma, *React. Polym.* 20 (1993) 1.
00. A. B. Dixit, G. D. Yadav, *React. Funct. Polym.* 31 (1996) 237.
01. L. B. Young, US Patent, 4, 301, 317 (1981) to Mobil Oil Corporation.
02. J. A. Kocal, US Patent, 5, 196, 574 (1993) to UOP (Des Plaines, IL).
03. J. F. Knifton, P. R. Anantaneni, P. E. Dai, US Patent, 5, 847, 254 (1998) to Huntsman Petrochemical Corporation (Austin, TX).

104. J. A. Kocal, D. J. Korous, US Patent, 5, 276, 231 (1994) to UOP (Des Plaines, IL).
105. J. F. Knifton, P. R. Anantaneni, US Patent, 5, 777, 187 (1998) to Huntsman Petrochemical Corporation (Austin, TX).
106. D. J. Stewart, D. E. O'Brien, US Patent, 6, 417, 420 (2002) to UOP LLC (Des Plaines, IL)
107. J. F. Knifton, P. R. Anantaneni, M. E. Stockton, US Patent, 5, 770, 782 (1998) to Huntsman Petrochemical Corporation (Austin, TX).
108. J. F. Knifton, P. R. Anantaneni, M. E. Stockton, US Patent, 3, 315, 964 (2001) to Huntsman Petrochemical Corporation (Austin, TX).
109. J. F. Knifton, P. R. Anantaneni, P. E. Dai, M. E. Stockton, Catal. Lett. Vol. 75, No. 1-2 (2001) 113.
110. B. Wang, C. W. Lee, T-X. Cai, S-E. Park, Catal. Lett. Vol. 76, No. 1-2 (2001) 99.
111. L. L. G. de Almeida, M. Dufaux, Y. B. Taarit, C. Naccache, Appl. Catal. A. Gen. 114 (1994) 141.
112. P. Meriaudeau, Y. B. Taarit, A. Thangaraj, J. L. G. de Almeida, C. Naccache, Catal. Today 38 (1997) 243.
113. M. Han, Z. Cui, C. Xu, W. Chen, Y. Jin, Appl. Catal. A. Gen. 238 (2003) 99.
114. S. Sivasanker, A. Thangaraj, J. Catal. 138 (1992) 386.
115. Z. Da, P. Magnoux, M. Guisnet, Catal. Lett. 61 (1999) 203.
116. W. Liang, Z. Yu, Y. Jin, Z. Wang, Y. Wang, J. Chem. Tech. Biotechnol. 62 (1995) 98.
117. W. Liang, Y. Jin, Z. Yu, Z. Wang, B. Han, M. M. He, E. Min, Zeolites, 17 (1996) 297.
118. Z. Da, Z. Han, P. Magnoux, M. Guisnet, Appl. Catal. A. Gen. 219 (2001) 45.
119. Z. Da, P. Magnoux, M. Guisnet, Appl. Catal. A. Gen. 182 (1999) 407.
120. S. Sivasanker, A. Thangaraj, R. A. Abulla, P. Ratnasamy, Stud. Sur. Sci. Catal. 75 (1993) 397.
121. P. Magnoux, A. Mourran, S. Bernard, M. Guisnet, Stud. Sur. Sci. Catal. 108 (1997) 107.
122. L. B. Zinner, K. Zinner, M. Ishige, A. S. Araujo, J. Alloys Comp. 193 (1993) 65.
123. L. B. Zinner, A. S. Araujo, J. Alloys Comp. 180 (1992) 289.
124. P. B. Venuto, Micropor. Mater. 2 (1994) 297.
125. ARCO Technology Inc. Hydrocarbon Processing, 64 (11) (1985) 127.

Chapter 2

Materials and Methods

"Imagination is more important than knowledge"

-Albert Einstein

The use of catalyst in commercial process industries is currently widespread. The nature of the catalytic process whereby a given reaction may be accomplished at lower temperature than that required for the homogeneous reaction is likely to lead the application of catalytic methods and catalysts to even more processes as fuel costs continue to rise. In view of this, there is always thrust for developing tailored catalysts for industrial applications. In fact, catalyst synthesis still seems to be an art to many material scientists. In the production of commercial catalysts, even a minute change in the preparation conditions change the quality of the catalyst. This points to the need of characterizing the catalyst thoroughly before use. The catalytic behavior of a laboratory catalyst can be better appreciated if one knows as much as possible of its physical properties as possible. The methods available nowadays for catalyst characterization vary widely in their complexity and sophistication ranging from really expensive adsorption techniques to highly sophisticated electron spectroscopy and microscopic techniques.

2.1 Preparation of the catalyst

Catalyst preparation was regarded as an art, where successful results were acquired by trial and error than scientific understanding of the process involved. However, in the past ten years scientists became more interested in the 'design' of catalyst with well-defined properties and a well-controlled preparation as a necessary prerequisite. The various processes involved in the preparation of acid catalyst link inorganic chemistry, colloidal chemistry, surface chemistry and cluster chemistry and the increasing research efforts have justified the organization of three international symposia on catalyst preparation. The 'supreme' aim of a successful preparation method is to distribute the active phase in the most efficient way i.e. in a highly dispersed form to obtain large specific surface areas and maximum activity per weight of active compound over the support surface.

Materials

The materials used for the preparation of binder free M-Y zeolites (M = H⁺, Na⁺, K⁺, and Mg²⁺) and various as-exchanged rare earth zeolites are given in Table-2.1.

Methods

A detailed discussion of the experimental procedures adopted to develop the catalyst systems for the present investigations is given in the following section.

Table 2.1. Materials used for the catalyst development.

Material	Supplier
HFAU-Y	<i>Sud-Chemie (India) Ltd.</i>
Ce (NO ₃) ₃ · 6H ₂ O.	<i>Indian Rare Earths Ltd. Kerala India.</i>
La (NO ₃) ₃ · 6H ₂ O.	<i>Indian Rare Earths Ltd. Kerala India.</i>
Sm (NO ₃) ₃ · 6H ₂ O.	<i>Indian Rare Earths Ltd. Kerala India.</i>
RE (NO ₃) ₃ · 6H ₂ O.	<i>Indian Rare Earths Ltd. Kerala India.</i>
NaCl	<i>SD fine Chemicals</i>
KCl	<i>SD fine Chemicals</i>
MgNO ₃	<i>SD fine Chemicals</i>

2 Preparation of MFAU-Y (M= Na, K, Mg)

MFAU-Y zeolite was prepared by ion exchanging HFAU-Y from a 0.1 M (0.05 moles per gram of zeolite) metal salt solution (NaCl, KCl and MgNO₃ for NaFAU-Y, KFAU-Y and MgFAU-Y respectively) at room temperature. The H-Y zeolite dispersed in metal salt solution is stirred for 24 hours and repeated the process 3 times. It was then filtered, washed with deionized water and dried at 333 K for over night. It was then placed in a muffle furnace and heated stepwise in constant flow of air. The temperature was raised from room temperature to 773 K over a period of 6 hours, and maintained at this temperature for 5 hours. Finally the sample was cooled to room temperature under ambient conditions.¹⁻³

3 Preparation of rare earth FAU-Y (RE= Ce³⁺, La³⁺, RE³⁺, Sm³⁺)

Rare earth exchanged zeolite is prepared by ion exchanging the MFAU-zeolites with a 0.5 M (0.025 moles of nitrate/g of zeolite) rare earth metal nitrate solution at 353 K for 24 hours. It was filtered, washed, made free of

nitrate ions and dried at 383 K over night in an air oven. All the samples were then calcined at temperatures from 423 to 773 K, and at 773 K for 5 hours with a heating rate of 12 K per minute with a constant air blowing over the sample (60mL/min).⁴⁻⁷

Catalyst Notations

Table 2.2. Notations used for the catalysts

Parent zeolites	Rare earth modified forms
H-Y	CeH-Y, LaH-Y, REH-Y
Na-Y	CeNa-Y, LaNa-Y, RENa-Y, SmNa-Y
K-Y	CeK-Y, LaK-Y, REK-Y
Mg-Y	CeMg-Y, LaMg-Y, REMg-Y

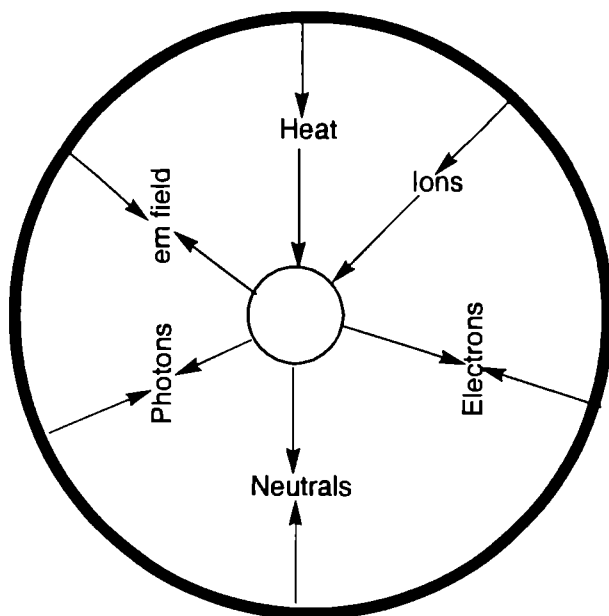
2.4 Zeolite characterization

Catalyst characterization is highly a relevant and important field in catalysis. The catalytic properties of the surface are determined by its composition and structure on the atomic scale and hence it is essential to know the exact structure of the surface including crystal defects, exact location of the active atom/site etc. Thus, from a fundamental point of view, the ultimate goal of catalyst characterization should be a look at the surface atom by atom and under specific reaction conditions.

Spectroscopic techniques

There are many ways to obtain information on the physico-chemical properties of a material. Scheme- 2.1 presents a scheme from which all techniques can be derived. All kinds of spectroscopies are based on some type of excitation as expressed by the ingoing arrow, to which the catalyst responds as symbolized by the outgoing arrow.

Scheme 2.1. A schematic representation of different spectroscopic techniques available for catalyst characterization.



Several approaches can be adopted to investigate the fundamental relationship between the state of a catalyst crystal and its activity. One would like to model the catalyst surface with that of single crystal. By using appropriate combinations of surface techniques, one can obtain desired characteristics on an atomic scale. The disadvantage, however, is that although one may be able to study the catalytic properties of samples under realistic conditions, most of the characterization is necessarily carried out in UHV and not under reaction conditions.

Energy Dispersive X-ray analyses (EDAX)

X-rays are one of the by products in an electron microscopic studies. The interaction of an electron with an atom produces two types of X-rays; characteristic emission lines and Bremstrahlung. Element characteristic X-rays

are emitted by the atom when the incident electron ejects a bound electron from an atomic orbital. The core-ionized atom is highly unstable and there arises two possibilities for decay; X-ray fluorescence and Auger decay. The first is the basis for the electron micro probe analysis and the second form the basis for the Auger electron spectroscopy.

The most convenient method to analyze the emitted X-rays is with energy dispersive X-ray detector located at a fixed position with respect to the sample. The detector is a liquid nitrogen cooled solid-state device made of lithium-doped silicon. The incident X-ray photon emits an electron with kinetic energy $E_{X\text{-ray}} - E_b$. (E_b = Binding Energy; B. E. of the photoelectron). The later dissipates its kinetic energy (K.E.) by creating electron-hole pair in the semiconductor, at the cost of 3.8 eV per pair. The number of electron-hole pair is reflected in the pulse height of the current, which can be measured if a voltage is applied over the detector. Hence, the pulse height is a measure of the K.E. of the photoelectron and hence the energy of the incident X-ray photon. The energy resolution is limited to 150 eV, implying that closely spaced X-ray lines cannot be resolved.

Energy Dispersive X-ray analyses (EDAX) were performed over a *JEOL JSM-840 A* (Oxford make model I6211 with a resolution of 1.3 eV) EDX instrument. Samples were prepared by dusting the zeolite powder onto double sided carbon tape, mounted on a metal stub. The samples were then sputter coated with a thin film of gold to reduce charging effects⁸ and a gold minimization procedure was adopted all the times. All these analysis were performed within an error limit of 5%.

II. Scanning Electron Microscopy (SEM)

Seeing the surface of a catalyst, preferably in the atomic scale is an ideal observation of every catalyst chemist. Unfortunately optical microscopy is of no

Due to this end, simply because the rather long wavelength of visible light does not enable the detection of features of particles smaller than one micrometers. Hence electron beams offer the best opportunity to visualize the catalyst surface. Electron microscopy is a rather straightforward technique to determine the size and shape of the particles. The SEM provides information relating to topographical features, morphology, phase distribution, compositional differences, crystal structure, crystal orientation, and the presence and location of electrical defects of a catalyst. The SEM is also capable of determining elemental composition of micro-volumes with the addition of X-ray or electron spectrometer and phase identification through analysis of electron diffraction patterns. The strength of the SEM lies in its inherent versatility due to the multiple signals generated, simple image formation process, wide magnification range, and excellent depth of field.⁹ The current generation of SEMs provide a resolution of about 1 nm at 30 kV operating voltage. However, the resolution degrades to 4 nm when the operating voltage is reduced to 1 kV.

SEM pictures of the samples were taken using a *JEOL JSM-840 A* Oxford build model No. 16211 with a resolution of 1.3 eV) scanning electron microscope using a field emission gun. Finely powdered sample is poured on to the top of a double-sided carbon tape on a metal stub. It is then sputter coated with a thin film of gold to increase the conductivity and to reduce charging effects.⁸

I. Powder X-ray Diffraction (PXRD)

X-rays were discovered at the end of nineteenth century by Roentgen and powder diffraction was developed as early as 1913 for the characterization of materials. The diffraction pattern is a fingerprint of any crystalline phase and powder diffraction is used extensively to identify the mixture phases, which generally constitute a catalyst. A conventional X-ray source consists of a target

which is bombarded with high energy electrons. The emitted X-rays arise from two processes. Electrons slowed down by the target, emit a continuous background spectrum of Bremsstrahlung superimposed on these narrow characteristic lines. Cu $K\alpha$ line with energy 8.04 keV and wavelength 0.154 nm arises because a primary electron creates a core hole in the K shell, which is filled by an electron from the L shell under emission of an X-ray.

X-ray diffraction is the elastic scattering of X-rays by atom in a periodic lattice. The scattered monochromatic X-rays that are in phase give constructive interference. Position, intensity, shape and width of diffraction lines give information on the samples. The spacing between two planes (hkl) d is related to diffraction angle 2θ by Braggs equation;

$$n\lambda = 2d \sin\theta; n= 1, 2, 3... \text{ is an integer.}$$

Thus, if we measure 2θ , at which constructively interfering X-rays leave the crystal, the Braggs equation give the corresponding lattice spacing, which are characteristic of a certain compound.

XRD pattern of a powder sample is measured with a stationary X-ray source (Cu $K\alpha$) and a movable detector, which scan the intensity of the diffracted beam as a function of 2θ between the incoming and the diffracted radiation. When working with samples like catalysts, an image of diffraction lines occur because a small fraction of the sample particles will be oriented such that certain crystal plane is at right angle θ with the incident beam for constructive interference.¹⁰

However, clear diffraction peaks are only observed when the sample posses sufficient long-range order. The advantage of this limitation is that the line width of diffraction peak gives information about the dimension of the reflecting planes. Thus, diffraction lines from perfect crystals are very narrow and sharp. Furthermore, for crystallite size below 100 nm, line broadening

occurs due to incomplete destructive interference in scattering directions where the X-rays are out of phase. The Scherrer equation relates crystallite size to line width (FWHM);

$$\langle L \rangle = k \lambda / \beta \cos \theta$$

$\langle L \rangle$ is a measure of the dimension of the particle in the direction perpendicular to the reflecting planes, β is the peak width at half height or FWHM, and k is a constant related to the crystal shape and often taken as 1. The Scherrer equation tells us that the XRD pattern at smaller wavelength gives sharper peaks. This is not only because λ becomes smaller but also because the diffraction lines shift to lower angles, which decrease the $1/\cos \theta$ term. Both these help to reduce the line broadening. Thus, by using *Mo K α* (17.44 keV and $\lambda = 0.07$ nm) X-ray one can obtain diffraction pattern from smaller particles than with *Cu K α* (8.04 keV, $\lambda = 0.15406$ nm) radiation.¹⁰⁻¹¹

The crystal structure studies of the as-exchanged and parent systems were performed by the powder XRD method using a *Rigaku D-max C* X-ray diffractometer with Ni-filtered *CuK α* radiation in an angular range of 2θ from 5 to 40° and identification of hkl values has done by performing indexing of XRD data using a common Experimental Module ($\lambda = 1.5406$ Å).

1. Infrared Spectroscopy (IR)

Over the last few years, infrared (IR) spectroscopy has rapidly developed into an important and extremely useful method of analysis. In fact, for certain research areas and applications, ranging from material science via chemistry to life sciences, it has become an indispensable tool because this fast and cost-effective type of spectroscopy provides qualitative and quantitative information not available from any other technique. It is useful to divide the infrared region into three sections; near, mid and far infrared.

Table-2.3; A depiction of different IR wavelength regions

Region	Wavelength range (mm)	Wave number range (cm ⁻¹)
Near	0.78 - 2.5	12800 - 4000
Middle	2.5 - 50	4000 - 200
Far	50 -1000	200 - 10

IR radiation does not have enough energy to induce electronic transitions as seen with UV. Absorption of IR is restricted to compounds with small energy differences in the possible vibrational and rotational states.¹² For a molecule to absorb IR, the vibrations within a molecule must cause a net change in the dipole moment of the molecule. The alternating electrical field of the radiation (remember that electromagnetic radiation consists of an oscillating electrical field and an oscillating magnetic field, perpendicular to each other) interacts with fluctuations in the dipole moment of the molecule. If the frequency of the radiation matches the vibrational frequency of the molecule then radiation will be absorbed, causing a change in the amplitude of molecular vibration.

Infrared spectroscopy is considered to be the first and most important modern spectroscopic techniques that found general acceptance in the area of catalysis and are among the most promising and most widely used methods for catalyst characterization. Very detailed structural information can be obtained from vibrational spectra. Several vibrational spectroscopies can be applied in situ conditions and are successfully used for studies of ill-defined high surface area porous materials. In solution where any diffraction techniques are not applicable, vibrational spectroscopy can provide information on phase transitions and change in composition of bulk catalyst material, their crystallinity and the nature of surface groups.

The infrared induced vibrations of the samples were recorded using a *PerkinElmer Impact 400FT Infrared Spectrometer* by means of KBr pellet procedure in the range of 400-4000 nm. Spectra were taken in the transmission mode and the samples were evacuated before making the pellet and the spectra were taken under atmospheric pressure and 293 K temperature.

2.1. UV-vis- Diffuse Reflectance Spectroscopy (UV-vis DRS)

In the field of molecular spectroscopy, absorption measurements with electromagnetic radiation covering the wavelengths between 200 nm and 2000 nm can be used for analytical applications. By convention, tags such as Ultraviolet (200-400 nm), visible (400-800 nm), and NIR (800-2500 nm) were given to special intervals of the spectrum, each yielding different specific information on organic and inorganic substances. The energy for electronic transitions between outer molecular orbitals corresponds to radiation of the first two spectral regions noted, whereas vibrational spectroscopy is connected to the infrared. Here, it can be further distinguished between near- and mid-infrared spectral sub regions, which are important for routine analytical work.

In the classic spectroscopy experiment, transmission measurements are performed to analyze the radiation absorption of samples. Today, an additional powerful measurement technique is diffuse reflectance spectroscopy, which can be applied advantageously to scattering samples such as powders and other dispersed systems. It often requires less sample preparation than for a spectrum recorded in transmission. After sample penetration, the radiation is diffusely scattered and partially absorbed before part of the radiation emerges back at the surface, from where it is detected using various optics and detectors. Besides identification of compounds, quantitative assays for active ingredients and fillers and in general formulation testing are available that often

require special chemometric tools. Trace analysis and the study of adsorbed chemicals are additional fields.

UV-vis-DRS usually contain a lot of low energy d-d, f-f transitions, and metal-metal charge transfer. There are two types of electronic transitions. First class includes following metal-centered (MC) transition; (1) $d \rightarrow d$ and $(n-1) d \rightarrow ns$ in transition metals, (2) $f \rightarrow f$ and $4f \rightarrow 5d$ in rare earth element, and (3) $ns \rightarrow np$ in main group elements. The second group involves charge transfer (CT) transitions from an occupied level centered on the donor atom to a vacant one centered on acceptor. This includes; (1). Ligand-to-metal (LMCT) and metal-to-ligand (MLCT) charge transfer. (2). Metal-to-metal charge transfer (MMCT) commonly known as the intra-valence transition as reported in the case of Fe_2O_3 ($Fe^{2+} \rightarrow Fe^{3+}$) or CeO_2 ($Ce^{3+} \rightarrow Ce^{4+}$). (3). Transition between molecular orbital ($n \rightarrow \pi^*$, $\pi \rightarrow \pi^*$) in inorganic or organic molecules or ions known as intra-ligand or ligand-centered (LC) charge transfer. Transitions of both classes occur in catalytic materials like zeolites.¹³⁻¹⁴

The diffuse reflectance UV-visible spectroscopy was performed over an *Ocean optics AD-2000* spectrometer (200-900 nm) with CC detector. The spectra were taken in the *absorption* mode under atmospheric pressure and room temperature.

VI. Nuclear Magnetic Resonance Spectroscopy (NMR)

NMR spectroscopy is one of the most recent techniques to be developed. With in a very short time of its discovery, it has emerged as a powerful tool for the elucidation of molecular structure and properties. The general approach applies to any NMR experiment irrespective of whether liquid or solid are studied. However, the origin and characterization of internal interactions which greatly affect the features of NMR spectra are quite different

for liquids and solid samples. The dominant structure-dependent interactions, which contribute to the shape and position of the NMR lines of solids, are;¹⁵⁻¹⁷

-) Dipolar interactions
- i) Chemical shift interactions
- ii) Quadrupolar interactions for nuclei with $I > \frac{1}{2}$.

These interactions are closely related to the structural environment of the nucleus under investigation, they are the main source of structural information from solid state NMR. However, the above interactions are responsible for considerable line broadening in NMR spectra of solids that may lead to serious problems in attaining sufficient spectral resolution. The reason for line broadening is that all the above interactions are anisotropic, i. e. depend on their orientations relative to the direction of magnetic field, B_0 . Therefore the shape and position measured by NMR lines depend strongly on the orientation of the nuclear environment, which defines the direction of the internal interactions. In liquids, the direction dependency is averaged by fast thermal motions of the molecules, and sharp lines are usually observed. Hence the spectra of polycrystalline samples are characterized by broad superposition of resonances arising from different orientations of crystallites, weighed by statistical probability with which each orientation may occur. The superposition of wide distribution of interactions of different strengths and their random orientation usually give rise to broad signals without characteristic shapes.¹⁷

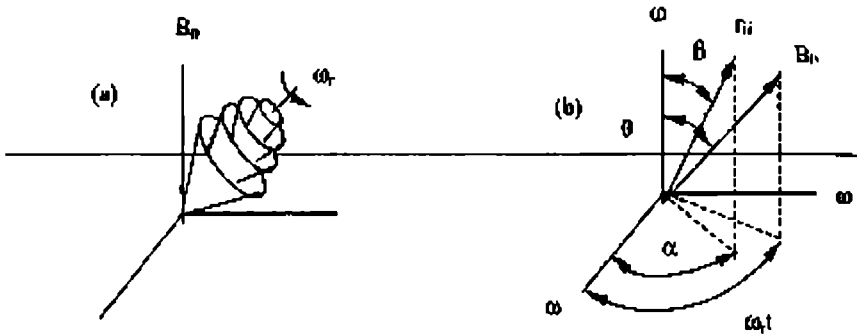
Various spin interactions result in the appearance of broad powder patterns. Thus for the measurement of well resolved NMR spectra of powder with individual resonance lines for inequivalent nuclei, special techniques have to be applied to remove or at least to reduce substantially the line broadening effects. The most important techniques are;

-) Dipolar decoupling, (ii) Magic angle spin, and (iii) Double oriented rotation (DOR).

Magic angle sample spinning

We know from the previous section that the line broadening in spin-1/2 solids mainly comes from the following anisotropic internal interactions: (1) Direct (homonuclear and heteronuclear) dipolar interactions, (2) Electron shielding interactions such as chemical shift. Below we will discuss the effect of MAS on each of them.

Figure 2.1. Schematic representation of magic angle sample spinning. (a) The unique internuclear vector r_{ij} moves along a cone whose axis is always inclined at θ relative B_0 . (b) r_{ij} and B_0 viewed in the rotor frame $[x]-[y]-[z]$.



The procedure of this technique consists of rotating the solid specimen about an axis inclined at the angle 54.7° to the direction of the magnetic field of the NMR magnet. Sufficiently rapid rotation about this particular axis removes most broadening interactions from the NMR spectra and gets the liquid-like high resolved NMR spectra. Magic angle spinning may be used on its own, and may also be combined with other line-narrowing techniques. For example, it may be combined with multiple pulse sequence (CRAMPS) to obtain high resolution NMR spectra, especially of hydrogen and fluorine nuclei, in solids; it may be combined with cross-polarization and high power heteronuclear decoupling methods to obtain the high resolution spectra from ^{13}C , ^{29}Si and other nuclei of low abundance. Of most importance in this dissertation is the combination with multiple quantum NMR spectroscopy.

Heteronuclear dipolar decoupling

Heteronuclear dipolar interactions between a nucleus A and another nucleus of the type B can be removed by irradiation of a strong rf field at the resonance frequency of the nucleus of the nucleus B, while measuring the spectrum of nucleus A. High power decoupling is widely used to remove the line broadening effects due to heteronuclear dipolar interactions with protons in the NMR spectra of compounds containing protons. Some prominent examples include; ^{13}C - ^1H interaction in organic molecules bonded to catalyst surface or ^{29}Si - ^1H interactions of surface SiOH groups and ^{27}Al - ^1H in aluminosilicates.¹⁵⁻¹⁶

Solid-state NMR experiments were acquired at 7.1 T with a Bruker DSX-300 spectrometer at 308 K. For all the experiments a standard 4 mm double bearing cylindrical Bruker probe was used. The detailed experimental parameter set-up is given in Table-2.3. XWINNMR software operating in a Unix environment on a Silicon graphic computer was employed to acquire and retrieve the data. Appropriate numbers of scans were accumulated to get a satisfactory signal to noise ratio. Detailed experimental conditions applied for various MAS NMR experiments are depicted in the Table below.

Table 2.3. Experimental conditions for different NMR experiments

Experimental parameter	^{27}Al	^{29}Si	^{23}Na	^1H
Effective Field (MHz).	78.19	59.63	79.97	300.00
Sample rotation frequency (kHz).	7	7	8	9
Pulse length (ms).	10	4	5.5	5
Pulse delay (sec.).	2	5	0.5	0.5
Internal standard.	$\text{Al}(\text{NO}_3)_3$	TMS	NaCl	TMS
Average number scans collected.	2000	3000	1200	200

VII. Surface Area and Pore Volume Measurements

The accessibility of catalyst surface to a reacting molecule is of considerable importance in the selection of a solid material, which is to function as an active catalyst for heterogeneous reaction. For a given catalyst, the greater amount of surface available to the reacting molecule, the better is the conversion to product. Very few catalyst preparation have the surface which are energetically homogeneous in the sense that all adsorption sites are equivalent and since the amount of energy is exchanged between each molecule of adsorbate and adsorbent site. If such a catalyst could be prepared then the activity would be directly proportional to the surface area exposed to the adsorbing gas.

Consistent with the definition given by *International Union of Pure and Applied Chemistry* (IUPAC), surface area is defined as the extent of total surface area as determined by given method under stated conditions.¹⁸⁻¹⁹ Despite its theoretical limitations, the Brunaur-Emmett-Teller (BET) method continues to be widely used for the evaluation of surface area from physisorption isotherm data. There are two stages in the application of BET procedure.

(1) It is necessary to derive the monolayer capacity n_m^a , defined as the amount of adsorbate required to complete a monolayer on unit mass of the adsorbent. The specific surface area a_s (BET), is then obtained from n_m^a by taking a value for the average area a_m , occupied by the adsorbate molecule (i. e., the monolayer cross-sectional area) in the filled monolayer.

Thus; a_s (BET) = $n_m^a \times L \times a_m$; where L is Avogadro constant.

In its original form, BET theory involved an extension of kinetic model of Langmuir to multilayer adsorption. It was postulated that under the steady state conditions of dynamic equilibrium the rate of adsorption in each layer is equal

the rate of evaporation from the layer. It was assumed that the molecules in the first layer are located on a set of equivalent surface sites and that these molecules are extended to the multilayer, which is composed of stacks of molecules. No allowance was made for the adsorbate-adsorbent interactions. To obtain a fairly simple equation, it is necessary to make the following assumptions;

- 1) In all layers after the first, the adsorption-desorption conditions are identical.
- 2) In all layers except the first the energy of adsorption is equal to the condensation energy. (3) When $p=p_0$, the multilayer has infinite thickness.

Based on these assumptions, Brunauer, Emmett and Teller arrived at the most useful form of equation.

$$\frac{p/p_0}{n^a (1-p/p_0)} = \frac{1}{n_m^a C} + \frac{C-1}{n_m^a C} \frac{p}{p_0}$$

Where c is a constant and is related exponentially to the energy of first layer adsorption, but it is now accepted that its value simply gives an indication of the isotherm shape and order of magnitude of adsorbent-adsorbate interactions.²⁰

The surface area and pore volume measurements were measured by low temperature (liquid nitrogen temperature) adsorption using *Micromeritics Gemini* surface area analyzer. All the results were reproducible within an error limit of less than 5%.

2.5 Characterization of acid sites on zeolites

Temperature Programmed Desorption of Ammonia (NH₃ TPD)

Temperature programmed desorption (TPD) or thermal desorption spectroscopy (TDS) as it is also called, is particularly useful in surface science,

where one studies desorption of gases from single crystals and polycrystalline foils into vacuum.

The theory behind NH_3 -TPD experiment was adopted from that of the *flash-filament* experiment used in surface science.²¹⁻²³ There are two assumptions: first, no readsorption of ammonia takes place during desorption; second the ammonia molecules are absorbed on a homogeneous surface without interaction among adsorbed molecules. These assumptions presume that all molecules desorb with same activation energy. It is assumed that the intracrystalline catalyst surface is homogeneous and the amount of ammonia desorbed in the experiment is less than that required for monolayer coverage.

Before going into the details, some concepts and vocabulary concerning this technique should be clarified;

When a gas or vapour is brought into contact with a solid, the solid takes up part of it. The molecules that disappear from the gas either enter the inside of the solid, or remain on the outside attached to the surface. The former phenomenon is termed *absorption* (or dissolution) and the latter *adsorption*. When the phenomena occur simultaneously, the process is termed *sorption*. The solid that takes up the gas is called the *adsorbent*, and the gas or vapour taken up on the surface is called the *adsorbate*.

Molecules and atoms can attach themselves onto surfaces in two ways. In *physisorption* (physical adsorption), there is a weak van der Waals attraction of the adsorbate to the surface. The attraction to the surface is weak but long ranged and the energy-released upon accommodation to the surface is of the same order of magnitude as an enthalpy of condensation (on the order of 20 kJ/mol). During the process of physisorption, the chemical identity of the adsorbate remains intact, i.e. no breakage of the covalent structure of the adsorbate takes place.

In chemisorption (chemical adsorption), the adsorbate sticks to the solid by the formation of a chemical bond with the surface. This interaction is much stronger than physisorption, and, in general, chemisorption has more stringent requirements for the compatibility of adsorbate and surface site than physisorption. The chemisorption may be stronger than the bonds internal to the free adsorbate, which can result in the dissociation of the adsorbate upon desorption (dissociative adsorption). In some cases, dissociative adsorption can be greater than zero, which means endothermic chemisorption, although uncommon, is possible.

The basic experiment has two main parts:

- Adsorption of one or more molecular species onto the sample surface at a certain temperature
- Heating of the sample in a controlled manner (preferably so as to give a linear temperature ramp) whilst monitoring the evolution of species from the surface back into the gas phase with a gas analyzer.

The data obtained from such an experiment consists of the intensity variation of each recorded mass fragment as a function of time (temperature).

It must be pointed out that if adsorbate molecules do react on the surface of the sample, reaction products may also be detected.²⁵

- The area under a peak is proportional to the amount originally adsorbed, i.e. proportional to the surface coverage.
- The kinetics of desorption (obtained from the peak profile and the coverage dependence of the desorption characteristics) give information on the state of aggregation of the adsorbed species
- The position of the peak (the peak temperature) is related to the enthalpy of adsorption, i.e. to the strength of binding to the surface. The higher the temperature is, the stronger the binding.

The complete desorption analysis can be very complicated, so many authors rely on simplified methods to obtain certain parameters such as the activation energy of desorption. These methods make use of easily accessible spectra features (temperature of the peak maximum, half width at half maximum of the peak).²⁶

In this study, desorption of ammonia from pure and as-exchanged rare earth zeolites have been analyzed by TPD. Zeolite powder was pressed into small discs. These discs (0.5 g) were introduced in a *stainless steel 340* reactor connected to a flow apparatus, a furnace to heat up the samples, a thermocouple, and temperature controller. Before NH₃ adsorption, discs were pre-treated in synthetic pure nitrogen (50 ml/min) at 773 K for 1 hour. Afterwards, temperature was decreased to the adsorption temperature (room temperature). At this temperature, a flow of NH₃ is passed through the reactor and allowed to equilibrate for 3 hours and the granules were quenched to room temperature. Finally, the flow of nitrogen was switched on (10 ml/min) and temperature was increased from room temperature to 873 K at a rate of 12 K/min. The desorbed species (NH₃) were analyzed by a conventional gas analyzer.

II. Cracking of probe molecules (cumene)

The acid sites on molecular sieves have been studied extensively with physical and catalytic characterization techniques. These include IR spectroscopy, measurement of adsorption desorption properties of probe molecules such as ammonia, pyridine etc. Acid catalyzed reactions include selected cracking of organic molecules. The most commonly used catalytic test reactions for zeolites involve cracking of n-hexane²⁷ (a-test developed by Mobil Corporation), n-butane²⁸, (Union Carbide) and n-decane²⁹ (used as a catalytic

acid amount test as well as determining the porosity of microporous materials) and cumene.³⁰

It is generally believed that the cumene cracking reaction requires acid sites of medium strength, i. e., Brønsted acid sites (BAS) in the case of FAU-type of zeolites.³¹ The purpose of this study is to dissect the component reactions of hydrocracking process, and to correlate them with specific catalytic sites. The incentive of course is to be able to tailor individual catalysts explicitly to feed stocks and to the products required.

Catalytic reaction was carried out in a fixed-bed, down-flow reactor with 1.6 cm internal diameter and 30 cm height. Catalysts (500 mg) were activated at 773 K for 12 hours in presence of oxygen, allowed to cool to room temperature in dry nitrogen (10 mL/h) and then heated to reaction temperature where it was kept for one hour to stabilize. The reactant was fed into the reactor in presence of constant flow of dry nitrogen. Product was collected after the fourth hour (after undergoing some deactivation) and identification was done using gas injection method on a *Chemito 8610 Gas Chromatograph* fitted with a FID detector and SE-30 column (Column temperature 383 K, injector temperature and detector temperature was 503 K).

2.6. Alkylation of benzene with higher olefins (C₈, C₁₀, and C₁₂ olefins)

Catalytic ability of the prepared systems was tested for the alkylation of benzene with a series of higher olefins such as 1-octene, 1-decene, and 1-dodecene. The aim was to increase the selectivity for the most biodegradable *p*-phenylalkane. The process has been optimized with respect to catalyst loading, reaction temperature, reactant to substrate molar ratio, weight hourly space velocity (WHSV), and time on stream. The nature of carbonaceous compounds inside the zeolitic pores and cages was also monitored during the reaction.

The catalytic experiments were carried out at atmosphere pressure in a flow type reactor equipped with a fixed bed-down flow reactor with a high sensitivity temperature controller (accuracy ± 5 K). Nitrogen was used as carrier gas in the reaction. The catalyst (1000 mg in the case of 1-octene and 1500 mg in case of 1-decene and 1-dodecene) was pressed binder free between ceramic beads in the reactor. Prior to alkylation reaction, the catalysts were heated in situ with a heating rate of 20 K/min to the final temperature of 773 K in presence of constant purging of air and kept over night at this temperature. The catalyst was then allowed to cool to reaction temperature (448 K) in dry nitrogen (10 mL/h) and kept for an hour to stabilize. Benzene (*SD Fine Chemicals*, India used after washing with sulfuric acid and 20% Na_2CO_3) and 1-alkene (purity 98% supplied by *Sigma-Aldrich* USA was used without further purification) in appropriate molar ratio was fed into the reactor at flow rate of 4mL/h (WHSV=3.46, 2.46, 2.45 h^{-1} or contact time=0.289, 0.407, and 0.408 h respectively for three 1-alkenes) by means of an infusion pump. The rate of product withdrawal was brought into equilibrium with the reactant introduction by controlling the pilot valve at the bottom of the reactor. Periodically samples of the stream were analyzed using a *Chemito* GC1000 Gas Chromatograph fitted with a FID detector and SE-30 capillary column. Column temperature was adjusted between 383 K and 548 K, injector temperature was 523 K and detector temperature was 523 K. Isomer determination was done using a *Shimadzu QP 2010-* GCMS with 30 m universal capillary column of cross-linked 5 % phenylmethylsilicone. The MS detector voltage was 1 kV. The m/z values and relative intensity (%) are indicated for the significant peaks. (Column temperature; 323-533 K and heating rate was 10 K/minute, injector; 513 K and detector; 563 K).

References

- F. Roessner, K. H. Steinberg, H. Winkler, *Zeolites* Vol. 7 (1987) 47.
- P. K. Dutta, R. E. Zaykoski, *Zeolites* Vol. 6 (1986) 423.
- K. Becker, K. H. Steinberg, H. Bremer, V. Kanazirev, ch. Dimitrov, K. Nestler, M. Ch. Minacev, *Chem. Tech.* 23 (1981) 296.
- M. Weihe, M. Hunger, M. Breuninger, H. G. Karge, J. Weitkamp, *J. Catal.* 198 (2001) 256.
- K. Gaare, D. Akporiya, *J. Phys. Chem. B.* 101 (1997) 48.
- R. Carvajal, P. J. Chu, J. H. Lunsford, *J. Catal.* 125 (1990) 123.
- M. Hunger, G. Engelhardt, J. Weitkamp, *Micropor. Mater.* 3 (1995) 497.
- R.A. Jonathan, N. Pervaiz, A.K. Cheetham, M.W. Anderson, *J. Am. Chem. Soc.* 120 (1998) 10754.
- A. K. Datye, "Electron Microscopy and Diffraction" in *Handbook of Heterogeneous Catalysis* (Ed. G. Ertl, H. Knozinger, J. Weitkamp) Vol. 2, Wiley VCH, (1999) p.497.
0. C. Suryanarayana, M.G. Norton, "X-Ray Diffraction- A Practical Approach", Plenum Press, New York & London 1998, p. 97.
1. G. Bergeret, "Structure and Morphology" in *Handbook of Heterogeneous Catalysis* (Ed. G. Ertl, H. Knozinger, J. Weitkamp) Vol. 2, Wiley VCH, (1999) p.464.
2. J. W. Neimantsverdriet, "Spectroscopy in Catalysis- An Introduction", VCH Verlagsgesellschaft, D-69451, Weinheim, Germany (1995) p. 194.
3. G. Blasse, *Struct. Bond.* 76 (1991) 153.
4. G. Moretti, "Valence States, Redox Properties" in *Handbook of Heterogeneous Catalysis* (Ed. G. Ertl, H. Knozinger, J. Weitkamp) Vol. 2, Wiley VCH, (1999) p.641.
5. M. Mehring, "Principles of High Resolution NMR in Solids", Springer-Verlag, Berlin (1983) p. 1.
6. C. A. Fyfe, "Solid State NMR for Chemists" CFC Press, Guelph (1985) p.1
7. G. Engelhardt, "Solid-State NMR" in *Handbook of Heterogeneous Catalysis* (Ed. G. Ertl, H. Knozinger, J. Weitkamp) Vol. 2, Wiley VCH, (1999) p.525.
8. J. Haber, *Pure Appl. Chem.* 63 (1991) 1227.
9. J. Rouquerol, D. Avnir, C. W. Fairbridge, D. H. Everett, J. M. Haynes, N. Pemicone, J. D. F. Ramsay, K. S. W. Sing, K. K. Unger, *Pure Appl. Chem.* 66 (1994) 1739.
0. S. Brunauer, P. H. Emmett, E. Teller, *J. Am. Chem. Soc.* 40 (1938) 309.

21. Y. Amemomia, R. J. Cvetanoic, *J. Phys. Chem. B.* 67 (1963) 144.
22. R. J. Cvetanoic, Y. Amemomia, *Catal. Rev.* 6 (1972) 21.
23. R. J. Cvetanoic, *Am. Chem. Soc. National Meeting*, Boston, 1972.
24. V. Amemomia, *Chemtech.* 128 (1976).
25. J. W. Neimantsverdriet, "Spectroscopy in Catalysis- An Introduction", VCH Verlagsgesellschaft, D-69451, Weinheim, Germany (1995) p. 11.
26. C. V. Hidalgo, H. Itoh, T. Hattori, M. Niwa, Y. Murakami, *J. Catal.* 85 (1984) 362.
27. P. B. Weisz, J. N. Miale, *J. Catal.* 4 (1965) 527.
28. W. W. Kaeding, C. Hu, L. B. Young, S. A. Butter, *J. Catal.* 69 (1981) 392
29. J. A. Martens, M. Tielen, P. A. Jacobs, J. Weitkamp, *Zeolites* 4 (1984) 98.
30. J. T. Miller, P. D. Hopkins, B. L. Meyers, G. J. Ray, R. T. Roginski, G. W. Zajac, N. H. Rosenbaum, *J. Catal.* 138 (1992) 115.
31. S. J. Decano, J. R. Sohn, P. O. Fritz, J. H. Lunnford, *J. Catal.* 101 (1986) 132.

Chapter 3

Zeolite Characterization

*An experiment is a question which science poses to Nature,
and the measurement is the recording of Nature's answer"*

-Max Plank

Catalyst characterization is a lively and highly relevant discipline in catalysis. In general it deals with the Material Science of Catalysis at a microscopic level or on the atomic scale. The catalytic properties of surface are determined by its composition and structure on an atomic scale. Hence it is not sufficient to know that the surface consists of a metal and a promotor, say iron and potassium or iron and molybdenum, but it is essential to know the exact structure of the catalyst surface, ranging from structural defects and exact position of the promotor atoms. Thus, from a fundamental point of view, the ultimate goal of a catalyst characterization should be a look at the surface atom by atom, and under specific reaction conditions. The well-defined surfaces of single crystals offer the best perspectives for an atom-by-atom characterization. Although occasionally atomic scale information can be obtained from real catalysts under in situ conditions. There are several ways to obtain information on the physico chemical properties of materials. These methods of catalyst characterization vary widely in their complexity and sophistication. At one end of the scale we have such simple and inexpensive techniques as gas adsorption and sophisticated electron spectroscopic and microscopic techniques on the other. Here, in this chapter, we shall discuss some most commonly used physico chemical techniques in catalysis research for the atom scale characterization of the prepared zeolite systems.

3.1 Chemical composition (EDX)

Energy dispersive X-ray analysis was used to calculate the chemical composition of the parent, binder free Na-Y, K-Y, Mg-Y, and their corresponding rare earth exchanged zeolites. The unit cell composition of the zeolite samples are listed in Table-3.2 and 3.2. The degree cation exchange was taken from the chemical analysis of the solid phase.

Table 3.1. Chemical compositions of pure H-Y, binder free Na-Y and various as exchanged rare earth zeolites.

Zeolite	Chemical composition ¹	Silica-alumina ratio ¹	Degree cation exchange (%) ¹
H-Y	H _{76.5} Al _{76.5} Si _{115.5} O ₃₈₄	1.5	-
Na-Y	Na _{78.5} Al _{78.5} Si _{113.5} O ₃₈₄	1.5	-
CeNa-Y	Ce _{10.7} Na _{44.3} Al _{76.4} Si _{115.6} O ₃₈₄	1.5	44.8
LaNa-Y	La _{10.5} Na _{45.0} Al _{78.5} Si _{115.5} O ₃₈₄	1.5	42.7
RENa-Y ²	La _{9.38} Ce _{1.21} Pr _{2.72} Nd _{3.10} Na _{27.27} Al _{78.5} Si _{115.5} O ₃₈₄	1.5	64.3
SmNa-Y	Sm _{12.9} Na _{39.8} Al _{78.5} Si _{115.5} O ₃₈₄	1.5	49.3

Note: ¹ As determined by Energy Dispersive X-ray analysis. ² RENa-Y is a mixed rare earth exchanged zeolite with La³⁺ as the main counter cation and small amounts of Ce³⁺, Pr³⁺ and Nd³⁺ etc. * All results are reproducible within an error limit of 5%

Table 3. 2. Chemical compositions of pure H-Y, binder free K-Y and Mg-Y, their various as-exchanged rare earth zeolites.

Zeolite	Chemical composition ¹	Silica-alumina ratio ¹	Degree cation exchange ¹
H-Y	H _{76.5} Al _{76.5} Si _{115.5} O ₃₈₄	1.5	-
K-Y	K _{74.09} Al _{74.09} Si _{117.91} O ₃₈₄	1.5	-
CeK-Y	Ce _{15.06} K _{30.78} Al _{76.25} Si _{115.57} O ₃₈₄	1.5	59.7
LaK-Y	La _{14.94} K _{31.43} Al _{76.25} Si _{115.75} O ₃₈₄	1.5	58.8
REK-Y ²	La _{10.01} Ce _{1.92} Pr _{3.31} Nd _{4.81} K _{15.27} Al _{75.42} Si _{116.58} O ₃₈₄	1.5	79.8
Mg-Y	Mg _{38.29} Al _{76.58} Si _{115.42} O ₃₈₄	1.5	-
CeMg-	Ce _{13.38} Mg _{17.74} Al _{75.62} Si _{116.38} O ₃₈₄	1.5	76.5
LaMg-Y	La _{13.08} Mg _{18.51} Al _{76.25} Si _{115.75} O ₃₈₄	1.5	75.7
REMg- ²	La _{9.98} Ce _{2.52} Pr _{4.21} Nd _{4.91} Mg _{13.68} Al _{75.78} Si _{116.22} O ₃₈₄	1.5	81.9

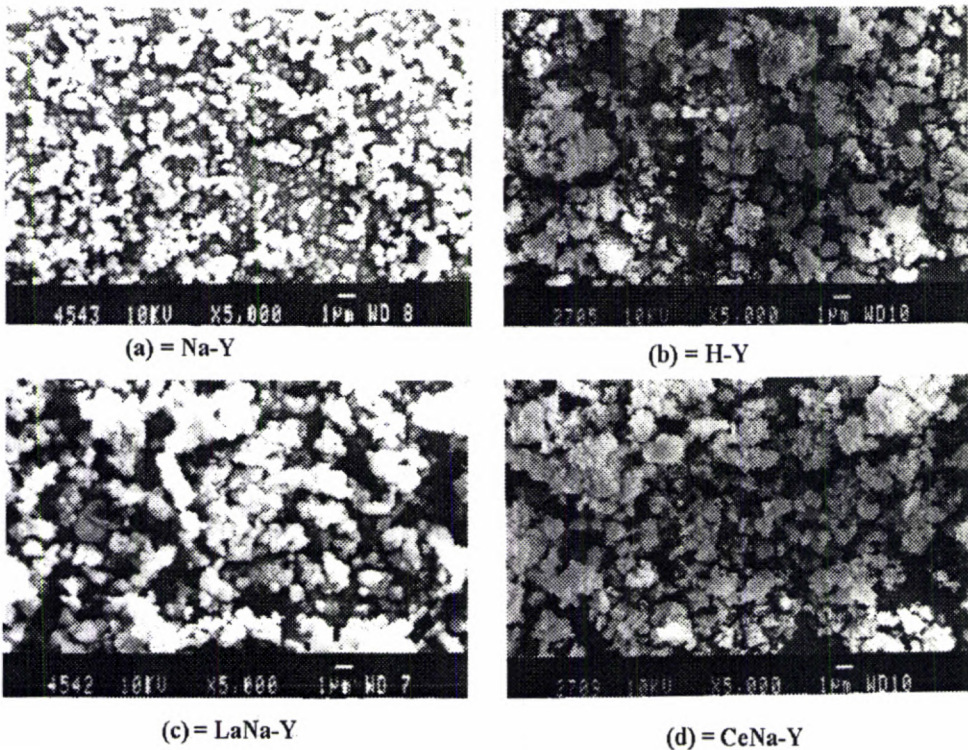
Note: ¹ As determined by Energy Dispersive X-ray analysis ² RENa-Y is a mixed rare earth exchanged zeolite with La³⁺ as the main counter cation and small amounts of Ce³⁺, Pr³⁺ and Nd³⁺ etc. * All results are reproducible within an error limit of 5%

3.2 Surface morphology (SEM)

In SEM, the image is obtained by scanning a finely focused probe in a raster pattern on the zeolite surface in synchrony with raster scan on a cathode ray tube (CRT). The emitted signals such as back scattered and secondary electrons are detected and are used to form images by modulating the brightness on the CRT. The magnification was determined by the ratio of the area scanned to the display area of the zeolite sample.¹⁻² Figure 3.1 depicts the scanning electron micrographs of representative samples recorded with a field emission gun; (a) binder free Na-Y, (b) pure H-Y, and as-exchanged CeNa-Y and LaNa-Y zeolites. The crystallites exhibit uniform morphology in the size range 80 – 100 nm with little twinning and intergrowth. It is seen that there is

significant decrease in the particle size of the materials on ion doping. The average particle size of H-Y zeolite is 100 nm and is decreased to around 80 nm on sodium and subsequent rare earth exchange. Despite this, the micrograms are seemed to be not well-resolved. Also, the particles seem to undergo agglomeration.

Figure-3.1. SEM micrograms of the pure H-Y, binder free Na-Y, and as-exchanged LaNa-Y and CeNa-Y zeolites.



The exact morphology determination was difficult due to the rather smaller particle size (in nanometer range). With the small zeolite particle (which might be agglomerated too), condense contrast that could be limiting the information that can be obtained by SEM. However, the major advantage of

Scanning electron micrographs is that bulk zeolite samples are studied. An average idea about the bulk morphology of the zeolite samples have been obtained from SEM studies.

3 Powder X-ray diffraction (PXRD)

X-ray powder diffraction patterns indicate uniqueness in structure, as they are fingerprints of individual zeolite structures. The powder patterns can also give information about crystallite size, percentage crystallinity, and incorporation of other elements into the framework. Of most of the zeolite and molecular sieve materials prepared, only a few have had their structures determined by single crystal technique. These include $AlPO_4$, clathrasils, zeolite-A and ZSM-5.³⁻⁶ Determining the structure from powder patterns always is met with many difficulties. Unresolved or overlapping peaks have resulted in poor data, impeding the attainment of reliable structure information.⁷ The Rietveld method has been most widely used as the refined procedure for structural studies from X-ray powder diffraction patterns of zeolites.⁸ The X-ray data include the relative intensity (I), which is based on the peak intensities relative to the strongest peak in the pattern ($I_0 = 100$).

Table 3. 3a. Results of XRD data indexing for pure H-Y, Na-Y, and as exchanged CeNa-Y and LaNa-Y zeolites

Sample	A	$h^2 + k^2 + l^2$	hkl	Bravais lattice.	Lattice parameter. $a = \lambda / 2(A)^{1/2}$ (nm)
a-Y	0.0044	6.4521	211	P	0.7380
-Y	0.0107	4.2500	200	P	1.1621
ceNa-Y	0.0101	0.3200	100	P	0.7667
laNa-Y	0.0082	0.3400	100	P	0.8504

continued in table-3.3b

From the earlier reports, it is clear that faujasite crystallizes with cubic unit cell with space group F3dm. The standard 'hand' method for calculating the unit cell parameters of a faujasite sample is,⁷

$$a = \lambda/2 (A)^{1/2}$$

Also, a quantitative measure of the percentage crystallinity of a zeolite is made by a summed height of approximately eight peaks in the X-ray diffraction pattern. The percentage crystallinity is taken as the sum of the peak heights of the unknown material divided by the sum of the peak heights of a standard material that has been designated as 100% crystalline.⁹ Indexing of the XRD data from the patterns of the samples confirm the lattice to be primitive. Table - 2 and Figure - 3 show the results of XRD analysis for representative samples and the patterns obtained by performing indexing of XRD data using a common Experimental Module taking $\lambda = 1.5406 \text{ \AA}$.⁷

Table 3. 3b. Results of XRD data indexing for pure H-Y, Na-Y, and as exchanged CeNa-Y and LaNa-Y zeolites

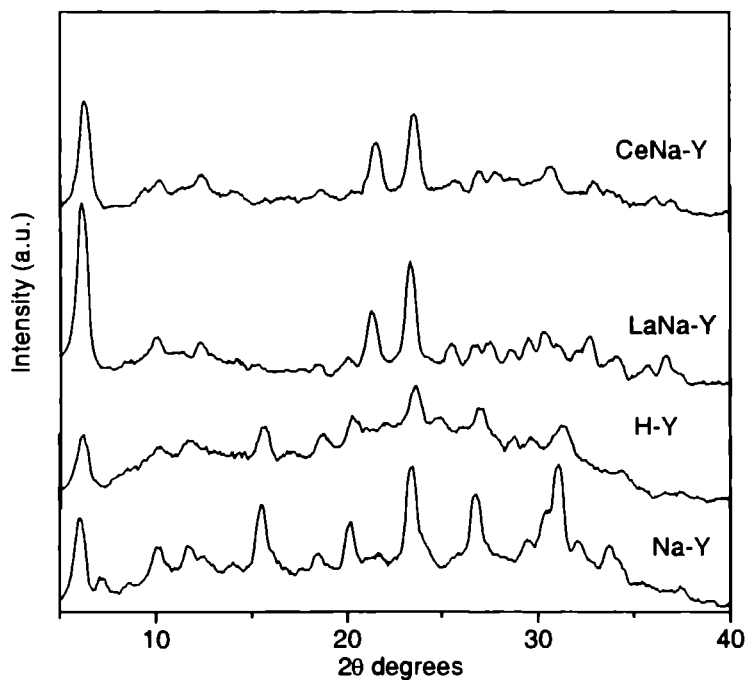
Sample	Lattice Constant. $d = \frac{a}{(h^2+k^2+l^2)^{1/2}}$ nm	Unit cell Volume. $V=a^3 (\text{\AA})^3$ (nm ³)	Crystallite size (D). $K \lambda / \beta \cos \theta$ (nm)	Crystallinity (%)	Space Group.
Na-Y	0.295	0.4020	23.44	100.00	F3dm
H-Y	0.564	1.5694	15.01	74.60	F3dm
CeNa-Y	1.355	0.4507	17.91	77.50	F3dm
LaNa-Y	1.4586	0.6150	22.40	98.50	F3dm

Percentage crystallinity of samples decreases in the order Na-Y > LaNa-Y > CeNa-Y > H-Y. This is due to the decrease in the electropositivity of the counter cation. Unit cell volume and lattice parameter of the samples decrease when sodium is exchanged with other cations like lanthanum and cerium. The

Crystallite size of the samples is in the order, Na-Y > LaNa-Y > CeNa-Y > H-Y. This is exactly the order of electronegativity decrease and hence the crystallite size decreases as the electronegativity of the counter cation decreases.

Thus the XRD patterns of the pure H-Y, Na-Y, and various rare earth exchanged zeolites confirm the stability of the framework towards the ion exchange method of catalyst preparation and subsequent high temperature calcinations. Infrared spectroscopy (section 3.4) in the framework region ($400-1300\text{ cm}^{-1}$) also supports this observation. Therefore we concluded

Figure 3.2. X-ray diffraction pattern of parent Na-Y zeolite and of the as-exchanged zeolites CeNa-Y and LaNa-Y recorded in the 2θ range of 5 to 40 degrees.



That the zeolite framework remains undamaged during ion exchange. Along similar lines, it can be assumed that other zeolites like binder free K-Y, Mg-Y

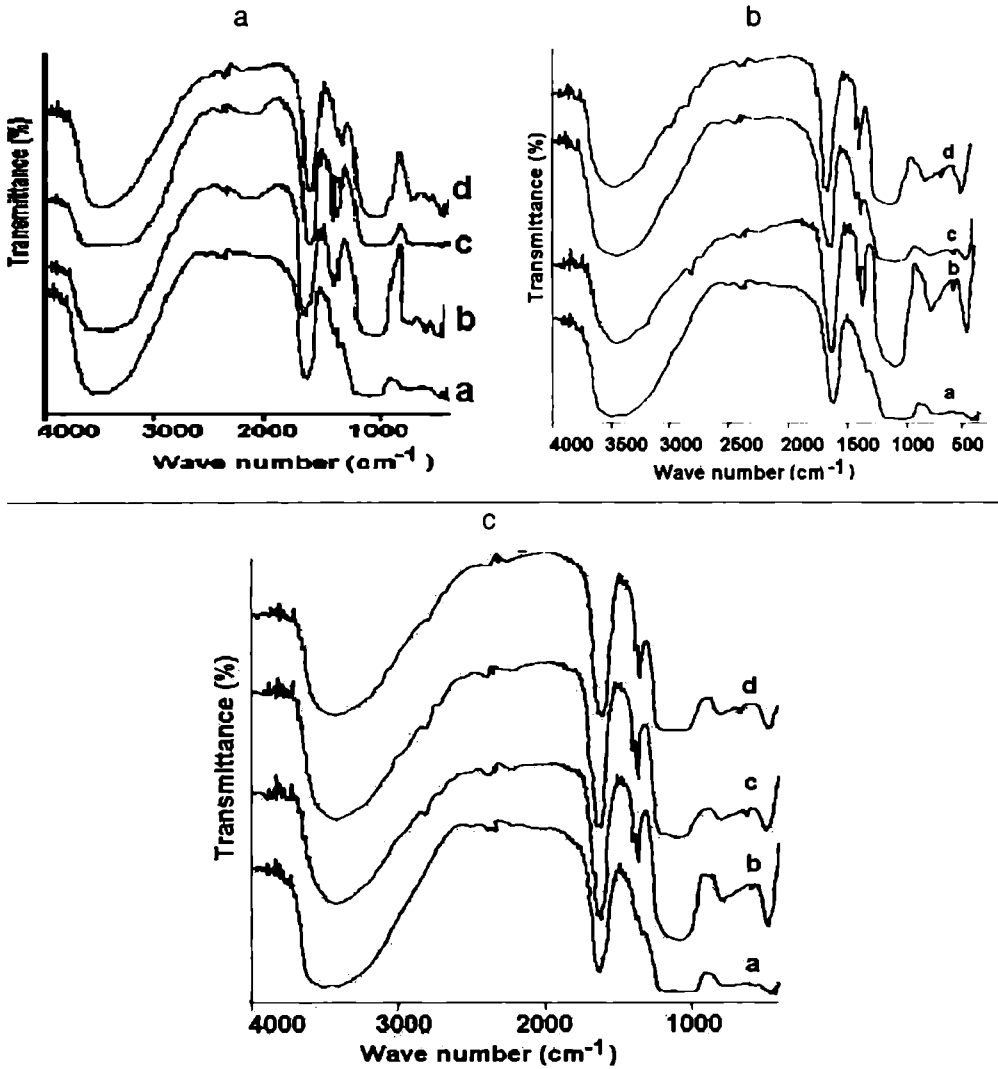
and their rare earth doped forms also have the X-ray diffraction patterns consistent with simple cubic crystal structure.

3.4 Vibrational spectral studies (IR)

Though X-ray diffraction is most widely used for the identification of zeolite structure types, other techniques have provided useful information as well. Perhaps, IR can give information about the structural details of the material. In addition, it is used to confirm the acid characteristics and isomorphous substitution.¹⁰ In recent years a number of aluminosilicates, including tecto-aluminosilicates have been investigated by IR spectra.¹¹⁻¹⁵ Fourier Transform infrared spectroscopy show bands characteristic of faujasite type of zeolites both in the framework ($400-1300\text{ cm}^{-1}$) and hydroxyl regions ($3000-4000\text{ cm}^{-1}$).¹¹⁻¹³ The framework region ($400-1300\text{ cm}^{-1}$) FTIR is a sensitive tool to indicate structural changes after sodium, potassium, magnesium, and rare earth exchange and the spectra of original Na, K, and Mg zeolites and their corresponding rare earth metal derivatives are displayed in Figure 3.3. The IR assignments for each framework bands are indicated in Table 3. 4.

Each zeolite appears to exhibit a typical IR pattern. In general the spectra can be divided into two classes; (1) those due to internal vibrations of the TO_4 tetrahedra which is the primary unit of the structure and which are not sensitive to other structural vibrations, and (2) vibrations which may be related to the linkages between tetrahedra.¹³ Class two vibrations are sensitive to the other overall structure, individual tetrahedra, in secondary structural units as well as their existence in the larger pore opening. Individual assignments to specific TO_4 tetrahedra are not possible. However, the vibrational frequencies represent the average composition. Typical IR spectra of different zeolites are given in Figure 3.3.

Figure 3.3. Vibrational spectra of various zeolite samples taken in the transmittance mode in the wave number range of 400-4000 cm^{-1} . 1. (a) H-Y, (b) Na-Y, (c) CeNa-Y, and (d) LaNa-Y. 2. (a) H-Y, (b) K-Y, (c) CeK-Y, and (d) LaK-Y. 3. (a) H-Y, (b) Mg-Y, (c) CeMg-Y, and (d) LaMg-Y.



From Figure 3.3 and Table 3.4, it is clear that the framework consists of strong vibration in the 1050-1100 cm^{-1} and a strong band around 450-490 cm^{-1} . These are assigned to the internal tetrahedral vibrations. The band around 1050 cm^{-1} is assigned to T-O asymmetric stretch. The next strong band is around 450 cm^{-1} region and is assigned to T-O bending. T-O stretching modes involving mainly the tetrahedral atoms are assigned in the region 750-800 cm^{-1} as shown in Table 3.4 and Figures 3.2.1, 3.2.2, and 3.2.3. The stretching modes are highly sensitive to the Si-Al composition of the framework and may shift to lower frequency with increasing the number of tetrahedral aluminium atom. However, above mentioned bending mode is not very sensitive.

Table 3. 4. IR spectral assignments of parent H-Y, binder free Na-Y, K-Y, Mg-Y, and their corresponding cerium and lanthanum doped derivatives.

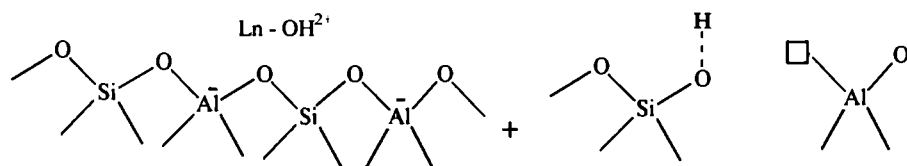
Zeolite	Assymmetric stretch (cm^{-1}) EL or IT ¹	Symmetric stretch (cm^{-1}) EL or IT ¹	Double ring ² (cm^{-1})	T-O bend ³ (cm^{-1})
HY	1050	771	570	457
Na-Y	1058	791	571	460
CeNa-Y	1078	777	578	468
LaNa-Y	1078	767	573	458
K-Y	1059	772	573	466
CeK-Y	1093	793	579	483
LaK-Y	1062	772	575	467
Mg-Y	1067	777	579	466
CeMg-Y	1087	787	580	472
LaMg-Y	1100	782	578	472

Note: ¹ EL, External linkage; IT, internal linkage. ² D₆R double ring units. ³ T= Si, Al.

The second group of frequencies which are sensitive to the linkages between tetrahedra, the topology and mode of arrangement of the secondary building units of the structure in the zeolites occurred around 550-600 cm^{-1} . In all the cases this band is around 570 cm^{-1} and is due to the presence of double

ings (D_6R) in the zeolitic framework structure. This confirms the presence of double rings or larger polyhedral units such as β -cages in the zeolite structure. bands of pore opening or pore motion ($300-420\text{ cm}^{-1}$) of the tetrahedral ring which form the pore opening in zeolites were not observed.¹⁶⁻¹⁸

The bands characteristic of the hydroxyl functions of the zeolites in the region of the infrared spectra around 3000 cm^{-1} have been associated with the acid nature and related to the acid activities of the molecular sieves.^{13, 16-17} However, the samples examined must be rigorously dried and maintained in that condition during the acquisition of the data. In addition, KBr wafer of the approximately 5 mg material have been used to produce a reasonable quality spectra, However, despite these precautions IR spectra does not provide a well resolved spectra in the hydroxy region. A band around 3400 cm^{-1} is observed for all zeolite samples. Hence, it must be stated that IR does not provide valuable information on the nature of different hydroxyl moieties in the zeolite. But, the vibrations in the range of $3400-3700\text{ cm}^{-1}$ must be due to the hydroxyl groups associated with the Bronsted acid nature in rare earth zeolites.^{9, 13} Furthermore, for FAU type of zeolites, it is reported that the BAS hydroxyl band occurred around 3660 cm^{-1} .⁹⁻¹⁰ The nature of trivalent or divalent cation also influences the position of the OH vibration on the structural incorporation of that element.⁹

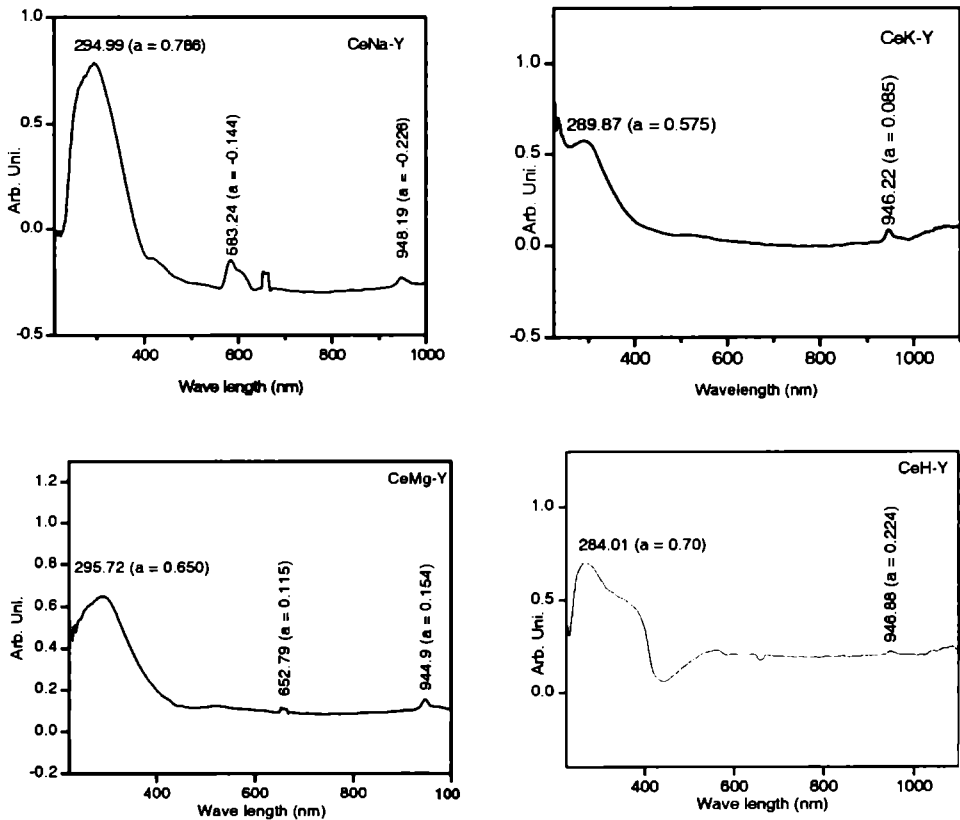


IR spectra thus confirm the presence of $[\text{Ln-OH}^{2+}]$ and $[\text{H}^+ \text{---} \text{O}^- \text{---} \text{Zeolite}]$ species after thermal treatment as shown in the above scheme. The acid hydroxyl groups are perturbed by the highly polarizing effect of rare earth cations in such a way as to increase the acid strength of the zeolite.

3. 5 UV-vis- diffuse reflectance spectroscopy

Figure-3.4 shows the UV-vis diffuse reflectance spectra of CeNa-Y, CeK-Y, CeMg-Y, and CeH-Y zeolites. These zeolites show a clear intense band around 300 nm with an absorbance greater than 0.55. A very small shoulder peak at 950 nm (absorbance < 0.22) is also observed for these samples. However, the peak in the low frequency range (around 300 nm)

Figure 3. 4. UV-Vis-Diffuse Reflectance Spectra of various cerium exchanged zeolites; CeNa-Y, CeK-Y, CeMg-Y, and CeH-Y in the range of 200-1000 nm.



is absent for other as-exchanged samples, whereas the higher frequency shoulder peak is observed for all rare earth zeolites around 950 nm (944.25 nm and 944.9 nm for LaK-Y and REK-Y respectively with absorbance 0.189 and 0.364). UV-vis-DRS is a sensitive method for the characterization of metal ion coordination on the zeolite surface. Position of the metal-to-ligand (MLCT), ligand-to-metal (LMCT) or metal-to-metal charge transfer spectra (MMCT) [eg. $f^2 \rightarrow Ce^{4+}$ or $Ce^{3+} \rightarrow Ce^{4+}$] depends on the ligand field symmetry of other metal ion.¹⁹⁻²¹ Depending on the coordination (or symmetry) and oxidation state of the metal ions, materials usually show two absorption bands; one at/ or around 300 nm and another around 400 nm. The electronic transition from cerium to oxygen require high energy for the tetra coordinated Ce^{4+} than the hexa coordinated one, i.e. the former at 300 nm is tetrahedrally coordinated metal center and the latter at 400 nm is due to hexagonally coordinated metal center.²² Therefore the absorption band centered around 300 nm for the CeK-Y zeolite is due to the presence of well-dispersed Ce^{4+} in a tetra-coordinated environment. This charge transfer peak is possible due to presence of the oxidizability in the oxidation state of cerium, ($Ce^{3+} \rightarrow Ce^{4+}$). Other as-exchanged samples do not show charge transfer bands predominantly due to the lack of oxidizable oxidation states in the metal cation as in the case of cerium. However, in the low energy region they exhibit very small shoulder peaks due to less intense $f \rightarrow f$ transitions. These peaks (652.79 nm in the case of CeK-Y) are very weak as these transitions are usually only slightly sensitive to the surrounding and appear at about the same frequency as in the free ion. Its appearance as a narrow band, however, are excellent fingerprints of the rare earth ions in the zeolites.²³ UV-vis DRS confirms the presence only one type of well dispersed cerium species in the tetra coordinated atmosphere. Applying the same concept it can be induced that other rare earth cation (La^{3+} , RE^{3+} etc)

too are present in a tetra-coordinated ligand field, which is the potential active site for the reaction

3.6 MAS Nuclear magnetic resonance studies

I. ^{23}Na MAS NMR

The determination of the cation distribution has involved a number of techniques ranging from X-ray and neutron diffractions, infrared spectroscopy etc. However, with diffraction techniques, stationary cations can be located, and only half of the cations can often be located for zeolite samples. IR too can provide limited information on cation distribution in zeolites.²⁴⁻²⁵ High field ^{23}Na NMR is applied widely for the correct determination cation distribution in zeolites²⁶⁻²⁸ The quantitative evaluation of ^{23}Na MAS NMR spectra allows one to determine the population of different cation sites. Welsh and Lambert observed two lines in the ^{23}Na MAS NMR spectrum; one at -9 ppm which is assigned to sodium cations in the large cavities on cation position SII and non-localized sodium cation in the large cavities. Second one at -13 ppm was assigned to sodium cations located on cation position SI' in the sodalite cages.²⁹ However, Bayer et al. attributed the line at -9 ppm to hydrated sodium ions on position SI' and SII'.³⁰ A line at 5.5 ppm occasionally observed in the spectra of hydrated lanthanum exchanged faujasite zeolite is ascribed to sodium cations in hexagonal prisms (SI). Challoner and Harris observed line in the static spectra of hydrated Na-Y, which they assumed to be due to the satellite transitions ($\pm 1/2 \leftrightarrow \pm 3/2$) of sodium nuclei undergoing isotropic tumbling.³¹

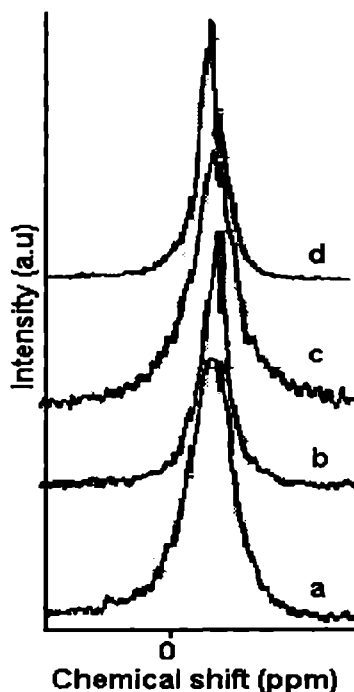
^{23}Na NMR spectra of Na-Y and different as-exchanged zeolites calcined at 773 K are shown in Figure 3-5. ^{23}Na NMR spectra of dehydrated RE-Y zeolites give three peaks at chemical shift values -13 , -31 and -63 ppm. Engelhardt et al. proposed the peak at 13 ppm is due to Na cations located at the center of the hexagonal prisms on position SI or SII of the sodalite cages,

which will be a low field Gaussian line (GL).³² Even at 773 K the Na cations will not be fully dehydrated and the simulation of ^{23}Na NMR spectra of dehydrated samples may have an additional line at -24 ppm, which has been assigned to the incompletely dehydrated Na cations. Sodium cations located close to the center of six membered ring window on position SI' and SII show a high field (-61 ppm) quadrupole pattern (QP) with a quadrupole frequency of $\nu_q = 2.1$ MHz, an asymmetry parameter of $\eta = 0.25$ and an isotropic chemical shift of -8 ppm.³³ Massiot et al. identified the contribution of this QP line to the central peak as 16%. The non-localized Na^+ ions in the large cavities of the faujasite are observed at an NMR shift of -9 ppm.³⁴ The peak at -13 ppm was found to be caused by two components, the component that is characterized by a quadrupolar interaction causing a field dependent shift and a signal at $\nu = 2\nu_H$ in the two dimensional quadrupolar nutation spectra is attributed to Na^+ enclosed in the sodalite cages. All the base exchanged samples exhibit a single peak between -8.95 and -10.57 ppm.

The absence of peak at -13 ppm suggest the absence of localized Na^+ ions in the sodalite cages of zeolite framework. The absence of peaks at -24 and -61 ppm confirm the non-existence of incompletely dehydrated Na^+ ion and sodium cation located close to the centre of six membered ring window on positions SI and SII.^{33, 36} A single peak at or around -9 ppm confirms that all the Na^+ ions in the samples are non-localized. Pure Na-Y shows a chemical shift of -10.57 ppm and all the base-exchanged forms show chemical shifts lower than this. These shifts in the peak positions can be explained by the electrostatic repulsive force between Na^+ ions and other bulky rare earth cations. The shift value of CeNa-Y and LaNa-Y are -10.55 and -8.95 ppm respectively. Ce^{3+} induced a very small difference in the peak positions from La-Y (0.02 ppm). The line width at half height (or full width half maximum, WHM), $\Delta\nu_{1/2}$, of the MAS spectra of Na-Y, CeNa-Y and LaNa-Y are 1062,

549.32 and 451 Hz respectively, which is much smaller than the spinning speed of 7 kHz in the MAS NMR experiments. As expected, the sodium- exchanged

Figure 3. 5. ^{23}Na MAS NMR spectra of (a) parent Na-Y zeolite and of the as-exchanged zeolites (b) CeNa-Y, (c) LaNa-Y, and (d) SmNa-Y zeolites recorded at a resonance frequency of 79.97 MHz with a sample spinning speed of 8 kHz.



form exhibits the maximum and the lanthanum the least width at half height. The large value of $\Delta\nu_{1/2}$ corresponds to large quadrupole interactions of its sodium nuclei. This increase of line width is probably due to a reduced mobility of either the sodium ions or water molecules in the zeolite. Similar to any other NMR experiments of the same samples, La^{3+} exchanged zeolite-Y shows unusual peak position and $\Delta\nu_{1/2}$. This rather complicated result could be explained using the migration probabilities of La^{3+} ions from the large cages to the small β - cages and preferential formation of Brønsted acidity in sodalite in

presence of more electropositive counter cations. This observation correlates well with the results obtained from ^{27}Al , ^{29}Si and acid amount determination experiments like TPD and thermodesorption studies.

^{27}Al MAS NMR

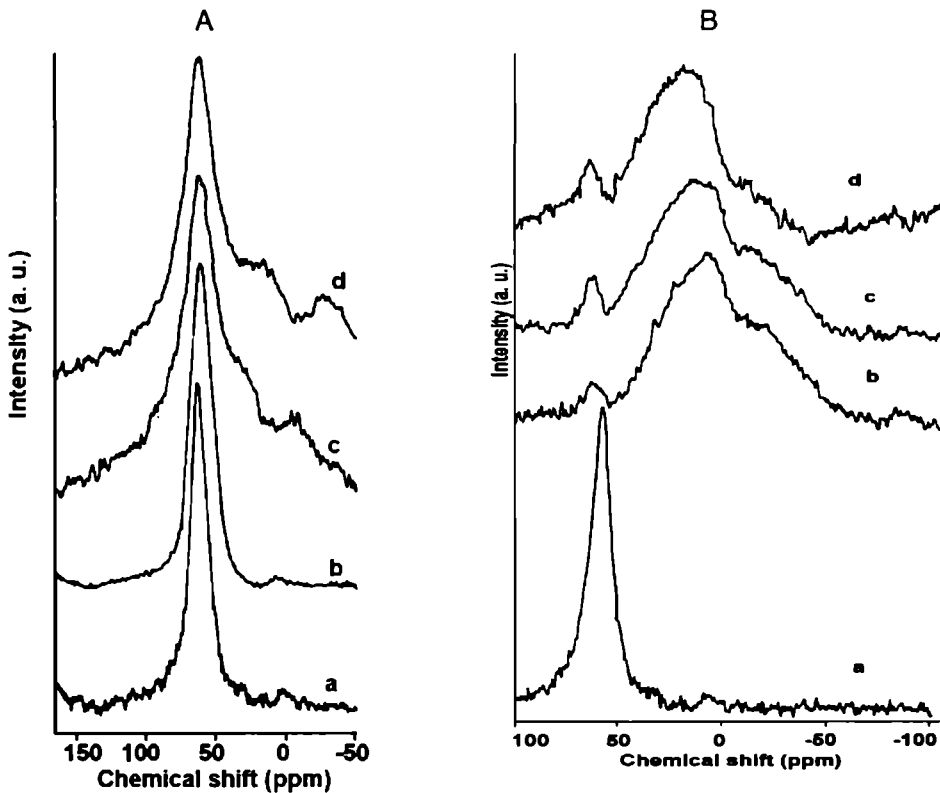
In principle, ^{27}Al is a favorable nucleus for NMR and it has 100% natural abundance with chemical shift range of about 450 ppm. ^{27}Al magic-angle spinning NMR spectroscopy is a unique technique providing direct information on the local environment of this nucleus in zeolite structure.^{33, 36-41} From ^{27}Al NMR data the discrimination between tetrahedral framework and octahedral non-framework species is possible. As the tetrahedral Al atoms and the associated hydroxyl protons constitute the active sites in many catalytic reactions, careful control and quantitative knowledge of Al concentration is highly demanding.⁴²⁻⁴⁴ ^{27}Al spectra of zeolites are, in general, much simpler than their ^{29}Si counterparts since according to Loewenstein's rule (which forbid AlOAl pairing) only one tetrahedral aluminium environment exists in the aluminosilicate framework. A narrow line at 60 ± 5 ppm is observed for tetrahedral aluminium in hydrated zeolites, indicating weak quadrupolar interactions due to distortion from tetrahedral symmetry of the framework AlO_4 environments. In contrast to the hydrated cation containing zeolites, very strong quadrupolar interactions were observed for ^{27}Al nuclei in Al-OH-Si sites of dehydrated hydrogen forms of zeolites, rendering these Al atoms "NMR invisible" in conventional ^{27}Al MAS NMR spectra due to excessive line broadening.⁴⁵⁻⁴⁶

The ^{27}Al MAS NMR spectra of calcined samples give rise to only one resonance peak around 60ppm due to aluminium in a tetrahedral environment, which is typical for zeolitic framework aluminum (Figures 3.6a. A, B and 3.6b. C and D). But, some samples show a small peak at 0 ppm, which is due to the extra framework octahedral aluminum formed by leaching during thermal

exchange. Absence of peak around 80 ppm confirm the lack of $\text{Al}(\text{OH})_4^-$ species. Perhaps, most of the zeolites show a peak around 30 ppm confirming the presence of penta-coordinated aluminium species. There is still some controversy on the nature of species that has chemical shift lying between tetrahedral framework aluminium and conventional octahedral non-framework aluminium. In fact the nature of this species can vary as a function of sample preparation. Gilson et al. proposed the formation of penta-coordinated aluminium species at a chemical shift of ~ 30 ppm.⁴⁷ Later studies by Ray and Samoson assigned 30 ppm peak to species such as that proposed by Gilson et. al.⁴⁸ It has been reported that the ^{27}Al NMR spectroscopy of zeolites is sensitive to the oxygen coordination of aluminium atoms and to the strain of the framework AlO_4 tetrahedra.^{40, 43, 45, 49} The appearance of the broad line in the ^{27}Al MAS NMR spectrum is due to strain in the Al-O-T bonds caused by the presence of bulky or highly charged cations. This spectral broadening increases in the order of $\text{H-Y} < \text{Na-Y} < \text{K-Y} \cong \text{Mg-Y}$. A similar observation is seen in the case of rare earth exchanged forms. Broadening is caused by the distribution of chemical shifts due to aluminium atoms in the locality of strained (due to vicinity of heavy or bulky cations) and non-strained framework. Aluminium with spin 5/2 is involved in quadrupolar interaction with electric field gradients caused by the electric changes in the surrounding of the Al nuclei. These electric field gradients are small for symmetric charge distribution i.e., for fully hydrated and mobile Na, K or Mg cation in the large cavities. But, they are larger for non- symmetric charge distribution, eg., for residual cation located close to the centre- of six membered oxygen ring, such as position Si' in the sodalite cages.⁴⁷ The greater line width for K and Mg suggests a greater quadrupolar influence and enhanced probability of a residual cation being at or near to the small cage (Si'). Parent H-Y shows a chemical shift of 61.29 ppm. All other as- exchanged zeolite systems exhibit a chemical shift less than this

value. This shift in the peak position to high field region can easily correlated to the strain of the AlO_4 framework due to the presence of bulky or heavily charged counter/residual cations.

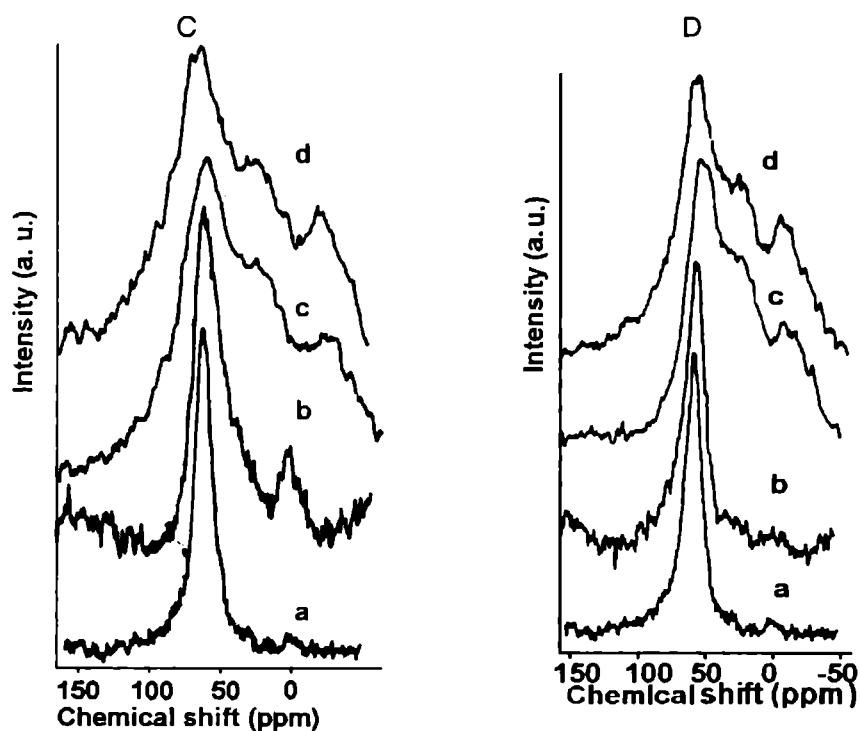
Figure 3.6.a. ^{27}Al MAS NMR spectra of zeolites [A]; H-Y (a), Na-Y (b), K-Y (c), and Mg-Y, [B]; zeolite H-Y, and of the as-exchanged zeolites (b) CeH-Y, (c) LaH-Y, and (d) REH-Y recorded at resonance frequency of 78.19 MHz with sample spinning speed of 7 kHz.



However, the spectra of as-exchanged rare earth H-Y, namely CeH-Y, LaH-Y, and REH-Y, are much broader and are completely featureless (FWHM

> 2000 Hz). The usual tetrahedral peak becomes weak in intensity and the octahedral one much stronger (Figure 3.6a. B).

Figure 3.6b. ^{27}Al MAS NMR spectra of zeolites [C]; H-Y (a), and as-exchanged zeolites CeNa-Y (b), CeK-Y (c), and CeMg-Y, [D]; H-Y (a), and as-exchanged zeolites LaNa-Y (b), LaK-Y (c) and (d) LaMg-Y recorded at resonance frequency of 78.19 MHz with sample spinning speed of 7 kHz.



However, we cannot overemphasize on the identity of each peak in these thickly protonated zeolites. This broadening effect however, is attributable to the fact that dipolar interactions arising from the local magnetic fields at ^{27}Al nucleus associated with magnetic moments of the surrounding protons (residual cations).^{39, 45, 50}

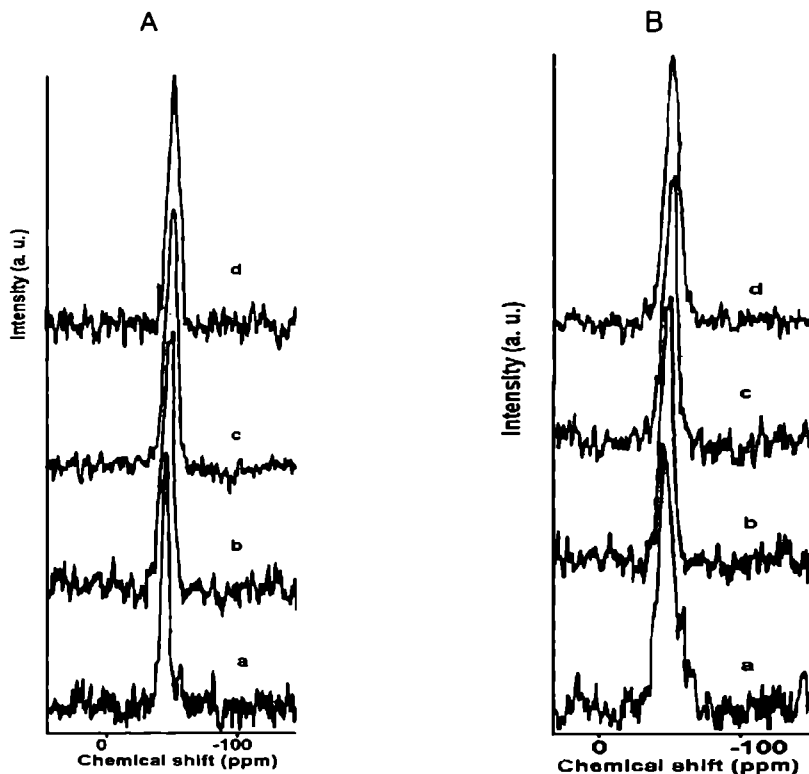
I. ^{29}Si MAS NMR

^{29}Si NMR studies have provided many insights into the structure and chemistry of zeolites. Signals originating from crystallographically inequivalent silicon atoms now can be resolved and related to structural parameters. Full range of ^{29}Si chemical shifts is over 500 ppm wide, but most shifts are found in the narrower range; ca. 120 ppm. Pioneering studies in high resolution solid state ^{29}Si NMR spectroscopy have been performed by Lippmaa et al. who carried out the first comprehensive investigation of a variety of silicates and aluminosilicates.⁵¹ High resolution solid state ^{29}Si NMR with magic angle spinning has been shown to be effective in determining the Si, Al ordering in zeolites, providing direct information of the local environment of silicon atom.⁵² The technique has been widely applied to many zeolites for the structural identification.⁵³⁻⁶⁵ ^{29}Si peak positions shift either to the lower field or to the higher field through the nature of the counter cations. This shift can also be due to the change in the Si-O-Si or Si-O-Al bond angles.^{44, 66-67} It has also been applied for the identification of framework in the zeolites. Q-unit is used to indicate the different silicate atoms in the systems. In zeolites, the Q-unit is always Q4, where four silicate or alumina surrounds each silicate units. Generally they are noted as Si(nAl) or Si(4-n)Si, indicating that each Si atom is linked through oxygen to n aluminium and 4-n silicon neighbors.⁴⁴

Figures - 3.7a. A and B and 3.7b. C and D show the ^{29}Si NMR spectra of pure H-Y and as-exchanged Na-Y, CeNa-Y and LaNa-Y calcined at 773 K. Applying ^{29}Si NMR spectroscopy, Chao et al. found that the exchange of zeolite Na-Y with lanthanum and cerium cations and subsequent dehydration bring about high field shift of Si(nAl) signals, where 'n' is the number of aluminium atoms in the second coordination sphere of the resonating silicon atom.⁶⁶ The chemical shifts of Na-Y and as-exchanged CeNa-Y and LaNa-Y

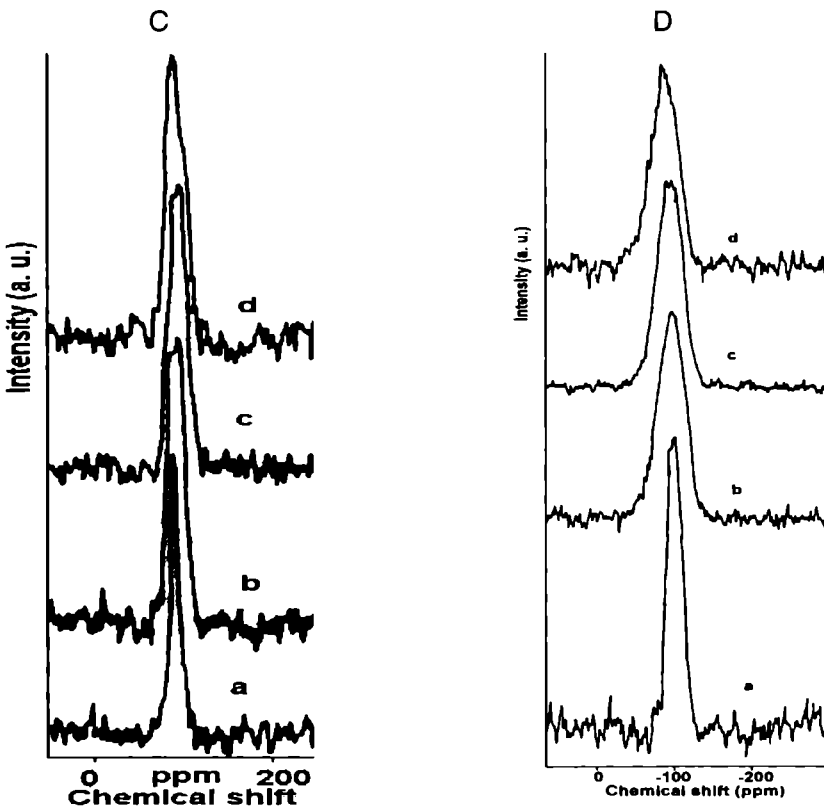
are -88.699 , -89.822 and -89.338 ppm respectively. This high field shift is due to the local strain of the framework SiO_4 tetrahedra in the neighborhood of extra framework positions occupied by bulky cations. The main central peak in the as-exchanged zeolites shows three shoulder peaks which might be originating from $\text{Si}(n\text{Al})$ with $n=3, 2$ and 1 whereas the central peak must be that of $\text{Si}(\text{OSi})_4$ unit. The spectrum of exchanged zeolites showed slightly different shapes.

Figure 3. 7a. A and B; ^{29}Si MAS NMR spectra of parent zeolites [A]; H-Y (a), Na-Y (b), K-Y, (c) and Mg-Y [B]; CeNa-Y (a), H-Y (b), CeK-Y (c), and CeMg-Y zeolites recorded at a resonance frequency of 59.63 MHz with sample spinning speed of 7 kHz.



The spectra of rare earth zeolites are different from H-Y, Na-Y, K-Y or Ag-Y zeolites. There is predominant increase in the line width on exchange with rare earth metals (see Figures-3.7 A-D). It is reported that ^{29}Si spectra are not perturbed by La cations in the super cages (cation sites SI or SII) of zeolite AU-Y, only by La cations in sodalite cages (cation sites SI¹ or SII¹) can perturb the spectra.⁶⁶ The criterion for having La in the sodalite cage is

Figure 3. 7b. C and D; ^{29}Si MAS NMR spectra of parent zeolites [C]; LaNa-Y – (a), H –Y (b), LaK-Y, (c) and LaMg –Y [D]; H-Y (a), CeH-Y (b), LaH-Y (c), and REH-Y zeolites recorded at a resonance frequency of 59.63 MHz with ample spinning speed of 7 kHz.



activation temperature. In the case of FAU-Y zeolite, migration of rare earth cations is known to start at 80°C.⁶⁷ A perturbation of the ²⁹Si spectra by cations in the super cages is very difficult to understand, as it is essentially very low. Hence the perturbation is considered to be caused by cation in the sodalite cages. Cerium or lanthanum occupies SI' site (Y zeolite has 16 such sites). The difference in the line shapes for CeM-Y and LaM-Y is correlated to the migration of these cations from super cages SI to small cage SI'. La³⁺ cation is known to undergo a rapid exchange between SI and SI' sites within the NMR time scale.^{33, 66-67} High field shifts in the spectra of the as-exchanged samples is also due to this perturbation owing to the presence of these cations in the sodalite cages. During heating and dehydration, La³⁺ ions (diameter 0.23nm) strip off their hydration shell and migrate from super-cages into the small cages or hexagonal prism cavities^{24, 68-69}. Hence the cation distribution in rare earth zeolite varies with heat treatment. The repulsive interaction of sodium ions is responsible for the migration of lanthanum and cerium cations into the small cages. This is more pronounced in the case of LaM-Y. This cation migration influences the number of bulky cations (La³⁺ and Ce³⁺) that are accessible for the formation of Brønsted acid sites (BAS) that are available for a reaction according to Hirschler-Plank mechanism.⁶⁹ According to this generally accepted mechanism BAS are formed in zeolites containing multivalent cations upon thermal removal of most of the water initially present in the zeolite pores. In the local electrostatic fields, water dissociates, and the proton formed together with a negatively charged oxygen framework produces the so-called bridging hydroxyl group that is a catalytically active BAS. This is again confirmed by the low acid amount value from NH₃-TPD studies.⁷⁰⁻⁷² A possible explanation for the perturbation and change in the chemical shift values is; when La³⁺ and Ce³⁺ are exchanged with sodium, potassium or magnesium cations in the sodalite cage, one rare earth cation replaces three Na⁺ or K⁺ or

.5 Mg^{2+} . The net result is therefore two empty cation positions. The unfilled SI' sites in the region of Al may induce a perturbation of ^{29}Si spectra that is equivalent to the presence of La^{3+} and Ce^{3+} .

The location of extra-framework cations depends on a number of factors, such as the framework type, the presence of adsorbed molecules, the framework composition, the degree of ion-exchange etc. All these parameters influence the surface structure and composition and are therefore important for understanding the physicochemical properties.⁷³ There are 16 SI sites per unit cell of zeolite-Y. SI', SII and SII' have the same multiplicity of 32 cations per unit cell. Dendooven et al. reported that the occupancy of better co-ordinated sites is favored at elevated temperatures (above 623 K) and better co-ordinated site is SI in dehydrated CaY zeolite.⁷⁴ There are many reports on the cation distribution in Y zeolites.⁷⁵⁻⁷⁶ Based on model calculation, Van Dun et al. concluded that the sites preference are $\text{SI} > \text{SII} > \text{SI}'$ for monovalent cations and $\text{SI} > \text{SI}' > \text{SII}$ for divalent cations in dehydrated zeolites.⁷⁷ Since SI is energetically the most favorable site for monovalent and divalent cations, it might be the most favorable site for trivalent cation too. As the association energy of La^{3+} ions and the faujasite framework (-3000 kJmol^{-1}) is far greater than that for sodium cation (-393 kJmol^{-1}) in the dehydrated state, lanthanum ion is more preferred than sodium ion for occupancy of SI center. However, the number of orbital electrons in lanthanum is ca. 6.5 times greater than that of sodium and this should be considered on assigning the occupancy of cation sites.⁷⁸ For dehydrated LaNa-Y zeolites the electron count at super cage cation position (SI and SII) is lower than that at sodalite cation positions (SI' and SII'). Hence, it is concluded that upon dehydration of zeolites rare earth cations migrate from super cages into the small cages (mostly SI'), while sodium cations localized at SI. ^{23}Na MAS NMR experiments also expose the presence of non-localized Na^+ ions in the large cavities of rare earth exchanged NaFAU-Y zeolite. We, therefore

conclude that the residual cations preferably occupy a super cage cationic position in the rare earth-Y zeolitic structure.

IV. $^1\text{H} - ^{27}\text{Al}$ - Dipolar decoupling studies

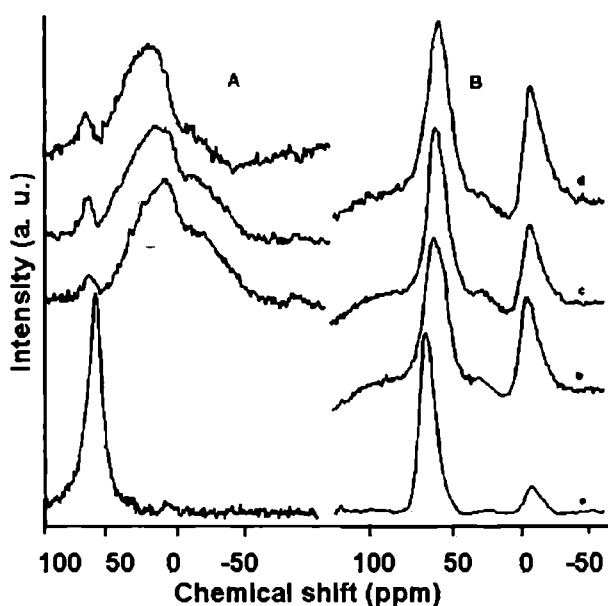
An important application of ^{27}Al MAS NMR to zeolite is the perfect identification and characterization of non-framework aluminium species formed, for example, by various treatments (thermal or hydrothermal) of zeolites as usually applied in the preparation of zeolites catalysts and during their practical day to day use.^{39-40, 43-45, 70-71} Non-framework aluminium is preferably a six fold AlO_6 coordination and gives rise to a signal at about 0 ppm, i. e. well separated from that of the four- coordinated framework aluminium, which gives rise a peak around 60 ± 5 ppm.^{33, 70-71} However, line broadening effects such as quadrupolar interactions, heteronuclear dipolar interactions etc cause major distortions and may complicate the quantitative interpretation of the spectra.³⁹ Furthermore four-coordinated non-framework Al (which will be quantitatively absent in most cases) in strongly distorted AlO_4 environment has been detected in hydrothermally treated zeolites by broad signals which heavily overlap with the signal of tetrahedral framework aluminium in the MAS NMR spectra. As shown in Figure 3.7, the framework Al in the rare earth exchanged HFAU-Y zeolite is broadened and is fully featureless. There is in effect no peak at 0 ppm or at/around 58 ppm. This could be explained as an effect of strong heteronuclear dipolar interactions arising from the local magnetic interactions observed at aluminium nucleus associated with magnetic moments of the surrounding nuclei, i. e. protons in these highly protonated zeolites. The local field modifies the resonance frequency of the nucleus. This dipolar interaction is independent of field strength and could not be avoided by increasing the external magnetic field. The heteronuclear interactions in the case of rare earth exchanged samples are so strong that it makes the spectra totally featureless as seen in the Figure-3.8A. For all the rare earth exchanged samples the

Tetrahedral and octahedral aluminium peaks are interchanged in intensity. For CeH-Y, LaH-Y, and REH-Y zeolites the tetrahedral peak positions were 63.05, 1.38, and 62.68 ppm, whereas the octahedral peaks were at 8.77, 17.03, 8.11 ppm respectively. In the case of pure HFAU-Y zeolite the tetrahedral peak was at 61.29 ppm and octahedrally coordinated one was not seen. For rare earth exchanged zeolites, the octahedral peak was very strong and was highly shifted in the frequency scale. The tetrahedral Al peak was very weak. However, for common zeolites it should be reverse, i. e., the tetrahedral peak should be strong and octahedral one weak.

The reversal of broadening, peak intensity, and positions could be explained as an effect of dipolar interaction arising from local magnetic fields at aluminium nucleus by the surrounding nuclei (mainly from ^1H , as the zeolites are thickly protonated). This effect could be removed to a large extent by the irradiation of a strong rf field at the resonance frequency of ^1H , while measuring the spectrum of ^{27}Al . The high-power dipolar decoupling is widely used to remove line broadening effects due to heteronuclear dipolar interactions with proton in the NMR spectra of proton containing samples.^{39, 45}

The effect of $^1\text{H} - ^{27}\text{Al}$ decoupled MAS NMR spectra of HFAU-Y, CeH-Y, LaH-Y, and REH-Y zeolites are shown in Figure-b. Analysis was done at a spinning speed of 8 kHz. All the zeolites show a strong peak around 55 ppm, (for pure H-Y it is at 59.85 ppm) and a small peak around 0 ppm corresponding to those of octahedral Al as expected for a zeolite. The intensity of the octahedral peak (0 ppm) increases from H-Y to REH-Y. This is rather expected as there is possibility of formation of non-framework aluminium upon thermal exchange and subsequent high temperature activation.

Figure. 3.8. Effect ^1H - ^{27}Al dipolar decoupling magic angle spinning NMR on heavily protonated ReH-Y zeolites (a) pure H-Y (b) CeH-Y, (c) LaH-Y, and (d) REH-Y). (A) Without dipolar decoupling and (B) with ^1H - ^{27}Al dipolar decoupling recorded with a resonance frequency of 78.19 MHz for ^{27}Al and 300.08 MHz for ^1H with a sample spinning rate of 8.0 kHz.



The full width half maximum (FWHM) for both the peaks (one for aluminium in the tetra-coordination around 58 ppm and other for the same in the octahedral surrounding around 0 ppm) of the pure H-Y and different rare earth exchanged zeolites has been calculated. These values are shown in Table-3.5. There is a small peak at 3.74 ppm for H-Y zeolite and is assigned to octahedral aluminium. This peak was not observed in the simple ^{27}Al MAS NMR of the sample. All the rare earth exchanged zeolites exhibit this peak around 0 ppm and the intensity increases from pure H-Y to rare earth form. This is rather expected as there are chances of dealumination during ion exchange and subsequent thermal activation.

Table 3.5. Full width half maximum values of both tetrahedral and octahedral aluminium peaks for pure H-Y zeolite and different rare earth exchanged zeolites as obtained from $^1\text{H} - ^{27}\text{Al}$ decoupling MAS NMR experiments recorded at 78.19 MHz in case of aluminium and 300.08 MHz in the case of proton with a sample spinning frequency of 8.0 kHz.

Zeolite	Tetra-coordinated aluminium (Hz)	Octa-coordinated aluminium (Hz)
H-Y	800.0	714.0
CeH-Y	1202.0	910.7
LaH-Y	1019.0	947.0
REH-Y	1209.0	957.0

Rare earth exchange not only increases the intensity of the octahedral peak but also shifts its position from 3.74 ppm to around 0 ppm. The peak positions are 0.23, -0.54, and -0.47 ppm respectively for CeH-Y, LaH-Y, and REH-Y zeolites. Similarly the peak position for the tetrahedral aluminium also shifts on exchange with rare earth metal ions. The peak positions are 59.85, 55.33, 6.14, and 55.74 ppm for pure H-Y, CeH-Y, LaH-Y, and REH-Y zeolites. The p -field shift in the peak position is correlated to the strain in the T-O-T framework in presence of bulky rare earth metal ions.⁷⁰⁻⁷¹ As shown by different NMR spectral techniques, lanthanum exchanged H-Y zeolite exhibits rather unusual peak position when compared to CeH-Y. This is explained as an effect of migration of La^{3+} ions from super cage cation locations to small cage positions (sodalite) in the zeolite structure. The effect of migration of rare earth cations on the physicochemical properties of rare earth zeolites are discussed in previous NMR sections; 3.5a, 3.5b, and 3.5c. Very sharp increase in the intensity of the octahedral peak confirms dealumination during catalyst

preparation. However, these non-framework aluminium acts as potential Lewis acid-centers during catalytic reactions.

$^1\text{H} - ^{27}\text{Al}$ decoupling MAS NMR experiments also confirm the presence of penta-coordinated aluminium (peak around 30 ppm) for rare earth exchanged zeolites. Simple MAS NMR spectra have not provided clear information about this aluminium species. The peak positions are 29.81, 31.21, and 30.81 ppm for CeH-Y, LaH-Y, and REH-Y zeolites respectively. Broadening of peaks in other rare earth zeolites could also be reduced by applying $^1\text{H} - ^{27}\text{Al}$ dipolar decoupling. Thus, we conclude that $^1\text{H} - ^{27}\text{Al}$ dipolar decoupling can resolve different kinds of aluminium in rare earth exchanged Y zeolites.

3.7 Surface area and pore volume measurements

In order to get an idea about the number of active sites per unit area of the catalyst, we have performed the surface area and pore volume measurements. The number of active sites per unit area is defined as the ratio of acidity and surface area. Number of active sites per unit area is directly correlated to the catalytic activity of the system. The micro pore volume has a major role in the selectivity of the product. Surface area and pore volume of the parent and as-exchanged samples are shown in Table 3.6. The data were reproducible within an error limit of 5%. Surface and pore volume increase invariably on exchange with rare earth cations. But the sodium- exchanged form shows a very low surface area and pore volume. The increase of surface area might be due to the decrease in the crystallite size when moving from the sodium form to the rare earth modified forms. As expected, LaNa-Y has a low value of these parameters compared to

Table 3.6. Surface area and pore volume measurements, and number of active sites per unit area of H-Y, Na-Y, K-Y, Mg-Y and their rare earth derivatives determined by low temperature nitrogen adsorption method.

Zeolite	Textural properties			
	BET Surface area (m ² /g) ¹	Langmuir surface area (m ² /g) ¹	Pore volume ² (cc/g)	No of active sites per unit area ³ (mmol/m ²)
H-Y	398	593	0.266	0.0034
Na-Y	254	389	0.232	0.0030
CeNa-Y	484	697	0.296	0.0046
LaNa-Y	441	650	0.287	0.0032
PrNa-Y	468	684	0.291	0.0039
SmNa-Y	498	712	0.302	0.0053
Y-Y	181	321	0.214	0.0039
CeK-Y	473	684	0.303	0.0027
LaK-Y	435	648	0.277	0.0022
PrK-Y	461	667	0.295	0.0024
SmK-Y	301	438	0.252	0.0043
CeMg-Y	497	728	0.312	0.0046
LaMg-Y	455	681	0.294	0.0023
PrMg-Y	471	707	0.306	0.0043
CeH-Y	511	731	0.340	0.0040
LaH-Y	464	679	0.288	0.0036
PrH-Y	483	699	0.301	0.0042

Note: ¹ Values are reproducible within an error limit of $\pm 5\%$. ² Total pore volume measured at 0.9976 p/p₀. ³ Number of active sites per unit area is the ratio of total acidity and the BET surface area.

CeNa-Y, which is in accordance with the above argument. This observation can easily be correlated to the results from various NMR and acidity measurement experiments. The very high surface area of RENA-Y may

be due to the greater percentage of sodium exchange and by the combined effect of various counter cations.

The catalysts have high surface area and pore-volume. Catalysts of high surface area in general have exceedingly complex pore structures. Thus this experimental method cannot be expected to provide an evaluation of the 'absolute' surface area or pore size (or pore volume). Also, for practical reasons it is increasingly difficult to make accurate measurements of nitrogen isotherms at 77 K. Thus, we acknowledge that there could be an inconsistency in the surface area and pore volume measurements up to $\pm 5\%$. In spite of the above recommendation, it is generally recognized that for textural characterization, no other readily available method can offer the same scope and overall reliability as gas adsorption at liquid nitrogen temperatures.

3. 8 Characterization of acid sites in zeolites

I. Temperature Programmed Desorption of Ammonia (NH_3 -TPD)

The acid strength distribution of the parent and various as exchanged zeolites are presented in Table-3.7. The table describes the distribution of acidity in three temperature regions of 373-473 K (weak acid sites), 473-673 K (medium acid strength) and 673-873 K (strong acid sites). Hence, NH_3 -TPD presents the acid site distribution in zeolites rather than the total acidity. Amount of ammonia desorbed by each sample varies with the nature of rare earth cation present. All the rare earth exchanged samples invariably show high value of acidity. CeNa-Y and SmNa-Y have the maximum acidity and pure Na-Y the least among different sodium derivatives. However, for all the rare earth exchanged zeolites, the amount of ammonia desorbed in the high temperature region (673-873 K) is low.

Table 3. 7. Temperature programmed desorption of ammonia studies on pure H-Y, Na-Y, K-Y, Mg-Y and their rare earth derivatives.

Zeolite	Ammonia desorbed (mmol/g)			Total acid amount
	W ^{1,2}	M ²	S ²	
H-Y	0.69	0.41	0.33	1.43
Na-Y	0.59	0.12	0.05	0.77
ZeNa-Y	1.45	0.59	0.20	2.24
LaNa-Y	0.92	0.42	0.13	1.48
RENa-Y	0.70	0.68	0.46	1.83
SmNa-Y	1.21	1.09	0.34	2.64
K-Y	0.40	0.20	0.09	0.71
ZeK-Y	0.62	0.38	0.23	1.23
LaK-Y	0.47	0.35	0.12	0.94
REK-Y	0.52	0.37	0.21	1.10
Mg-Y	0.60	0.51	0.18	1.29
ZeMg-Y	1.21	0.63	0.44	2.28
LaMg-Y	0.71	0.43	0.28	1.42
REMg-Y	0.94	0.76	0.31	2.01
ZeH-Y	1.10	0.60	0.31	2.02
LaH-Y	0.51	0.71	0.46	1.68
REH-Y	0.68	0.86	0.49	2.03

Notes: ¹ Ammonia desorbed in the temperature 373-473 might contain some physisorbed ammonia too. ² W (373-473), M (473-673), S(673-863) indicates weak, medium, Strong acid sites

Catanach et al. identified three desorption peaks for Y type of zeolites located at 463, 513 and 673 K which corresponds to the loss of about 45 (49.45%), 28 (30.77%) and 18 (19.78%) molecules of ammonia per unit cell.⁷⁹

Dehydroxylation occurs only at 963 K. Lok et al. proposed that the first NH_3 -TPD (below 473 K) peak is associated largely with weakly chemisorbed NH_3 molecules rather than physically adsorbed NH_3 molecules for high silica to alumina ratio zeolites. The second peak (between 473-673 K) is associated with NH_3 molecules adsorbed on zeolite hydroxyl groups (the Brönsted acid sites) and the third NH_3 -TPD peak (between 673-873) is desorption from very strong BAS or LAS. The first and second desorption peaks usually account for most of the ammonia adsorbed and the third peak is usually very small in absolute amount.⁸⁰ All the as-exchanged zeolites show steady observation for the above statements. The values in parenthesis (of Table-2) show the fraction of the amount of ammonia desorbed in the specific temperature ranges. Ammonia desorption occur mainly in the temperature range of 373-473 and 473-673 K. Very strong BAS/LAS are comparatively low in the case of as-exchanged zeolites than H-Y where ammonia desorption occurs mainly in the middle region.

As seen in the Table-3.5; the total amount of ammonia adsorbed by each sample varies with the nature of cation present. Irrespective of the cations, all samples show high values of acidity in the weak and medium regions. Among the samples, CeNa-Y and CeMg-Y, and CeH-Y zeolites show maximum acid amount. Acid amount increases from potassium to sodium to magnesium to proton for a fixed rare earth cation. Binder free Na-Y and K-Y exhibit very low acid amount. The effect of sodium ions on the activity of Brönsted type of zeolites in acid catalyzed reactions has been recognized very early especially in the case of faujasite type of zeolites. It was proposed that the residual Na^+ ions have a poisoning effect on the acidity i.e.: a particular Na^+ ion, present within the decationated zeolite, has a neutralizing effect over a large number of the existing protons.⁸¹⁻⁸³ Recently, it has been shown that the effect of residual Na^+ ions was to weaken the Brönsted acid sites, without actually neutralizing more than one Brönsted site per Na^+ ion. As the Na content decreases on

exchange of Na with rare earth cations, there is an increase in the acid amount. Along similar lines it may be said that the more basic K^+ ions might have a stronger poisoning power on the Brønsted acid sites. Indeed potassium exchanged zeolites show much low acid amount compared to sodium, magnesium or proton rare earth zeolites. Binder free Mg-Y zeolite is much more acidic compared to Na-Y or K-Y zeolites. The very specific influence of Mg^{2+} cation in introducing greater acidity in its parent as well as rare earth modified forms is due to its very high polarizing power which affects the OH bond strength through the lattice.⁸⁴⁻⁸⁵ Low value in the acidity of LaNa-Y, LaK-Y and LaMg-Y is due to the formation of inaccessible Brønsted acid sites (BASs) in the small cages upon heat treatment. These inaccessible BASs in the small cages are formed by the migration of La^{3+} from super cage to small cages in the electrostatic repulsive field of residual cations.^{69-70, 86} This migration is most in the case of magnesium cation and consequently shows the maximum variation in acidity from the parent form Mg-Y.

Corma et al. reported that the Brønsted acidity in rare earth exchanged zeolites are generated by the hydrolysis of rare earth cations at Si' in the sodalite and super cages.⁶⁷ The acid strength variation among different rare earth exchanged zeolite can be explained using the well-established Pauling's principle. According to the principle of electronegativity equalization, the strength of BAS depends on the nature of cation present and decreases in the series $HLi-Y > HNa-Y > HK-Y$.⁸⁸⁻⁸⁹ O'Donoghue and Barthomeuf found a decrease of catalytic activity in the dehydration of 2-propanol at 388 K in the same order.⁸⁹ Pertaining the same principle, acidity should follow the order $SmNa-Y > CeNa-Y > LaNa-Y$. Indeed acidity follows the same order. The specific influence of Ce and Sm is most likely due to the high polarizing power and rather small size (even though in the rare earth series size does not vary much) compared to La, which affects the OH bond through

the lattice. A comparatively low acidity of LaNa-Y, LaK-Y, LaMg-Y, and LaH-Y could be due to the presence of large number of La³⁺ ions in the small cages (SI' sites) due to migration (migration behavior is already explained in ²⁹SiMAS NMR; section-3.5c) than Sm³⁺ and Ce³⁺ in the cases of SmNa-Y and CeM-Y (M = K⁺, Mg²⁺, and H⁺) zeolites respectively.

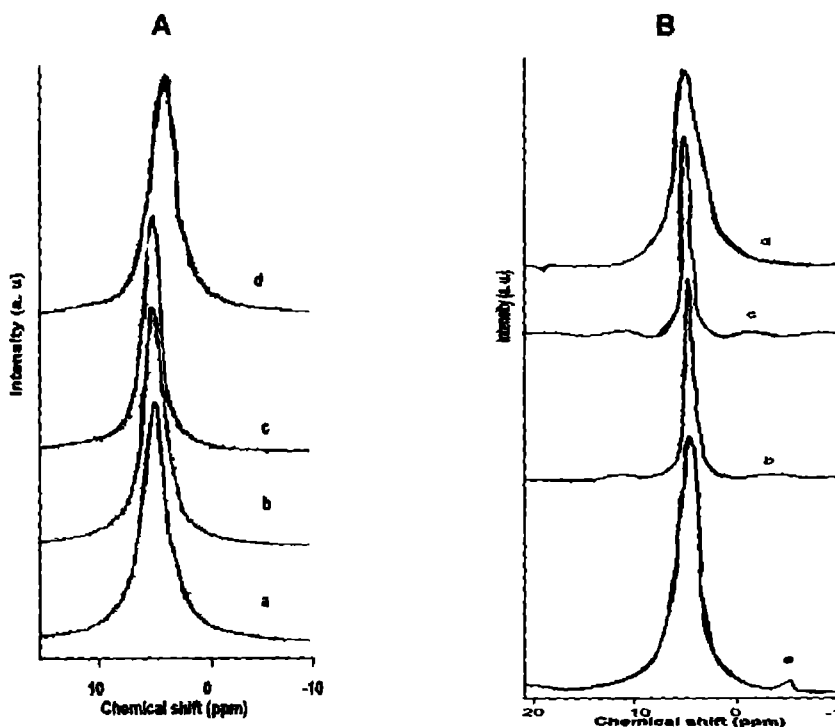
BAS is formed in zeolites containing multivalent cations upon thermal removal of water initially present in the pores. In the local electrostatic fields, a water molecule dissociates and the proton formed together with negatively charged oxygen framework gives the so-called bridging hydroxyl groups that are the catalytically active BAS. BAS that are formed in the small cages are non-accessible acid centers. However, cation migration influences the number of cations that are available for the formation of accessible BAS according to Hirschler-Plank mechanism during thermal treatment.⁶⁹ In the local repulsive interaction rare earth cations migrate from super cages to small cages and is maximum in the case of lanthanum cations (as evidenced by the ²⁹Si NMR). The influence of repulsive interaction on the cation distribution in the small cages of zeolite Y was discussed earlier by Van Dum and Mortier.⁷⁴

II. ¹H MAS NMR Spectroscopy

To collect more information about the Brønsted acid sites (BAS) in the large and small cages of various as-exchanged faujasite-Y zeolite systems, ¹H MAS NMR spectra of samples were taken after calcining at 773 K in MAS mode (Figures 3.9A and 3.9B). ¹H MAS NMR can characterize Brønsted acid amount as it directly probes the protons and their environments. In principle ¹H MAS-NMR chemical shifts are correlated with the proton donor ability of BAS and hence can provide information about the Brønsted acidic strength.⁹⁰⁻⁹⁴ But zeolites have BAS sites involving framework oxygens at crystallographically different positions, i.e. bridging hydroxyls freely vibrating in large cages or

channels next to bridging hydroxyls in small cavities delineated with 6 rings or 8-rings of T-atoms.⁹⁰ Since the bridging hydroxyls interact with several framework oxygen, ¹H fast MAS-NMR spectroscopy at very high field is a powerful technique for the atoms, these interactions may give rise to different downfield chemical shift in the ¹H NMR spectra, mostly reflecting an increase in Brønsted acidic strength.⁷⁰ Proton-proton interactions will cause extreme line broadening and lowered resolution when the zeolite cages have a high density of protons.⁹¹

Figure 3.9. ¹H MAS NMR spectra of dehydrated (773 K) zeolites [A] (a) H-Y, (b) Na-Y, (c) CeNa-Y, and (d) LaNa-Y (1) and [B] (a) H-Y, (b) CeH-Y, (c) LaH-Y, and (d) REH-Y (b), recorded at a resonance frequency of 300.08 MHz with a magic-angle spinning speed of 9 kHz.



^1H MAS NMR spectra of all zeolites revealed a single, relatively sharp Brönsted signal with a chemical shift value between 4.0 to 5.25 ppm. Parent Na-Y has a chemical shift of 5.11 ppm. Chemical shifts of as-exchanged CeNa-Y and LaNa-Y were 4.17 and 4.92 ppm. The chemical shift values of rare earth exchanged H-Y zeolites are; 4.5, 4.9, and 4.26 ppm respectively for CeH-Y, LaH-Y, and REH-Y zeolites. The relative large shift of the signal in the case of CeNa-Y and REH-Y zeolites could be taken as an indication of high Brönsted acidity.^{70, 95} LaNa-Y and LaH-Y show a down field shift, which might be due to local strain of the zeolitic framework. Lanthanum cations migrate from the large cages to small cages and preferentially form Brönsted acid sites in these cages during dehydration or calcination steps. This reduces the number of accessible Brönsted acid sites (BAS) in the zeolitic framework and hence shows a comparatively down field shift in their spectra.

III. Cumene cracking

There are several well-established methods for the quantitative determination of zeolite acidity. Some of the important analytical techniques includes; UV-Visible spectroscopy, temperature programmed desorption (TPD) of amines, microcalorimetry, solid state NMR spectroscopy (^1H MAS NMR), infrared spectroscopy, photo acoustic spectroscopy, different thermodesorption studies of probe molecules (TG/DTA), and catalytic test reaction such as cracking of isobutene, hexane, decane and cumene.^{44, 80, 96-106} Classical molecular mechanics calculations on extended systems using force fields deduced from ab initio quantum-chemical calculations are also used for calculating the local distortions in zeolites around the protonic site.¹⁰⁷⁻¹⁰⁸ Cumene cracking is widely used to distinguish between the amount of Brönsted acidity and Lewis acid amount.

We have studied the influence of the calcination temperature of the material on the cracking and dealkylation activities of cumene. As the calcination temperature increases from 623 K to 773 K, the total conversion increases. Formation of benzene (formed through the dealkylation of cumene on BAS) increases and that of α -methyl styrene (formed by the dehydrogenation of cumene over LAS) decreases. This is consistent with the well-accepted Hirschler-Plank mechanism of the formation of Brønsted acidity in zeolites⁶⁹. According to this mechanism, BAS are formed in zeolites containing multivalent cations upon thermal removal of most of the water initially present in the pores. In the local electrostatic fields, a water molecule dissociates, and the proton together with a negatively charged oxygen framework gives the so called bridging hydroxyl groups that are the catalytically active BAS for benzene formation through dealkylation of cumene.

Further we have evaluated the effect of temperature on the conversion of cumene and of the formation of benzene and α -methyl styrene. Formation of α -methyl styrene decreases and that of benzene increases. This is consistent with the generally accepted mechanism of increase of conversion with temperature due to decrease of activation energy for the reaction. Kinetic studies show that activation energy is maximum at 473 K and least at 673 K. It is assumed that at low temperatures activation energy favors predominantly benzene and to some extent α -methyl styrene. However, at high temperatures favors maximum benzene formation. In the present case, as the reaction temperature increases to 673 K, α -methyl styrene formation becomes almost nil, whereas that of benzene increases. Hence at higher temperatures, the acid sites become fully Brønsted in nature.

Table 3. 8. Product distribution during the cracking of cumene over pure H-Y, Na-Y, K-Y, Mg-Y, and their corresponding rare earth exchanged zeolites.

Zeolite	Cumene reacted (%)	Selectivity (%)			
		Benzene	α -Methyl styrene	Ethylbenzene	Others ¹
H-Y	30.9	87.4	5.2	3.3	4.1
Na-Y	8.2	68.3	14.2	4.8	12.7
CeNa-Y	39.5	93.7	1.4	3.9	1.0
LaNa-Y	31.7	88.3	2.9	3.2	5.6
RENa-Y	32.8	91.8	1.7	2.9	3.6
SmNa-Y	35.1	92.1	1.1	4.2	2.6
K-Y	6.8	63.2	13.2	5.2	18.4
CeK-Y	33.3	90.5	1.3	2.4	5.8
LaK-Y	27.2	88.1	1.7	3.1	6.1
REK-Y	28.4	90.6	1.8	2.1	6.5
Mg-Y	24.4	82.5	6.6	4.2	6.7
CeMg-Y	42.5	95.3	1.4	2.7	0.6
LaMg-Y	33.4	91.2	2.5	3.3	1.4
REMg-Y	32.9	92.7	2.1	3.1	1.7
CeH-Y	40.1	92.9	1.8	3.9	1.4
LaH-Y	35.6	91.2	2.0	4.0	2.8
REH-Y	40.6	93.3	2.7	2.1	1.9

Notes: Reaction conditions: temperature: 623 K, flow rate: 4 mL/hour, catalyst amount: 500 mg, the time on stream: 4 hours, and steady supply of nitrogen (10 mL/h).

Table 3.8 illustrates the cumene cracking ability of various zeolite materials. Pure Na-Y and K-Y have very low activity towards the reaction. The effect of sodium and potassium ions on the activity of Brønsted type of zeolites

in acid catalyzed reactions has been recognized very early especially in the case of faujasite. It was proposed that these residual cations have a poisoning effect on the acidity i.e.: a particular Na^+ or K^+ ion present within the decationated zeolite has a neutralizing effect over a large number of the existing protons⁸¹⁻⁸². Recently, it has been shown that the effect of residual Na^+ ions was to weaken the Brønsted acid sites, without actually neutralizing more than one Brønsted site per Na^+ ion. Binder free Mg-Y converts comparatively larger amounts of cumene and produce larger amounts of benzene. This enhancement in the activity/selectivity is due to the high polarizing power of magnesium cation.

All the as-exchanged forms show cracking activity more than that of Na-Y, K-Y or Mg-Y. Lanthanum forms of sodium, potassium, magnesium, and even proton- Y zeolites show lower conversion of cumene than the corresponding cerium or mixed rare earth exchanged materials. This could be explained by the low acidity values of LaNa-Y and LaK-Y zeolites due to the migration of La^{3+} ions from the super cages (SI) to small cages (SII) in the local repulsive electrostatic field of residual and counter cations on thermal treatment.¹⁰⁹⁻¹¹¹ This migration creates catalytically inaccessible Brønsted acid centers in the small cages by the hydrolysis of lanthanum ions.⁷⁰ Rare earth exchanged sodium forms invariably show greater cracking activity over the potassium derivatives due to their greater acidity values (from ammonia TPD). The creation of stronger acidity in magnesium and sodium derivatives is explained in terms of Sanderson's principle of electronegativity equalization; the strength of Brønsted acid sites depends on the nature of alkali cation and is expected to decrease in the order $\text{Mg-Y} > \text{Na-Y} > \text{K-Y} > \text{Rb-Y}$ etc i.e. acidity decreases as the electropositivity of the residual cation increases.⁷⁰

Figure: 3.10. A probable one- to- one correlation between the total amount of ammonia desorbed (as studied by NH₃ TPD) and cumene converted for different catalysts (a and b) and amount of ammonia desorbed and benzene formation during the cracking of cumene (c and d).

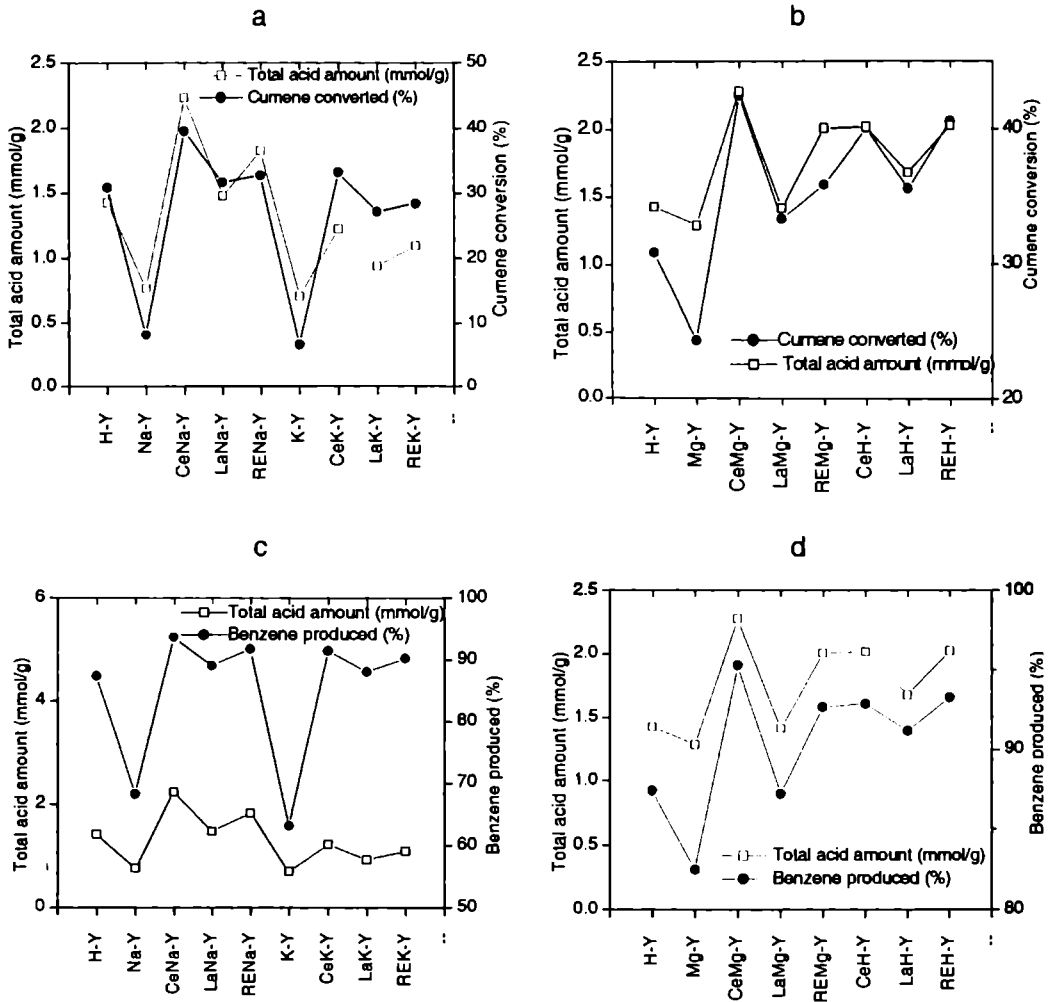


Figure-3.10a and 3.10b; represents the comparison of the total amount of ammonia desorbed from the zeolite systems with conversion of cumene. It

shows a perfect one-to-one correlation between the total acidity and conversion. K-Y and Na-Y with their weak acid structure exhibit least ability to crack/dealkylate cumene. REH-Y and CeMg-Y with their maximum acid amount convert the maximum amount of cumene under standard reaction conditions. Therefore, we conclude that dealkylation and cracking of cumene is a function of the total acid structural properties of the as-exchanged rare earth zeolites.

Figure-3.10c and 3.10d; show the perfect correlation between the amount of ammonia desorbed during ammonia TPD and formation of benzene while cumene cracking. Benzene is known to be produced over BAS and pure binder free zeolites such as K-Y and Na-Y with their low Brønsted acid amount produce the least amount of benzene. The poisoning effects of Na^+ ions on BAS are widely reported and it is not surprising that Na-Y or K-Y produce a comparatively low amount of benzene.¹⁰⁹ As expected lanthanum exchanged varieties produce lower amounts of benzene than their cerium or mixed rare earth counterparts. From the present study, we conclude that the improvement in the acid structural properties of H-Y, Na-Y, K-Y, and Mg-Y zeolites upon rare earth exchange is in the Brønsted acid amount.

3.9 Conclusions

Different physicochemical characterization techniques have been effectively employed for the proper understanding of the probable influence of rare earth cations on the textural and structural properties of rare earth zeolites. From the detailed studies, we arrived at following conclusions.

1. PXRD, Energy Dispersive X-ray Analysis, infrared spectroscopy studies confirm that the zeolite framework remain intact even after multi step metal ion exchange at moderately high temperatures.

2. Cerium exchanged zeolites (CeNa-Y, CeK-Y, CeMg-Y, and CeH-Y) show a strong band around 300 nm in the UV-vis diffuse reflectance spectroscopy. This band (which is a MLCT) confirms the distribution of cerium in a well-dispersed tetrahedral coordination, which is the catalytically active site. Other as-exchanged zeolites do not show this band due to the lack of flexible oxidation states such as $\text{Ce}^{3+} \rightarrow \text{Ce}^{4+}$. However, they do show small shoulder peaks in the low energy region due to forbidden $f \rightarrow f$ transitions.
3. ^{23}Na MAS NMR spectral studies on sodium exchanged rare earth zeolites confirm the presence of this residual cation in super cage cationic position (SII). Hence it may be induced that other residual cations (H^+ , K^+ , and Mg^{2+}) too occupy a super cage cation location in zeolite structure.
4. ^{27}Al MAS NMR spectra of all zeolites show a strong band around 58 ppm confirming the tetra coordination of aluminium in the structure. However, the spectra also show small shoulder peaks around 30 and 0 ppm corresponding to penta and hexa- coordinated aluminium respectively. The main central peak show major broadening on exchange of H^+ cations with sodium, potassium, magnesium, and rare earth metal ions. This could be taken as an indication of strain in the zeolitic framework. The broadening could be due to the distribution of chemical shifts due to aluminium atoms in the locality of strained (due to vicinity of heavy or bulky cations) and non-strained framework. This could also be due to the quadrupolar influence aluminium nucleus (Al spin 5/2 is a quadrupole nucleus). ^{27}Al MAS NMR spectra of the as-exchanged rare earth H-Y zeolites are completely featureless. Pure H-Y and its rare earth exchanged zeolites are thickly protonated and this result in strong dipolar interaction between proton and aluminium. FWHM is > 2000 Hz for all rare earth exchanged H-Y zeolites. For pure H-Y the FWHM is only 817.0 Hz.

5. In the ^{29}Si MAS NMR spectra central single peak corresponds to Q^4 Si(4Al) unit. Shoulder peaks represent other silicate units - Q^3 , Q^2 , Q^1 etc. Size and charge of residual cation has marked influence on the ^{29}Si MAS NMR chemical shift positions. Exchange of sodium cations with rare earth, potassium, and magnesium produce greater up field shifts in the spectra. This could be explained as an effect of the greater strain in the T-O-T zeolitic framework in presence of bulky and heavily charged cations in the extra-framework positions. Lanthanum exchanged zeolites exhibit unusual peak positions compared to cerium exchanged materials. Lanthanum cations tend to migrate from super cages to small cages upon thermal treatment according to Hirshler-Plank mechanism. Migration is responsible for the moderate acidity of La^{3+} exchanged zeolites as explained by temperature programmed desorption of ammonia.
6. Acid structural properties of different zeolites were determined by Temperature Programmed Desorption of ammonia (NH_3 -TPD), and cumene cracking test reaction. Lanthanum exchanged zeolites invariably show low acid amounts and decreased formation of benzene, which is a clear indication of their moderate acidic nature and catalytic activity. This is explained as an effect of cation migration.

References

1. J. R. Agger, N. Pervaiz, A. K. Cheetham, M. W. Anderson, J. Am. Chem. Soc. 120 (1998) 10754.
2. A. K. Datye, "Electron Microscopy and Diffraction" in Handbook of Heterogeneous Catalysis (G. Ertl, H. Knozinger, J. Weitkamp) Vol. 2, Wiley VCH, (1999) p.497.
3. J. J. Pluth, J.V. Smith, J.M. Bennett, Acta Crystallog. C42 (1986) 283.
4. W.M. Meier, C.Z. Baerlocher, Z. Kristallogr. 135 (1986) 339.
5. J.F. Chamell, J. Cryst. Growth. 8 (1986) 291.
6. K.J. Chao, J.C. Lin, Y. Wang. G.H. Lee, Zeolites, 6 (1986) 35.

7. C. Suryanarayana, M.G. Norton, "X-Ray Diffraction- A Practical Approach", Plenum Press, New York & London 1998, p. 97- 107.
8. H.M. Rietveld, *J. Appl. Crystallog.* 2 (1969) 65.
9. R. Szostak, "Molecular Sieves- principles of synthesis and identification" Van Nostrand Reinhold catalysis series, (1989), p. 349.
10. D. W. Breck, "Zeolite Molecular Sieves- Structure, Characterization and Uses" Wiley Intersci.Pub. Inc. 1973 p. 418.
11. F. Stubican, R. Roy, *Z. Kristallogr.* 115 (1961) 200.
12. B. D. Saksena, *Trans. Faraday Soc.* 57 (1961) 242.
13. E. M. Flanigen, H. Khatami, H. A. Szymanski, "Molecular Sieve Zeolites" *Advan. Chem. Ser.* 101, Am Chem. Soc. Washington, D. C. 1971 p. 201.
14. C. N. R. Rao, "Chemical Applications of Infrared Spectroscopy", Academic Press New York, 1963.
15. R. G. Milkey, *Amer. Minerl.* 45 (1960) 990.
16. L. B. Zinner, A. S. Araujo, *J. Alloys Comp.* 180 (1992) 289.
17. L. B. Zinner, K. Zinner, M. Ishige, A. S. Araujo, *J. Alloys Comp.* 193 (1993) 289.
18. H. Borchardt, F. Daniels, *J. Am. Chem. Soc.* 79 (1956) 41.
19. G. Blasse, *Struct. Bond.* 76 (1991) 153.
20. C. K. Jorgensen, "Adsorption Spectra and Chemical Bonding in Complexes", Pergamon, New York, 1962.
21. M. Gerloch, E. C. Constable, "Transition Metal Chemistry", VCH, New York, 1994.
22. S.C. Laha, P. Mukherjee, S.R. Sarkar, R. Kumar, *J. Catal.* 207 (2002) 213.
23. M. Che, F. B- Verduraz, "UV-Vis- and EPR Spectroscopies" in "Handbook of Heterogeneous Catalysis", Ed. G. Ertl, H. Knozinger, J. Weitkamp, Vol. 2, Wiley VCH, (1999) p.640.
24. D- S. Shy, S- H. Chen, J. Lievens, S-B. Liu, K-J. Chao, *J. Chem. Soc. Faraday Trans.* 87, 17 (1991) 2855.
25. E. F. T. Lee, L. V. C. Rees, *Zeolites*, 7 (1987) 143.
26. L.B. Welsh, S.L. Lambert, in "Characterization and Catalyst Development" Ed. S. A. Bradley, M. J. Gattuso, R. J. Bertolacini, Am. Chem. Soc. Washington DC. ACS Symp. Ser. 411 (1989) 262.
27. E. Kundla, A. Samoson, E. Lippmaa, *Chem. phys. Lett.* 83 (1981) 229.
28. A. Samoson, E. Lippmaa, *Chem. phys. Lett.* 100 (1983) 205.

Chapter 3

29. L.B. Welsh, S.L. Lambert in W-E. Flank and T.E. Whyte (Eds), "Perspectives in Molecular Sieve Science", (Am. Chem. Soc.), Washington, DC. 1998, p. 328.
30. H. K. Bayer, G. Pal- Barbely, H.G. Karge, *Mesopor. Mater.* 1 (1993) 67.
31. R. Challoner, R. Harries, *Zeolites*, 11 (1991) 265.
32. G. Engelhardt, H. Koller, P. Sieger, W. Depmeir, A. Samosan, *Solid State Nucl. Magn. Reson.*, 1 (1992) 127.
33. M. Hunger, G. Engelhardt, J. Weitkamp, *Microporous. Mater.* 3 (1995) 497.
34. D. Massiot, C. Bessada, J.P. Contunier, Jauldle, *J. Magn. Reson.* 90 (1996) 231.
35. C- F. Lin, K- J. Chao, *J. Phys. Chem. B.* 95 (1991) 9411.
36. J. Klinowski, *Chem. Rev.* 91 (1991) 1459.
37. P. J. Grobet, H. Geerts, J. A. Martens, P. A. Jacobs, *J. Chem. Soc. Chem. Commun.*(1987) 1688.
38. H. Klein, H. Fuess, M. Hunger, *J. Chem. Soc. Faraday Trans.* 91 (1995) 1813.
39. G. Engelhardt "Solid-State NMR" in *Handbook of Heterogeneous Catalysis* (Ed. G. Ertl, H. Knozinger, J. Weitkamp) Vol. 2, Wiley VCH, (1999) p.536.
40. J. Klinowski, *Colloids Surfaces*, 36 (1989) 133.
41. J. W. Akitt, *Annu. Rev. NMR Spectrosc.* 5A (1973) 465.
42. W. O. Hagg, R. M. Lago, P. B. Weisz, *Nature (London)*, 309 (1984) 589.
43. J. Klinowski, J. M. Thomas, C. A. Fyfe, G. C. Gobi, *Nature* 296 (1982) 533.
44. R. Szostak, "Molecular Sieves- principles of synthesis and identification" Van Nostrand Reinhold catalysis series, 1989, p. 339.
45. G. Engelhardt, D. Michel, "High Resolution Solid-State NMR of Silicates and Zeolites", Wiley, Chichester, 1987.
46. A. Samosan, E. Lippmaa, G. Engelhardt, U. Lohse, H.-G. Jerschke, *Chem. Phys. Lett.* 134 (1987) 589.
47. J.-P. Gilson, G. C. Edwards, A. W. Peters, K. Rajagopalan, R. F. Wormsbecher, T. G. Robeir, M. P. Shatlock, *J. Chem. Soc. Chem. Commun.* (1987) 91.
48. G. J. Ray, A. Samosan, *Zeolites*, 13 (1993) 410
49. M. Hunger, U. Scheuk, A. Buchhole, *J. Phy. Chem. B.* 104 (2000) 12230.
50. M. Mehring, "Principles of High Resolution NMR in Solids", Springer-Verlag, Berlin, 1983
51. E. Lippmaa, M. Magi, A. Samosan, G. Engelhardt, A. R. Grimmer, *J. Am. Chem. Soc.* 102 (1980) 4889.
52. E. Lippmaa, M. A. Alla, T. J. Pehk, G. Engelhardt, *J. Am. Chem. Soc.* 100 (1978) 1929.

53. M. T. Melchior, D. E. W. Vaughan, A. J. Jacobson, *J. Am. Chem. Soc.* 104 (1982) 4859.
54. J. Klinowski, J. M. Thomas, C. A. Fyfe, J. S. Hartman, *J. Phys. Chem. B.* 85 (1981) 2590.
55. E. Lippmaa, M. Magi, A. Samoson, M. Tarmark, G. Engelhardt, *J. Am. Chem. Soc.* 103 (1981) 4992.
56. C. A. Fyfe, G. C. Gobbi, J. Klinowski, J. M. Thomas, S. Ramdas, *Nature*, 296 (1982) 530
57. S. Ramdas, J. Klinowski, *Nature*, 308 (1984) 521.
58. K- J. Chao, J-Y. Chern, S- H. Chen, D-S. Shy, *J.Chem. Soc. Faraday Trans.* 86, 18 (1990) 3167.
59. C. A. Fyfe, J. H. O' Brien, H. Strobl, *Nature*, 326 (1987) 281.
60. S. Hayashi, K. Hayamizu, O. Yamamoto, *Bull. Chem. Soc. Jpn.* 60 (1987) 105.
61. J. H. Kwak, R. Ryoo, *J. Phys. Chem. B.* 97 (1993) 11154.
62. J. M. Thomas, C. A. Fyfe, S. Ramdas, J. Klinowski, G. C. Gobbi, *J. Phys. Chem. B.* 86 (1982) 3061.
63. J. Klinowski, M. W. Anderson, *J. Chem. Soc. Faraday Trans.* 1 (1986) 569.
64. R. H. Jarman, A. Jacobson, M. T. Melchior, *J. Phys. Chem. B.* 88 (1984) 5748.
65. K. A. Smith, R. J. Kirkpatrick, E. Oldfield, D. M. Henderson, *Am. Mineral.* 68 (1983) 1206.
66. K.J. Chao, J.Y. Chern, *J. Phys. Chem. B* 93 (1989) 1401.
67. K. Gaare, D. Akporiaye, *J. Phys. Chem. B.* 101 (1997) 48.
68. L. Moscou, M. Lakeman, *J. Catal.* 16 (1970) 173.
69. A.E. Hirschler, *J. Catal.* 2 (1963) 428.
70. M. Weihe, M. Hunger, M. Breuninger, H.G. Karge, J. Weitkamp, *J. Catal.* 198 (2001) 299.
71. B. Thomas, S. Sugunan, *Micropor. Mesopor. Matr.* 72 (2004) 227.
72. B. Thomas, S. Sugunan, *Indian J. Chem.* (in press)
73. W. J. Mortier, *J. Phys. Chem. B.* 79 (1975) 1447.
74. E. Dendooven, W. J. Mortier, J. B. Uytterhoeven, *J. Phys. Chem. B.* 88 (1984) 1916.
75. J. J. V. Dun, K. Dhaeze, W. J. Mortier, *J. Phys. Chem. B.* 92 (1988) 6747.
76. C. P. Herrero, *J. Phys. Chem. B.* 95 (1991) 3282.
77. J. J. V. Dun, W. J. Mortier, *J. Phys. Chem.* 92 (1988) 6740.
78. M. L. Costenoble, W. J. Mortier, J. B. Uytterhoeven, *J. Chem. Soc. Faraday Trans. I.*, 73 (1977) 466.
79. J. Catanach, E. L. Wu, P. B. Venuto, *J. Catal.* 11 (1968) 342.

Chapter 3

80. B. M. Lok, B. K. Marcus, C. L. Angell, *Zeolites*, 6 (1986) 185.
81. Y. Cao, R. Kessas, C. Naccacha, Y.B. Taarit, *Appl. Catal. A Gen.* 184 (1999) 231.
82. J. W. Ward, R. C. Hansford, *J. Catal.* 13 (1969) 364.
83. M. Muscas, J. F. Dutel, V. Solinas, A. Auroux, Y. B. Tarrit, *J. Mol. Catal. A Chem.* 106 (1996) 169.
84. R. W. Hansford, J. W. Ward, *Adv. Chem. Ser.* 102 (1971) 354.
85. C. Mirodatos, A. A- Kais, J. C. Verrine, P. Pichat, D. Barthomeuf, *J. Phys. Chem. B.* 80 (1976) 2366.
86. E. F. T. Lee, L. V. C. Rees, *Zeolites*, 7 (1987) 143
87. A. Corma, V. Fomes, F. W. Melo, J. Herrero, *Zeolites*, 7 (1987) 559.
88. Y. S. Chen, M. Guisnet, M. Kern, J. LK. Lemberon, *New J. Chem.* 11 (1987) 623.
89. E. O' Donoghue, D. Barthomeuf, *Zeolites*, 6 (1986) 267.
90. J. A. Martens, S. Souverijns, W. V. Rhijn, P. A. Jacobs, "Acidity and Basicity in Zeolites" in "Handbook of Heterogeneous Catalysis", (Ed. G. Ertl, H. Knozinger, J. Weitkamp), Vol. I (Wiley VCH), 1997, p. 324.
91. M. Stoker, *Stud. Surf. Sci. Catal.* 85 (1994) 429.
92. H. Pfeifer, D. Freude, M. Hunger, *Zeolites*, 5 (1985) 274.
93. P. A. Jacobs, W. J. Mortier, *Zeolites* 2 (1982) 226.
94. S. Khabtov, T. Chevreau, J. C. Lavelley, *Micropor. Mater.* 3 (1994) 133.
95. Hunger M, *Catal. Rev - Sci. E ng*, 39 (1997) 345.
96. W. E. Farneth, R. J. Gorte, *Chem. Rev.* 95 (1995) 615.
97. A. Brenner, D. A. Hucul, *J. Catal.* 56 (1979) 134.
98. J. Ravichandran, B. Sivasankar, *Ind. J. Chem.* 34A (1995) 127.
99. H. Pfeifer, D. Freude, M. Hunger, *Zeolites*, 5 (1985) 274.
100. T. Somasundaram, P. Ganguly, C. N. R. Rao, *Zeolites*, 7, 404 (1987).
101. A. Corma, V. Fomes, L. Formi, F. marquez, J.M. Triguero, D. Mascotti, *J. Catal.* 179 (1998) 451.
102. R. A Beyerlein, G. B Mcvicker, L.N Yacullo, L.N Ziemiak: *J. Phy.Chem.* 92, 1967 (1988).
103. J. T. Miller, P. D. Hopkins, L. Meyers, G. J. Ray, R. T. Roginshki, G. W.Zajac, N. H. Rosenbaum, *J. Catal.* 138 (1992) 115.
104. S. J. Decanto, J. R. Sohn, P. O. Fritz, J. H. Lunsford, *J. catal.* 101 (1986) 132.

Chapter 4

Friedel-Crafts Alkylation 1

"What men call knowledge is the reasoned acceptance of false appearance. Wisdom looks behind veil and sees"

-Sri Aurobindo

The aromatic alkylation is an important acid-catalyzed reaction in industry. For example, octylbenzene is prepared from the alkylation reaction of benzene with 1-octene, octanol, octyl halides etc. In general, this product is a fine chemical widely used as surfactant. Generally this is synthesized industrially using catalysts H_2SO_4 , H_3PO_4 , Hydrofluoric acid, boron trifluoride, and $AlCl_3$. Because of the problems of environmental pollution and corroding facilities in conventional industrial processes, and very low atom efficiency due to irreversible loss of catalysts, it is expected that new types of catalysts, which are well behaved and environmentally friendly, will be developed to replace the conventional catalysts. In recent years many solid acids including metal oxides, sulphides, acidic clays and zeolites have been found to be active for the alkylation reaction. An alkylation process that employs a fixed bed of a stable, non-sludging, solid catalyst has advantages. A successful solid-bed alkylation process demands a solid acid catalyst that is active, selective, regenerable, and stable over prolonged periods of operation in order to be economical compared to hydrofluoric acid or aluminum chloride.

105. J. H. Fleisch, B. I. Meyers, G. J. Ray, J. B. Hall, C. L. Manshall, *J. Catal.* **99** (1986) 117.
106. H. Bremer, U. Lohse, W. Reschetilowski, K. P. Wendland, *Z. Anorg. Chem.* **482** (1981) 235.
107. R. A. Saten, G. J. Kramer, *Chem. Rev.* **95** (1995) 637.
108. K. de Boer, A. P. J. Jansen, van Santen, *Chem. Phys. Lett.* **223** (1994) 46.
109. B. Herreros, P. P. Man, J. M. Manoli, J. Fraissard, *J. Chem. Soc. Chem. Commu* (1992) 464.
110. M. Hunger, G. Engelhardt, *Stu. Surf. Sci. Catal.* **84** (1994) 725.
111. K. Gaare, D. Akporiaye, *J. Mol. Catal. A. Chem.* **109** (1996) 177.

4.1 Alkylation of Aromatics

The alkylation of aromatic rings, called *Friedel-Crafts alkylation*, is a reaction of very broad scope. The products of the reaction are widely used in the large-scale synthesis of petrochemicals and a great variety of fine chemicals and intermediates. The essential feature of the reaction consists in the replacement of a hydrogen atom of an aromatic compound by an alkyl group derived from an alkylating agent. If the replaced hydrogen atom is on the aromatic ring, the reaction is an electrophilic substitution and is carried out in presence of an acid catalyst; if a hydrogen atom on the side chain of an aromatic is replaced, base catalysts or radical conditions are required. Hence it is concluded that the nature of alkylation product depends on the catalyst used (scheme-1). However, the overwhelming majority of commercial alkylations are acid catalyzed.¹

In view of the great theoretical and practical interest in alkylation reaction, there are several review articles which provide valuable information on both mechanistic and synthetic issues¹⁻⁶. Acid catalysts used for the reaction are metal halides and Brønsted acids containing acidic protons. These include acidic halides such as aluminium chloride, boron fluoride, and ferric chloride as metal halides. Protonic acids include sulfuric acid, hydrofluoric acid and phosphoric acid etc¹⁻².

Responsible care and sustainable development have become the paradigms of industrial production. It is therefore required that all industrial processes are optimized with respect to energy efficiency, chemical utilization, waste minimization etc.⁷⁻⁹ The efficient catalytic alkylation of aromatics *via Friedel-Crafts* reaction remains a challenge for the so called *clean technology*. Traditional methods rely the use of stoichiometric quantities of catalyst for the reaction. In this chapter, we would discuss the development of an effective

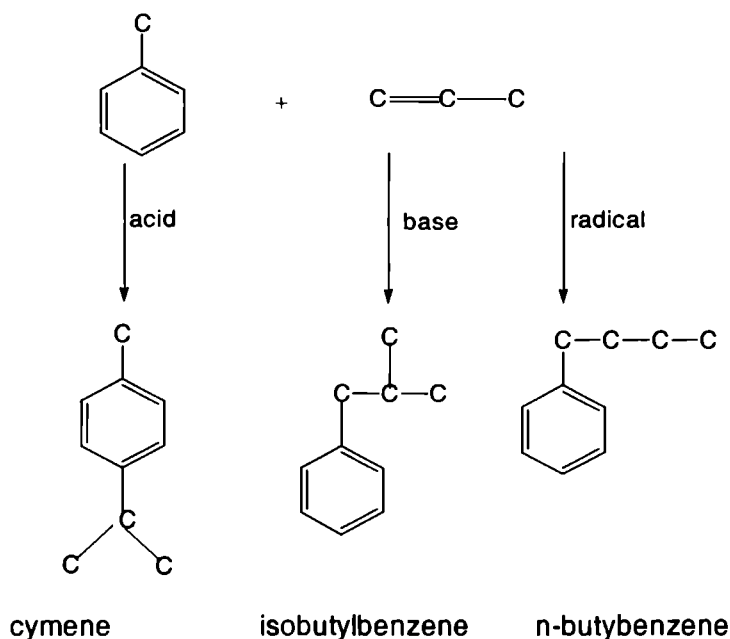
method for the alkylation of benzene with 1-octene. Of several materials used H-mordenite showed good activity while the rare earth version of zeolites noted for better stability towards reaction conditions.

The challenge for chemists and others is to develop new product processes and services that achieve the societal, economic and most importantly environmental benefits that are now required. This requires a new approach which reduce the material and energy intensity of chemical processes and products, minimize or eliminate the dispersion of chemicals to the environment, maximize the use of renewable resources and extend the durability and recyclability of products in which increases the industrial competitiveness.

It has been established that acidic halides, which are typically Lewis acids, have little or no activity for alkylation when used in the pure state. They are activated by the inadvertent presence or addition of small amounts of co-catalyst or promoters, such as water, alcohol or hydrogen halides. These co-catalysts interact with the Lewis acids to generate actual or potential Brønsted acids.¹⁰ Metal halides and Brønsted acid catalysts usually called Friedel-Craft catalysts have been extensively used in the past. They are highly active and allow the reaction to be carried out in the liquid phase at low temperatures. For example, hydrofluoric liquid acid was the alkylation catalyst of choice for the production of branched alkyl benzenes since 1960s. Alkylation reactions using HF is usually carried out in the temperature range 323-353 K. The HF technology is marked by high efficiency, superior product quality, and ease of use relative to other liquid acid catalysts. Even aluminium chloride too is used in ambient temperature conditions. However, the corrosiveness of HF acid and AlCl_3 had negative implications in terms of increased capital cost for the commercial plant as well as disposal of large amounts of neutralized waste products generated in the production process.

Alkylating agents are alkyl halides, alcohols, ether, alkanes, alkenes alkynes and dienes.¹¹ When alkyl halides are used, the reactivity order is $F > Cl > Br > I$.¹¹ However, large-scale alkylations use alkenes almost exclusively; they do not pose a by-product problem, and are quite inexpensively available from thermal catalytic cracking processes. Alkanes are used in commercially developed process, M-forming. It combines in situ alkene production via alkane cracking with simultaneous alkylation of aromatics by the alkenes.¹²

Scheme 4.1. Influence of catalyst type on products from reaction of toluene with propylene.



However, many of the above liquid acid catalysts are highly sensitive to water and extremely corrosive and needs special care in handling.¹³ The normal work-up procedure for reactions employing these acid catalysts involves a water quench which prevents the acid being reused and which on

subsequent neutralization leads to an aqueous salt waste stream. The disposal of this waste stream is a serious concern in these environmentally conscious days. Also, the handling of corrosive liquid acids has negative implications in terms of increased capital cost for the commercial plant. Since the catalysts are irreversibly lost in all the cases, the overall atom efficiency of the process is extremely low. All these make the choice of the catalyst really demanding. Solid acid catalysts are the best alternative for the reaction. An alkylation process that employs a fixed bed of a stable, nonsludging, solid acid catalyst has many advantages. The addition of solid acid catalysts removes the need for the quench step. In addition to being environmentally friendly, the solid acid catalyst is advantageous for enabling the use of quite ordinary metallurgy construction, easy separation of the product and elimination of HF acid or Al waste by-products. Additionally, their reusability is an added advantage.¹³

Many solid acids including metal oxides¹⁴⁻¹⁶, silicotungstic acid¹⁷, sulfated metal oxides^{9,18-19}, clays²⁰⁻²¹, cation exchanged resins,²²⁻²⁸ mesoporous materials²⁹⁻³², and most importantly microporous aluminosilicates, namely acidic zeolites (includes fluorided silica-alumina) are highly active for the alkylation of aromatics.^{21, 33-44} Unfortunately many of these solid acid catalysts such as clays and zeolites have significantly lower alkylation activities than the common homogeneous acids, although they give greatly improved reaction selectivity. Thus, while the reaction of benzene with linear alkenes using AlCl₃ occurs rapidly at room temperature, the corresponding reactions with zeolites occur only under forcing conditions of temperature and pressure.¹⁰ This is however, not necessarily a disadvantage. Alkylations are usually exothermic reactions. For example, the synthesis of ethyl benzene from benzene and ethylene occurs with a reaction enthalpy of -113 kJmol^{-1} . Operations at high temperature allow much of this heat to be economically recovered, in contrast to low temperature synthesis. A successful solid bed alkylation process

demands a solid acid catalyst that is active, highly selective, stable over prolonged period of operation and regenerable to be economical compared to hydrofluoric acid.

4.2 Alkylation of Benzene with 1-Octene

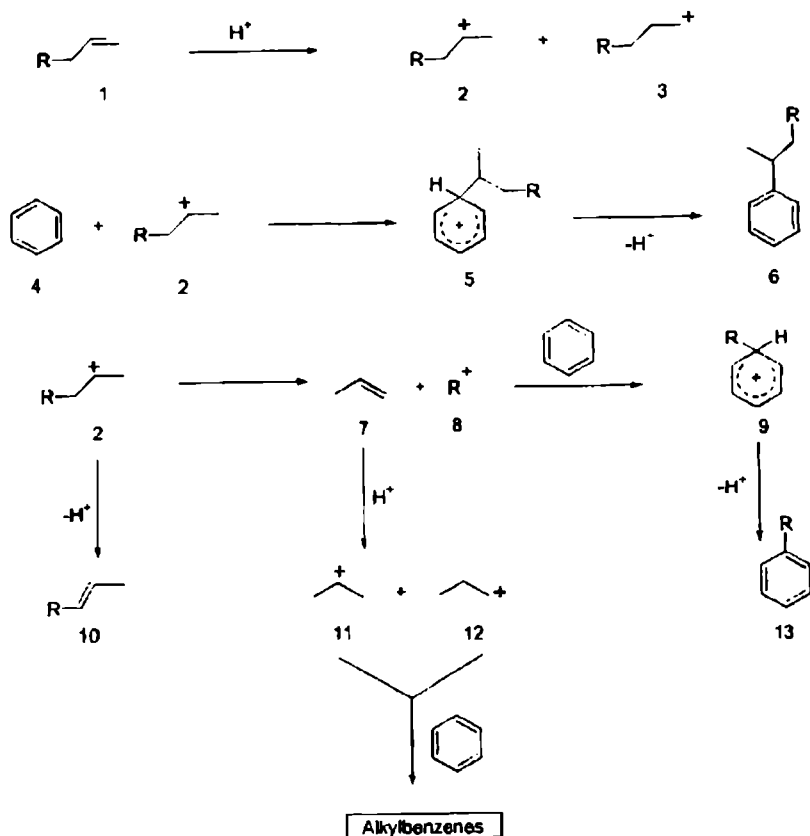
Earlier workers reported the formation of only one phenylalkane in the alkylation of benzene with long chain 1-olefins in the presence of Friedel-Crafts catalysts.⁴⁵⁻⁴⁶ Subsequent investigations by many workers have definitely established that isomerization occurs and that all the possible phenylalkanes are obtained except the 1-phenyl isomer.⁴⁷⁻⁴⁸ The generally accepted mechanism for Friedel-Crafts alkylation reactions involves interaction of the olefin with the catalysts to form a carbocation, the corresponding ion pair, or polarized complexes. This undergoes rapid isomerization in varying degrees and finally attacks benzene in what is considered to be the rate-determining step, to form the product.⁴⁹

The carbocation alkylation of arenes with detergent range of linear olefins via protonic acids typically produces mixed phenylalkanes that are positional isomers i.e., 2-phenyl, 3-phenyl, etc.⁴⁶ In the present case of 1-octene, four carbocations are possible and the relative stabilities of them increases towards the center of the chain. So the least stable is the primary ion (1- position) and due to its very low stability, 1-phenyl isomer is not detected in the product. On the basis of relative stabilities of the other carbocations (all secondary), it is expected that the isomer content increase towards the center of the chain. This is found to be so in the case of HF acid, in which the thermodynamic equilibrium is probably reached. However, in the case of HFAU-Y, rare earth exchanged zeolite-Y and H-mordenite zeolites, the 2-phenyl isomer content is greater suggesting the non-attainment of thermodynamic equilibrium.

Chapter 4

In the mechanism prescribed in scheme-2, a carbocation (2, 3 or 4) generated by accepting a proton from zeolite (2, 3 etc). 2-carbocation attacks benzene ring leading to the formation of an intermediate 5, which eliminate proton producing 2-phenyloctane (6). In a similar way the interaction of other carbocation isomers produce other phenyloctane isomers (not given). Multiple attacks of the carbocation on the benzene ring lead to the formation of dialkylates and trialkylates.

Scheme 4.2. Alkylation/cracking/isomerization reaction of 1-octene with benzene over zeolites.



The possible mechanism for the alkene cracking and isomerization are depicted in the remaining part of the scheme. However, these reactions occur to a limited extent under the given reaction conditions and the identification of those products was not done. Also, our main concern was to improve the selectivity towards the most desired 2-phenyl isomer.

The conversion of 1-octene and selectivity for the 2-phenyloctane were calculated according to the method proposed by J. L. G. de Almeida et al.²

$$\text{Conversion} = \frac{N_{A0} - N_A}{N_A} \times 100$$

where, N_{A0} is the initial number of moles of 1-octene and

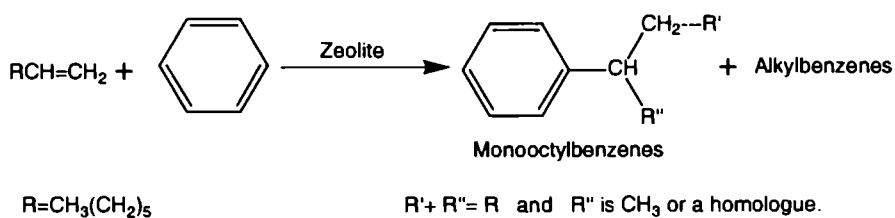
N_A is the number of moles of 1-octene at time t .

and

$$\text{Selectivity} = \frac{N_n}{N_{A0} - N_A} \times 100$$

where, N_n is the number of moles of product n . Also the alkylation of benzene with 1-octene is represented in scheme-1.

Scheme 4.3. Alkylation of benzene with 1-octene over zeolite catalyst leading to the formation of phenyloctanes.



4.3 Optimization of reaction conditions

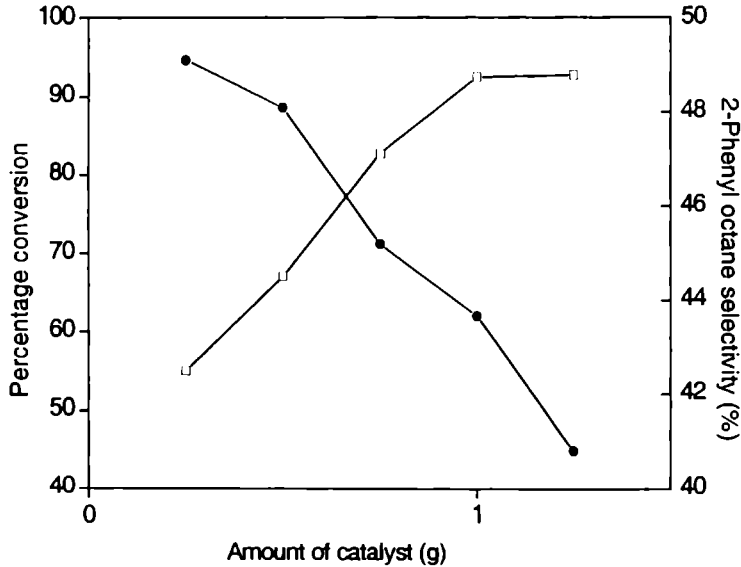
Reaction variables have a predominant influence for any reaction. Influence of parameters such as reaction temperature, benzene to 1-octene

molar ratio, concentration of the catalyst, and feed rate or weight hourly space velocity (WHSV, h^{-1}). The deactivation studies or time on stream (TOS) studies were performed for representative samples such as H-Y, CeNa-Y, LaNa-Y, K-, CeK-Y, Mg-Y, CeMg-Y, CeH-Y, and H-mordenite zeolites. Nature of carbonaceous compounds inside the zeolite cavities was done for H-Y and CeNa-Y zeolites.

Catalyst loading

Amount of catalyst loaded is one of the key parameters, which play an important role in determining the total conversion and the selectivity for a particular product. Total conversion of 1-octene and selectivity for 2-phenyloctane formation has been studied by varying the amount of the catalyst keeping the other variables constant. Figure-4.1 shows the dependence of the amount of catalyst on the conversion and selectivity. It is seen that with increment in the catalyst loading from 0.25 g to 1.25 g the total conversion increases from 55 to 62.7%. With the increase of catalyst loading the probabilities for reaction over the external surface acid sites is increased and the selectivity for 2-phenyl isomer decreases a little from 49.1 to 40.8%. However, at the same time other isomers (3-phenyl and 4-phenyl) are also detected. Also, with increase of the catalyst weight the adsorption and desorption of the reactants and products from the catalyst surface becomes slow providing enough time for the isomerization of the 2-carbonium ion formed to the internal carbocation (3 and 4-phenyl). This explains the decreased formation of 2-phenyloctane at high catalyst loadings.

Figure 4.1. Influence of amount of catalyst on the total conversion of 1-octene and selectivity for 2-phenyloctane.



(●) Selectivity of 2-phenyloctane, (□) 1-octene conversion

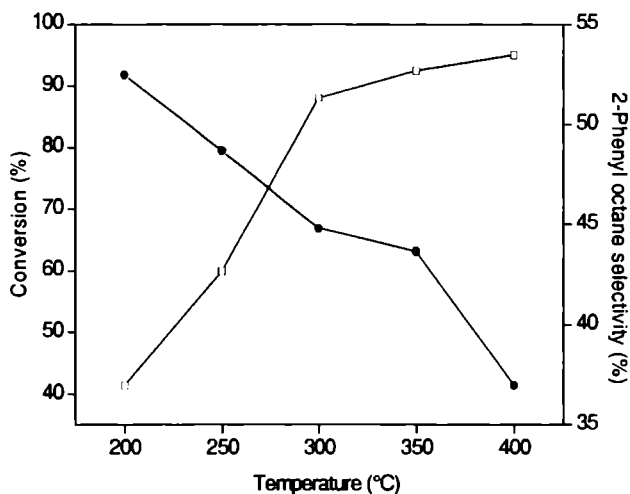
Notes: Catalyst- HFAU-Y, temperature 623 K, weight hourly space velocity- 3.43 h^{-1} , benzene to 1-octene molar ratio 20:1, TOS- 3 hours, and constant flow of nitrogen (10mL/h).

II. Influence of reaction temperature

Temperature of the catalyst bed has a predominant role in deciding the efficiency of the catalyst. For example, liquid acid catalysts such as HF acid or AlCl_3 catalyze alkylation reactions at low temperature, whereas a solid acid catalyst like zeolite catalyze the same reaction at an elevated temperature. Hence the conversion of the reactant and selectivity for a product could be suitably adjusted by varying the temperature. Influence of temperature on the alkylation of benzene with 1-octene was studied over a range from 473 to 673 K at a temperature interval of 50 K. The total conversion and selectivity for 2-phenyloctane

at various temperatures are shown in Figure 4.2. It is seen that at 473 K there is good selectivity for 2-phenyloctane formation even though the conversion is low.

Figure 4.2. Influence of temperature on the total conversion of 1-octene and selectivity for 2- phenyloctane.



(●) Selectivity of 2-phenyloctane, (□) Conversion of 1-octene

Votes: Catalyst- H-Y, catalyst amount- 1000 mg, weight hour space velocity- 3.43 h^{-1} , benzene to 1- octene molar ratio 20:1, TOS- 3 hours, constant flow of nitrogen (10mL/h).

This could be explained as follows. In the reaction of benzene with α -olefin such as 1-octene in presence of zeolite catalysts at higher temperatures, it is evident that the intermediate carbocation undergoes a series of fast hydride shifts to produce the isomer ions. However, evidence has been obtained which suggests that the hydride transfers, though rapid are not instantaneous³⁶⁻³⁷, and some of the carbocations may react before undergoing rearrangement.³⁸ Therefore, it is of interest to find out if the isomerization of carbocation is fast enough to allow the isomeric ions to attain the equilibrium distribution before they attack benzene. Now, as the temperature increases isomerization of 2-

carbonium ion to other isomer through fast hydride shifts which increases the probability of formation of other phenyl isomers such as 3 and 4-phenyloctane with a corresponding decrease in the 2-phenyl isomer formation. Also, as the temperature increases from 473 to 673 K, the total conversion increases at the expense of selectivity. This might be due to the increasing probabilities of catalytic cracking, rapid equilibration of the olefin isomer or easy diffusion of the bulkiest LAB isomer out of the zeolite cavities at higher temperature. At 673 K the selectivity was only 37 %.

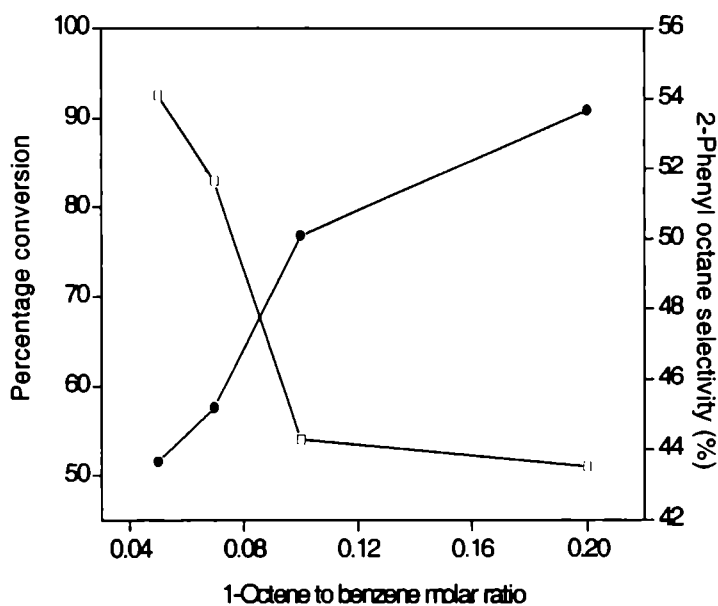
III. Effect of molar ratio (solvation effect)

The effect of molar ratio between benzene and 1-decene is presented in Figure-4.3. It is seen that as the molar ratio of benzene and olefin increases from 1:1 to 1:25, the conversion of alkene and selectivity of 2-phenyldecane increases. Selectivity towards monoalkylated product goes up from 82.2 to 92.1%. There is a corresponding decrease in the dialkylate formation. This could be explained in terms of solvation effect of benzene in higher molar ratios. In the alkylation of benzene with 1-octene, the solvation of the reaction intermediates by solvent molecules apparently reducing the differences in their stabilities, which results in greater formation of 2-phenyldecane. This effect is practically absent when the molar ratio of benzene and 1-decene is 1:1. Excess benzene acts as solvent. The studies on the effect of molar ratio of benzene and 1-octene on the 2-phenyl isomer selectivity confirms such an observation (2-phenyldecane selectivity was 20.9% when the molar ratio is 1:1 and 48.5% when it was 25:1). The involvement of solvent in certain reactions of free radicals involving the selectivity of chlorine atom has been reported by Russel.⁵⁰ Stock and Brown have suggested that this applies equally well to electrophilic reagents in aromatic substitution reactions.⁵¹⁻⁵² Other examples involving the change of reactivity of the reagent due to interaction with the

solvent have been observed in connection with the reaction of molecular chlorine with benzene.⁵³

The solvation effect of benzene in the reaction is further confirmed by performing the reaction in presence of diluent non-polar liquid. We used n-hexane for this purpose. The three reagents are taken in the molar ratio of 1:8.75:10.45 (benzene to olefin ratio is well within the industrial range) and passed through the catalyst (H-Y zeolite) at the reaction temperature and feed rate as usual. Total conversion was 66.8% and the selectivity for the 2-phenyl isomer was only 33.9%. The 2-phenyl isomer selectivity

Figure 4.3. Conversion of 1-octene and selectivity for 2-phenyloctane as a function of molar ratio of benzene and 1-octene



(□) Selectivity of 2-phenyloctane, (•) Conversion of 1-octene

Notes: Catalyst- HFAU-Y, catalyst amount- 1000 mg, weight hour space velocity- 3.43 h^{-1} , reaction temperature- 623 K, TOS- 3 hours, constant flow of nitrogen (10 mL/h).

decreases from 46.1 to 33.9%. This could be explained as follows; addition of large amounts of n-decane removes benzene from the immediate vicinity of the intermediate ion pairs and magnifies the difference in their stabilities. Actually the solvation of carbonium ion slows down the rate of isomerization to the internal isomers and thereby increasing the rate of alkylation reaction with benzene. Thus, the addition of n-decane not only reduces the rate of attack of carbonium ion on the benzene but also promote isomerization to the more stable internal isomers by removing the solvation effect of benzene around the carbonium ion. Also, since benzene is taken in excess, the reaction is supposed to follow pseudo unimolecular mechanism.

IV. Influence of feed rate (or weight hourly space velocity)

Feed rate is an important parameter in vapor phase reactions. The influence of WHSV on catalytic activity of H-Y zeolite was checked by conducting the reactions at four different space velocities. Data on Table 4.1 shows the variation of conversion and selectivity with change of flow rate (or weight hourly space velocity, h^{-1}) over the representative H-Y zeolite. As the flow rate increases from 3 to 5 mL per hour (2.57 to 4.28 h^{-1}) the conversion decreases from 94.6 to 80.9% whereas the selectivity increases from 35.9 to 46.7%.

Table 4.1. Conversion of 1-octene and selectivity for 2-phenyloctane as a function of weight hour space velocity of reactant.

Flow rate (ml/hour)	Weight hourly space velocity (h^{-1})	Percentage conversion	2-Phenyl octane selectivity (%)
3	2.57	90.6	55.90
4	3.43	92.6	53.71
5	4.28	80.9	46.71
6	5.15	79.45	50.54

Notes: Catalyst- HFAU-Y, reaction temperature- 623 K, amount of catalyst- 1000 mg, 1-octene to benzene molar ratio- 1:20, TOS- 3 hours, constant flow of nitrogen (10 mL/h).

Lower space velocities imply higher contact time ($1/WHSV$) for the reactants on the active sites and hence increased conversions. This increase in selectivity might be due to the less time the reactants spend inside the pores of the zeolite, which reduces the chances of isomerization of 2-carbocation to 3 and 4 isomers.

4.4 Activity of different systems

Table-2 demonstrates the catalytic activity of the pure binder free sodium zeolite, HFAU-Y, various rare earth exchanged Na-Y zeolites, H-mordenite, H-10 montmorillonite and a lab made 1:1 silica-alumina. Binder free sodium exhibits very low activity towards the reaction.

Table 4.2. Conversion of 1-octene and selectivity for 2-phenyloctane over different Na-Y zeolite, different RE-exchanged zeolites and some other common alkylation catalysts during the alkylation reaction.

Catalyst system	Alkene conversion (%) ¹	2-Phenyl octane selectivity (%)	Dialkyl benzenes (%)	Others ² (%)
Na-Y	13.0	40.0	1.6	58.4
H-Y	92.6	43.6	2.0	54.4
LaNa-Y	81.4	61.0	4.0	35.0
PrNa-Y	71.8	56.0	2.1	41.9
RENa-Y	74.5	61.7	3.8	34.5
SmNa-Y	82.1	62.5	4.3	33.5
H-Mor	94.1	74.0	1.4	24.6
H-10 Mont	71.2	33.1	0.9	66.0
SiO ₂ -Al ₂ O ₃	68.4	32.5	1.1	66.4

Notes: Reaction temperature- 623 K, amount of catalyst- 1000 mg, 1-octene to benzene molar ratio- 1:20, weight hourly space velocity- 3.43 h^{-1} , time on stream 3 h, constant flow of nitrogen (10 mL/h). ¹ Alkene conversion include small amount of double bond isomerization and subsequent alkylation. ² Others include mainly 3-phenyl and 4-phenyloctanes, 1-octene isomers, and small amounts of other lower alkylbenzenes formed during the reaction through cracking of 1-alkene and further alkylation.

Exchange of Na⁺ ions with rare earth cations improve the activity considerably. Silica-alumina exhibits lower activity and selectivity than the as-exchanged forms. However, H-mordenite (used as model alkylation catalyst for the reaction throughout) produce very high amount of 2-phenyl isomer due to its very specific shape selectivity.

Table 4.3. Conversion of 1-octene and selectivity for 2-phenyloctane over parent K-Y zeolite, different as-exchanged K-Y zeolites and some other common alkylation catalysts

Catalyst system	Alkene conversion (%) ¹	2-Phenyl octane selectivity (%)	Dialkyl benzenes (%)	Others (%) ²
K-Y	12.5	42.2	1.4	56.4
H-Y	92.6	43.6	2.0	54.4
K-Y	12.5	42.2	1.4	56.4
CeK-Y	73.1	60.8	3.6	35.6
LaK-Y	65.0	57.5	1.9	40.6
REK-Y	69.4	60.2	2.8	37.0

Notes: Reaction temperature- 623 K, amount of catalyst- 1g, 1- octene to benzene molar ratio- 1:20, weight hourly space velocity- 3.43 h⁻¹, time on stream 3 h, constant flow of nitrogen (10 mL/h). ¹ Alkene conversion include small amount of double bond isomerization and subsequent alkylation. ² Others include mainly 3- phenyl and 4-phenyloctanes, 1-octene dimers, and small amounts of other lower alkylbenzenes formed during the reaction through cracking of alkene.

Table-4.3 depicts the percentage conversion and selectivity of binder free K-Y zeolite, pure HFAU-Y and different as-exchanged rare earth exchanged K-Y zeolites. As in the former case of Na-Y, K-Y could produce nominal conversion of 1-octene. HFAU-Y has very high conversion under the reaction condition, but at the expense of selectivity for the desired product. Here also, exchange of the residual cation (K⁺) with rare earth metal ion enhances the catalytic activity as well as selectivity for the 2-phenyl isomer.

Table 4.4. Conversion of 1-octene and selectivity for 2-phenyloctane over different Mg-Y zeolite, different as-exchanged rare earth Mg-Y zeolites during the alkylation reaction.

Catalyst systems	Alkene Conversion (%) ¹	2-Phenyl octane selectivity (%)	Dialkyl benzenes (%)	Others (%) ²
Hg-Y	42.3	48.4	2.1	49.5
H-Y	92.6	43.6	2.0	54.4
Hg-Y	42.3	48.4	2.1	49.5
LaMg-Y	84.7	66.7	4.4	28.9
LaMg-Y	70.3	58.2	2.5	39.3
LaEMg-Y	78.1	63.4	2.4	34.2

Notes: Reaction temperature- 623 K, amount of catalyst- 1g, 1-octene to benzene molar ratio- 1:20, weight hourly space velocity- 3.43 h⁻¹, time on stream 3 h, constant flow of nitrogen (10 mL/h). ¹ Alkene conversion include small amount of double bond isomerization and subsequent alkylation. ² Others include mainly 3-phenyl and 4-phenyloctanes, 1-octene dimers, and small amounts of other lower alkylbenzenes formed during the reaction through cracking of alkene.

Table-4.4 presents a clear picture of the total conversion of 1-octene and the corresponding selectivity for the 2-phenyloctane isomer with pure Mg-Y zeolite and its rare earth modified forms. Pure Mg-Y converts much more 1-octene than the corresponding Na or K forms. Exchange of Mg²⁺ ions with rare earth ions further improve the conversion and selectivity for the formation of the desired 2-phenyl isomer to a great extent. However, even then these zeolites are far less active compared to H-mordenite zeolite.

Table 4.5. Conversion of 1-octene and selectivity for 2-phenyloctane over parent HFAU-Y zeolite and different as-exchanged rare earth H-Y zeolites.

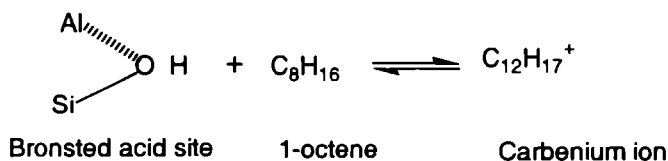
Catalysts system	Alkene conversion (%) ¹	2-Phenyloctane selectivity (%)	Dialkyl benzenes (%)	Others (%) ²
Na-Y	13.0	40.0	1.6	58.4
H-Y	92.6	43.6	2.0	54.4
HCe-Y	89.5	62.1	5.2	32.3
HLa-Y	78.5	56.8	3.7	39.5
HRE-Y	82.7	58.4	4.3	37.3

Notes: Reaction temperature- 623 K, amount of catalyst- 1g, 1- octene to benzene molar ratio- 1:20, weight hourly space velocity- 3.43 h⁻¹, time on stream 3 h, constant flow of nitrogen (10 mL/h). ¹ Alkene conversion include small amount of double bond isomerization and subsequent alkylation. ² Others include mainly 3- phenyl and 4-phenyloctanes, 1-octene dimmers, and small amounts of other lower alkylbenzenes formed during the reaction through cracking of alkene.

Tables- 4.2 to 4.5 show the percentage conversion of 1-octene and selectivity for the 2-phenyloctane under the given reaction conditions over HFAU-Y and different as-exchanged rare earth zeolites. Pure HFAU-Y shows the highest conversion among all the zeolites. However, the selectivity for the desired product is very less. When the H⁺ ions are subsequently replaced with rare earth metal ions such as Ce³⁺, La³⁺ and RE³⁺, the selectivity for 2-phenyl isomer increases at the expense of a nominal decrease in the total conversion of the olefin.

Binder free sodium and potassium Y zeolites show very low activity and selectivity for the conversion of 1-octene to 2-phenyl isomer. The effect of sodium ions on the activity of Brønsted type of zeolites in acid catalyzed reactions has been recognized very early especially in the case of faujasite type of zeolites. It was proposed that the residual Na⁺ ions have a poisoning effect on the acidity i.e. a particular Na⁺ ion, present within the decationated

zeolite, has a neutralizing effect over a large number of the existing protons.^{42, 53, 54-57} Recently, it has been shown that the effect of residual Na⁺ ions was to weaken the Brønsted acid sites, without actually neutralizing more than one Brønsted site per Na⁺ ion. Since potassium is much more basic in nature than sodium this negative effect on the BAS might be more pronounced. It is indeed more evident as seen in Table-3. The alkylation ability of all the potassium derivatives is far inferior to the corresponding sodium zeolites. As the sodium content decreases on exchange of it with rare earth cations, there is an increase in the Brønsted acidity as evidenced by thermodesorption studies of 2,6-DMP adsorbed samples. An increased strength of Brønsted acid strength would increase the lifetime of the intermediate carbocation generated by taking a proton from zeolite by the C₈ olefin. This improves the chances of addition of the carbocation to the benzene molecule, thus improving the alkylation of benzene with 1-octene.⁵⁴



Consistent with the increase in Brønsted acidity, all the rare earth exchanged zeolites exhibit better conversion of 1-octene and selectivity for 2-phenyloctane than the pure binder free Na-Y zeolite. Among different rare earth forms, CeNa-Y and SmNa-Y shows maximum conversion and selectivity. This is in agreement with their maximum Brønsted acidity. LaNa-Y and RENa-Y, LaK-Y and REK-Y and LaMg-Y and REMg-Y all show comparable activity and selectivity for the desired 2-phenyl isomer. Upon heat treatment lanthanum ions tend to migrate from super cation site (SI) to small sodalite cation site (SI') thus producing BAS, which are non-accessible. Consequently LaNa-Y zeolite shows low acidity [both total acid amount (from NH₃-TPD) as

well as Bronsted acidity (from thermodesorption of 2,6-DMP, performed only for sodium derivatives)]. The specific influence of La^{3+} ion is discussed in detail in the previous chapters. This weak acid structure might be the reason for the moderate activity of LaNa-Y zeolite towards the alkylation reaction. From the chemical composition studies it is seen that in the case of RENa-Y, the main counter cation is La^{3+} with small amounts of Ce^{3+} , Pr^{3+} , Nd^{3+} , and Sm^{3+} . It has similar acid structure (both total as well as BAS). This explains the comparable activities of LaNa-Y and RENa-Y towards the reaction.

All rare earth exchanged Mg-Y and H-Y zeolites were found to be catalytically more active than their corresponding rare earth exchanged Na-Y and K-Y counterparts for the alkylation of benzene with 1-octene. For the various residual cations (H^+ , Na^+ , K^+ and Mg^{2+}) activity follows the order $\text{H}^+ > \text{Mg}^{2+} > \text{Na}^+ > \text{K}^+$. The difference in activity could be correlated with the concentration of available OH groups in the zeolite structure.⁵⁸ Weihe et al. reported that the concentration of bridging OH groups in the large cages, i. e., of BAS accessible to hydrocarbons, was at least 20% lower in LaK forms than the corresponding LaNa form in FAU-Y and EMT zeolites for carefully dehydrated samples.⁵⁸ ^{139}La MAS NMR spectroscopy of the dehydrated zeolites indicate that the concentration of La^{3+} ions in the large cages is clearly lower for LaK zeolite than for the corresponding LaNa form. Consistent with this observation rare earth exchanged K zeolites show far inferior activity compared to sodium counterpart. The presence of large potassium (0.302 nm) hinders the formation of accessible BAS in the large cages (repulsive interactions of large potassium ions enhance the migration of rare earth cations from large cages into small cages.⁵⁸ This repulsive interaction is very much smaller in the case of sodium (0.204 nm) cations) i. e. bridging OH groups are preferentially formed in the small cages where they are not accessible for the hydrocarbons used as reactants in the study. This influence of residual cations

On physico-chemical and catalytic activity of various zeolites is reported elsewhere.⁵⁹⁻⁶¹ It is therefore stated that the availability of accessible BAS is one of the key factors which determines the catalytic activity of zeolites.

Magnesium cation too produces greater migration of counter cations from super cages to small cages due to its greater charge and larger diameter. The repulsive interaction is more in the case of magnesium and it induces greater strain on the framework and effects even greater migration of rare earth cations from super to small cages compared to the corresponding sodium or potassium derivatives and the number of accessible BAS might be even lower in this case. However, magnesium derivatives exhibit better alkylation activity compared to K or Na derivatives. The very specific influence of Mg cations, which improves significantly the catalytic performance by introducing a high acid strength, is most likely due to its high polarizing power which effects the OH bond strength through the lattice.⁶²⁻⁶³ This effect seems to outplay the effect of cation migration. It was reported previously that another small and highly polarizing cation Li^+ , also exhibit increased acid strength and catalytic activity.⁶⁴

Table- 3.6 in chapter-3 presents the number of active sites per unit area of the catalyst. As-exchanged zeolites show comparatively large number of active sites per unit area than the pure binder free Na-Y zeolite. SmNa-Y has the maximum number of such sites among different rare earth zeolites. Comparing the number of active sites and the activity/selectivity of the zeolites, there is a perfect correlation between the two in the case of rare earth exchanged zeolites. SmNa-Y with maximum number of such sites effects the best conversion and has maximum selectivity for the 2-phenyloctane. Na-Y zeolite, as expected with its minimum number of active sites is nearly inefficient as an alkylation catalyst. There is wide difference in the product distribution between different rare earth exchanged zeolites, pure H-Y and H-Mor. Two main reasons attributed by Alul for the difference in the product distribution are

(1) the existence of two equilibrium steps, one for the olefin (1-octene) and another for the phenyloctanes (products) and (2) the differences in the rate of two reactions; olefin isomerization and alkyl benzene isomerization over the catalyst.⁶⁵ Over the as-exchanged zeolites these two equilibrium steps seems to be the same and have almost the same conversion and selectivity to the desired product.

To compare the activity of different as-exchanged zeolite-Y systems with standard catalytic systems, alkylation of benzene with 1-octene was performed over H-mordenite. It shows much high activity and selectivity for this reaction, 94.1 and 74.7% respectively. This variation in activity is due to their structural difference. HMOR has a bi-directional pore system with parallel circular 12-ring channels (0.65 x 0.70 nm) and elliptical 8-ring channels (0.26 x 0.57). However, it practically functions as unidirectional pore system as the 8-ring channels do not allow the passage of the common organic molecules whereas, H-Y or its modified systems have large cavities (1.3 nm diameter) along with the 3-D pore systems (0.73 nm). The shape selectivity associated with the zeolites has its origin in the well-defined pore structure, which could be manipulated to some extent. Since diffusional restrictions are often encountered in zeolites with larger substrates, the quest for other materials that have large pore dimension has been the subject of intense research. K-10 montmorillonite clay is a layered alumino-silicate with an octahedral layer sandwiched between two tetrahedral layers. This, unlike any other zeolites used does not have a regular pore structure. The structure of the clay constitutes micropores and mesopores. The amount of mesopores is often less when compared to the amount of micropores. This explains the reduced surface area and pore volume when compared to zeolites. However, the average pore size is greater than zeolites (>1.0 nm).⁶⁶⁻⁶⁸ In the case of H-mordenite, shape selectivity appears to play an important role producing

maximum 2-phenyl isomer. However they suffer from very fast deactivation as evident from time on stream studies (see next section; 4.5). It is seen that K-10 montmorillonite and silica-alumina show much inferior alkylation ability than the zeolites and produce much lower amounts of 2-phenyl isomer. The lack of shape selectivity in both the cases must be the reason for their inferior ability for the formation of 2-phenyl isomer.

4.5 Deactivation studies

Though zeolites possess very high activity and selectivity for the production of 2-phenyl isomers, unfortunately they are not very stable, and stability is one of the most important qualities for an industrial catalyst. Because of the fast deactivation, catalyst regeneration is inevitable and very important for the industrial application of the catalyst. The conventional method of catalyst regeneration is to burn the deactivated catalyst with air or oxygen. However, since alkylation of benzene with higher olefins like 1-octene, 1-undecene etc. on zeolite catalyst is usually operated under relatively low temperature and reactants and products are in the liquid phase. There will be large amounts of reactants and products adsorbed in the pore structure of the catalyst and identification of these trapped compounds are important for understanding the nature and cause of deactivation of the catalyst.^{21, 42, 68} It has been proposed that the deactivation is due to the formation and trapping of heavy alkylate (known as coke) in the pores and cavities of zeolites.⁶⁸⁻⁷⁷ Da et al. proposed that the deactivation of large pore zeolites like H-FAU, H-MOR, etc. during the alkylation of toluene with 1-heptene, is due to heptyltoluenes locked in the pores.⁶⁸ Deactivation cannot be completely avoided and regeneration of catalyst by coke removal is inevitable for the industrial application of the catalyst.⁶⁹⁻⁷¹ Generally, coke removal is carried out through oxidative treatment under constant flow of air at high temperature. The

regeneration temperature has great effect on the activity of the regenerated catalyst. The product distribution for the deactivated and the regenerated zeolite catalyst is almost identical.^{69-71, 73, 75}

Alkylation reaction was carried out for 14 hours continuously over the zeolite catalyst (HFAU-Y, CeNa-Y, LaNa-Y, CeK-Y, CeMg-Y, CeH-Y, and H-mordenite) and products were collected at intervals of 2 hours. The deactivated catalyst was taken out from the reactor, extracted many times with acetone, dried in the oven at 383 K overnight and XRD profile taken. It was then kept in a silica crucible inside the muffle furnace and was then calcined at different temperatures in the range of 423-773 K and at 773 K for 5 hours with a heating rate of 12 K/ min with a constant air blowing over the sample (as described in the experimental section).

. Comparing these patterns, we see that the patterns are missing or their intensities are diminished for the deactivated zeolite. This is clearly due to the deposition of coke. But upon regeneration of the deactivated sample, all the peaks reappeared with almost same intensity. Carrying out the reaction with the regenerated sample we could get a maximum conversion of 91.5% and selectivity 43.5%, which is very close to the conversion obtained for the fresh catalyst.

The conversion and selectivity as a function of reaction time (or TOS) is shown in Tables-4.6 and 4.7 and Figure-4.4. The percentage conversion of 1-octene increases initially from second hour to approximately six hours whereas; the selectivity for 2-phenyloctane increases very slowly from second hour. The total conversion at 10 hours time was 90.3%, while the selectivity was 52.9%. Maximum selectivity of 57.5% was observed after 12 hours in the case of H-Y zeolite. Also, H-mordenite seems to undergo very fast deactivation with time and it lost as much as 40% activity (H-Y lost mere 12% activity under similar reaction conditions and TOS) in 14 hours (conversion at forth the hour was 94.9% and

at 14 hours 59.4%). At the same time the selectivity for the desired 2-phenyl isomer increases slightly to 80.9%. All the as-exchanged zeolites exhibit better stability (CeNa-Y lost almost 9% activity in 14 hours) than H-Y or H-mordenite zeolites. Thus, we conclude that rare earth exchange of zeolite-Y invariably enhances the resistance towards deactivation.

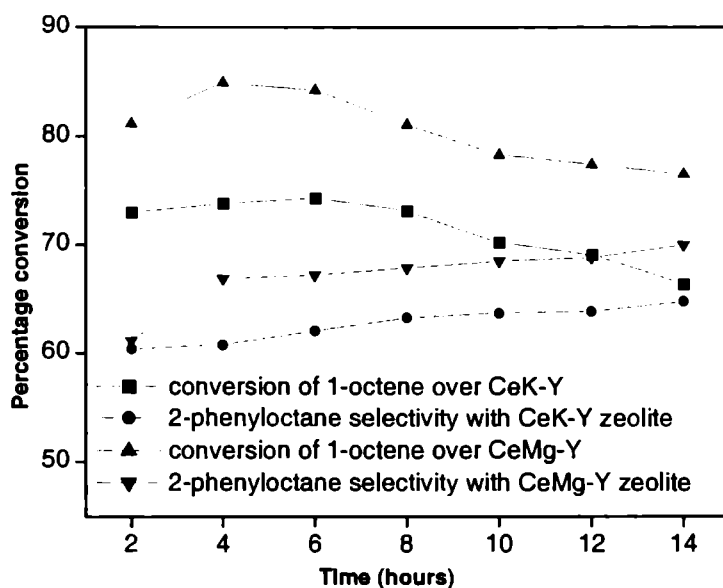
Table 4. 6. Deactivation of H-Y zeolite and rare earth exchanged CeNa-Y and LaNa-Y zeolites during the alkylation of benzene with 1-octene.

Catalyst system	Time (hours)							
	2	4	6	8	10	12	14	
H-Y	Conversion for 1-Octene (%)	64.0	92.6	92.8	93.2	90.3	84.2	81.1
	Selectivity for 2-Phenyloctane (%)	34.5	43.7	51.8	50.7	52.9	57.5	56.7
	Dialkylbenzenes (%)	3.9	3.5	3.2	3.2	2.4	2.3	2.0
CeNa-Y	Conversion for 1-Octene (%)	77.3	81.0	80.8	80.4	80.3	79.2	78.9
	Selectivity for 2-Phenyloctane (%)	64.5	66.1	66.3	66.9	67.5	67.7	68.9
	Dialkylbenzenes (%)	4.5	4.2	3.9	3.4	3.2	1.7	1.1
LaNa-Y	Conversion for 1-Octene (%)	71.9	76.9	72.4	72.2	72.0	71.2	70.4
	Selectivity for 2-Phenyloctane (%)	61.5	64.1	64.4	64.6	64.6	64.9	65.3
	Dialkylbenzenes (%)	3.4	2.8	2.0	1.8	1.6	1.6	1.5

Notes: Reaction temperature- 623 K, amount of catalyst-1g, 1-octene to benzene molar ratio- 1:20, weight hourly space velocity- 3.43mL, constant flow of nitrogen (10mL/h).

Da et al. reported that during the alkylation of toluene by 1-heptene, a very strong retention of monoheptyltoluene (MHT), biheptyltoluene (BHT) and triheptyltoluene (THT) inside the HFAU-Y microporous.⁷⁵ The distribution of the compounds occluded in the zeolite pores changes with reaction time; the percentage of MHT increases with time at the expense of BHT and THT. This could be due to pore mouth transalkylation reaction between bi and tri alkylation products trapped inside the zeolite pores and toluene molecules.⁷³ Again, Da et al. proposed that the deactivation of HFAU zeolite during the alkylation of toluene with 1-dodecene is mainly due the blocking of pores by monododecyltoluene (MDT), bidodecyltoluene (BDT) and tridodecyltoluene (TDT) etc.^{69, 73}

Figure 4. 4. Influence of reaction time on the percentage conversion of 1-octene and selectivity for the formation of 2-phenyloctane over as-exchanged CeK-Y and CeMg-Y zeolites



Notes: Reaction temperature- 623 K, amount of catalyst-1g, 1- octene to benzene molar ratio- 1:20, weight hourly space velocity- 3.43mL, constant flow of nitrogen (10mL/h).

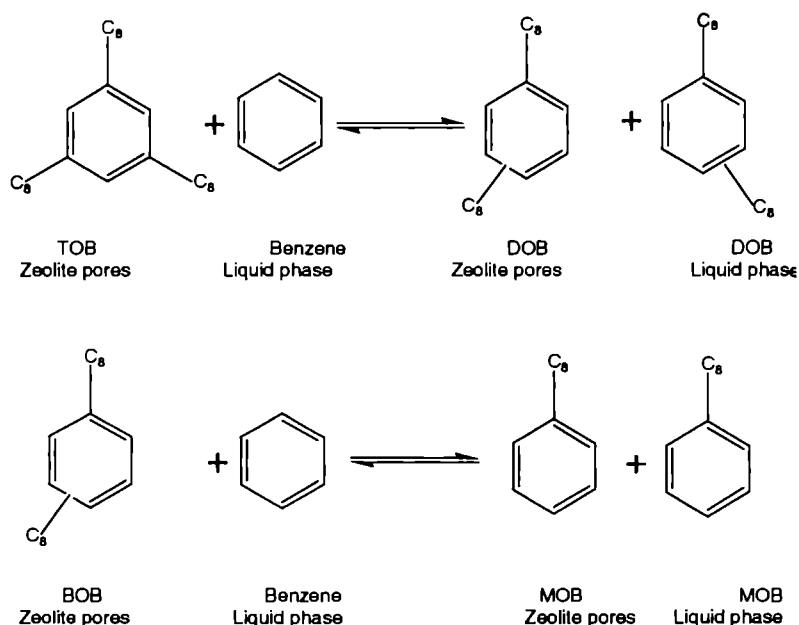
Most bulky TDT are mainly located in the super cages of the crystallites, causing deactivation by pore blockage. There are other similar reports in the literature.⁶⁹ Applying the similar observations in the present case the deactivation of zeolites in the alkylation of benzene with 1-octene might be due to the occlusion of monoctylbenzene (MOB), dioctylbenzene (BOB), trioctylbenzene (TOB) and some bulky aromatic molecules such as alkyltetraline etc. Improved porous structure of the Na-exchanged zeolites effects a better diffusion of the product formed and hence shows comparatively better stability than the pure HFAU-Y zeolite. The results shown in the Table-6 show that the zeolite catalysts used have a considerable resistance for deactivation and attain a steady state upon progression of the reaction. The increase in selectivity of 2-phenyloctane ought to be due to the blocking of unwanted pores of the catalyst upon coking. This blocking prevents the diffusion of isomerized products like 3 or 4-phenyloctane coming out of the zeolite pores.

Table-4.7. Deactivation of CeH-Y and H-mordenite zeolites during the alkylation of benzene with 1-octene.

Zeolite		Time (hours)						
		2	4	6	8	10	12	14
CeH-Y	Conversion for 1-Octene (%)	84.1	88.6	84.2	81.1	79.2	78.2	76.3
	Selectivity for 2-Phenyloctane (%)	60.9	62.5	63.8	63.9	65.1	66.3	66.9
H-mordenite	Conversion for 1-Octene (%)	81.2	94.9	89.0	81.0	70.2	62.5	59.4
	Selectivity for 2-Phenyloctane (%)	73.0	74.0	74.9	75.2	77.0	79.1	79.5

Notes: Reaction temperature- 623 K, amount of catalyst-1g, 1-octene to benzene molar ratio- 1:20, weight hourly space velocity- 3.43mL, constant flow of nitrogen (10mL/h).

Scheme 4.4. Probable transalkylation reaction pathway during the deactivation of zeolite catalyst on benzene alkylation with 1-octene, which explains an increase in the 2-phenyloctane content with time.



4.6 Nature of the carbonaceous compounds blocked inside the zeolite pores

To study the mechanism of deactivation, it is essential to clarify the coke composition clearly. The deactivated zeolites were prepared in a down flow reactor at 623 K with benzene to 1-octene-mole ratio 1:20 and weight hourly space velocity of 3.43 h^{-1} . After introducing the reaction mixture for specified time, it is cleaned by passing benzene for 2 hours. Zeolite is then dissolved in hydrofluoric acid and the organic compounds were extracted using methylene chloride.^{73, 79-81} The nature of the compounds blocked depend on the nature of the reaction, the time on stream and mainly the nature of the zeolite.

From the alkylation of benzene with 1-octene, whatever the reaction, the main compounds retained inside the zeolite pores are monoalkylbenzenes (MOBs). Beside these products octane dimer and trimer (formed by the polymerization of 1-octene under acidic conditions), dialkylbenzene (DOB) and trialkylbenzene (TOB) were formed. They constituted the non-desorbed products from H-Y and other rare earth exchanged Y zeolites. Table 5 shows the distribution of these three mainly as a function of time on stream. Among different MOBs, 3-isomer LAB and 4-isomer LAB are found to be more and they cause more deactivation as they diffuse much slower than that of the 2-isomer and are easier to be retained inside the pores of the zeolite catalysts. The shape selective catalyst hence, benefits products distribution, but the heavier molecules will block the pores of the catalyst and deactivate the catalyst.

The difference in the deactivation of zeolite H-Y and various rare earth exchanged-Y zeolites is mainly the difference in the retention of the reaction products in the pores of the zeolite and slightly to the difference in the distribution and strength of Brønsted acidity. It is seen from Table-4.8 that there is a very strong retention of mono, bi and tri alkylation products inside the FAU-Y micropores. In both the cases the compounds trapped inside the pores changes with time and the percentage of MOB increases with time, at the expense of DOB and TOB. It could be explained by pore mouth transalkylation reaction between bi and trialkylation (a probable trans alkylation pathway is shown in scheme-3 in the deactivation section) products trapped inside the pores and benzene molecules.^{69, 73} From pore volume measurements it is seen that the rare earth exchanged forms have larger pore volume compared to the binder free Na-Y or K-Y and MOB or DOB can easily diffuse out of the pore mouth. Hence mostly in the rare earth modified forms the chances of pore blockage is less and possibility of compound trapped inside the pore decreases.

However, in HFAU-Y there is always a chance of pore blockage due to BOB or TOB etc owing to the rather small pore opening compared to the other rare earth modified zeolites.

Scheme 4.5. Probable molecules (or coke composition) trapped inside the zeolite pores during the alkylation of benzene with 1-octene.

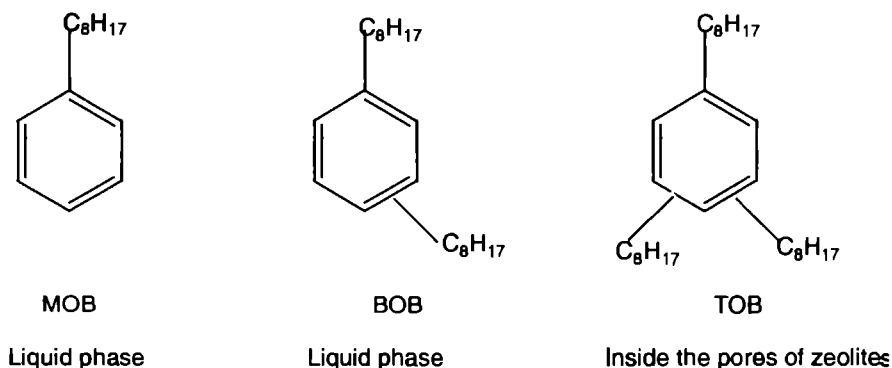


Table 4.8. Nature of the carbonaceous compounds blocked inside the zeolite pores

	Time on stream (h)	Coke (wt.%)	Coke composition (wt.%)			
			MOB ¹	BOB	TOB	Others ²
H-Y	2	20	38.5	32.5	13	16
	4	34	50.5	30	10	9.5
	8	39	73.5	20	5	1.5
CeNa-Y	2	17	37	35	11	17
	4	23	52.5	30	8	9.5
	8	28	65	18	7	10

Notes: Reaction temperature- 623 K, amount of catalyst-1000 mg, 1- octene to benzene molar ratio- 1:20, weight hourly space velocity- 3.43mL, constant flow of nitrogen (10mL/h). ¹ Among different monooctylbenzenes (MOBs) the 3 and 4 isomers is the maximum. ² Include different aromatic species such as naphthalene, some lower alkyl benzenes like toluene and ethyl benzene etc and other lower hydrocarbons formed through cracking.

Limitation in desorption of the MOB isomer from the pores of HFAU zeolite is the main reason for its low selectivity of 2-phenyloctane and rather fast deactivation over the rare earth exchanged FAU-Y zeolites. CeNa-Y, as seen in the table is highly stable to drastic reaction conditions when compared to H-Y. Under similar reaction conditions and same time on stream, H-Y undergoes more coking (34% in four hours) than CeNa-Y (23% in four hours). This resistance to deactivation of the rare earth zeolite is due to the improvement in the pore structure, which to some extent prevents the accumulation of MOB in the pore mouth.

7 Conclusions

Alkylation of benzene with 1-octene is performed over a series of solid acid catalysts such as pure H-Y zeolite, binder free Na-Y, K-Y, Mg-Y, and their corresponding rare earth exchanged forms, H-mordenite, K-10 montmorillonite, and silica-alumina. All these materials except for Na-Y and K-Y are found to be highly active for the reaction. From the alkylation studies, we arrived at following conclusions.

Pure HFAU-Y zeolite shows very high activity for the alkylation of benzene with 1-octene. However the selectivity for 2-phenyloctane is very low. This alkylation reaction of benzene with 1-octene over Y-zeolite is perfectly described by a pseudo-first order equation with respect to alkene. Y-zeolite exhibits a selectivity of 90-95 percentage towards linear alkyl benzene and principal by-products are dialkylindanes and dialkyltetralines was detected. Moreover, Y-zeolite do not seems to exhibit shape-selectivity effects.

Binder free Na-Y and K-Y zeolites exhibit poor activity towards benzene alkylation with 1-octene. Their low activity is explained as due to the poisoning effects on BAS.

3. Subsequent exchange of sodium and potassium with rare earth counter cations seems to enhance the catalytic activity considerably. Changes in the sodium and potassium content of these zeolites, already almost completely protonated, are responsible for the alkylation reaction due to the increased acid strength.
4. Binder free Mg-Y zeolite and its rare earth derivatives are far more active than K-Y or Na-Y zeolites. The very specific influence of magnesium cation, which improves significantly the catalytic performance by introducing a high acid strength, is most likely due to its very high polarizing power compared to K^+ or Na^+ , which effects the OH bond strength through the lattice.
5. Among different rare earth exchanged zeolites REM-Y and LaM-Y (where $M = Mg^{2+}$, K^+ , Na^+ , and H^+) zeolites exhibit comparable catalytic activity and selectivity for 2-phenyl isomer. This could be explained as an effect of lanthanum ions. It is to be remembered at this point that REMg-Y also have lanthanum ion as the main counter cation. LaM-Y and REM-Y have activities lower than that of the corresponding CeM-Y zeolite. The very specific influence of lanthanum cations could be explained by considering the migration tendency from super cages to small cages in rare earth zeolites. Lanthanum with diameter of 0.232 nm migrates from super cage cationic positions to small cage cation locations. This kind of migration is influenced by the size and charge of the residual cations and is most pronounced in the case of magnesium cation. The repulsive interactions of large and highly charged residual cations enhance the migration of La ions into small cages. This prevents the formation of accessible BAS in the large cavities i.e., bridging OH groups are preferentially formed in small cages and are not accessible for hydrocarbons used in this reaction and hence a decreased conversion of 1-octene. Cerium migration is not

so pronounced as La migration and in this case there will be greater amounts of accessible bridging OH groups effecting better conversion of alkene.

H-mordenite, which is used as a standard alkylation catalyst show the highest selectivity for 2-phenyl isomer and conversion of 1-octene (74.0 and 94.1% respectively). The greater selectivity is owing to an effective one-dimensional pore opening system and its medium pore, which cause no restriction for the diffusion of the products out of the zeolite pore system. Here, shape selectivity appears to play a role. However, it undergoes it very fast deactivation with time. Our studies show that it lost almost 40% of its initial activity in 14 hours.

Rare earth exchanged zeolites are far more stable towards vigorous reaction conditions compared to H-Y zeolite. H-Y lost almost 12% of its initial activity in 14 hours, while rare earth exchanged zeolites in general, lost only around 9% of the activity in same TOS. Hence both H-Y and ReM-Y are far more stable compared to H-mordenite, which is a much better catalyst during the initial stages of the reaction.

The deactivation of the catalysts is caused by a jam of bulkier molecules, such as MOB, (including 3 and 4 isomers) BOB and TOB which are too big to move quickly in the intracrystalline pores of the zeolites, so they deposit first in the intracrystalline pores and then gradually in the larger pores.

Time on stream (TOS) studies shows that amount of MOB in zeolite pores increases with time and there is a corresponding decrease in the amounts of BOB and TOB. This observation is due to the transalkylation of them with benzene producing MOB at the zeolite pore openings. This is

consistent with our observation of an increase in 2-phenyloctane content with time over zeolite catalyst.

Thus we conclude that for the alkylation of benzene with long chain olefins such as 1-octene, rare earth exchanged zeolites, mordenite and H-Y zeolites not only has the advantage of good selectivity for 2-phenyl isomer, no corrosive and environmental problems and high atom efficiency, but also can be regenerated repeatedly (regeneration recovers more than 95% of the activity). Rare earth zeolites are far superior as far as stability to process time is concerned. Hence these are very promising catalyst for industrial applications.

References

1. G. A. Olah, "Friedel-Crafts and Related Reactions", Wiley-Interscience publishers, New York, 1963.
2. H. Pines, "The Chemistry of Catalytic Hydrocarbon Conversions", Academic Press, New York, 1981.
3. W. Keim, M. Roper, "Ullmann's Encycl. Ind. Chem." 5th Ed., VCH, Weinheim, 1985, p. 185.
4. P. B. Venuto, *Micropor. Mater.* 2 (1994) 297.
5. G. A. Olah, "Friedel-Crafts Chemistry", Wiley, New York, 1073.
6. Kirk-Othmer, "Encyclopedia of Chemical Technology", 4th, Ed. Wiley, New York, 1991.
7. J. H. Clark, *Green Chem.* 1 (1999) 1.
8. R. A. Sheldon, R. S. Downing, *Appl. Catal. A. Gen.* 189 (1999) 163.
9. G. D. Yadav, A. A. Pujari, *Green Chem.* 1 (1999) 69.
10. G. A. Olah "Friedel-Crafts and Related Reactions", Wiley Interscience publishers, New York, Vol. 1 (1963) p. 205
11. J. March, "Advanced Organic Chemistry - Reactions, Mechanisms, and Structure", Fourth Edition, John Wiley and Sons, p. 534 (1992).
12. N. Y. Chen, W. E. Gaewood, R. H. Heck, *Ind. Eng. Chem. Process Des. Dev.* 26 (1987) 706.
13. J. A. Kocal, B. V. Vora, T. Imai, *Appl. Catal. A. Gen.* 221 (2001) 295.
14. C. Hu, Y. Zhang, L. Xu, G. Peng, *Appl. Catal. A. Gen.* 177 (1999) 237

Chapter 4

5. T. Okhara, N. Mizuno, M. Misono, *Adv. Catal.* 41 (1996) 113.
6. Y. Izumi, N. Natsume, H. Tamamine, K. Urabe, *Bull. Chem. Soc. Jpn.* 62 (1989) 2159.
7. R. T. Sebulsky, A.M. Henke, *Ind. Eng. Chem. Process. Des. Develop.* Vol. 10, No. 2 (1971) 272.
8. J. H. Clark, G. L. Monks, D. J. Nightingale, P. M. Price, J. F. White, *J. Catal.* 193 (2000) 348.
9. P. M. Price, J. H. Clark, K. Martin, D. J. Macquarrie, T. W. Bastock, *Org. Process. Res. Dev.* 2 (1998) 221.
10. H. M. Yuan, L. Zhonghui, M. Enze, *Catal. Today.* 2 (1988) 321.
1. S. Shivashanker, A. Thangaraj, *J. Catal.* 138 (1992) 386.
2. E. R. Lachter, R. A. da S. S. Gil, D. Tabak, V. G. Costa, C. P. S. Chaves, J. A. dos Santos, *React. Funct. Polym.* 44 (2000) 1.
3. J. Klein, H. Widdeke, *Chem. Ing. Tech.* 51 (1979) 560.
4. C. Buttersack, H. Widdeke, J. Klein, *J. Mol. Catal. A. Chem.* 35 (1986) 77.
5. C. Buttersack, H. Widdeke, J. Klein, *J. Mol. Catal. A. Chem.* 35 (1986) 365.
6. C. Buttersack, J. Klein, H. Widdeke, *React. Polym.* 5 (1987) 181. A. Chakrabarti, M. M. Sharma, *React. Polym.* 20 (1993) 1.
7. A. B. Dixit, G. D. Yadav, *React. Funct. Polym.* 31 (1996) 237.
8. X. Hu, M. L. Foo, G. K. Chuah, S. Jaenicke, *J. Catal.* 195 (2000) 412.
9. X. Lin, G. K. Chuah, S. Jaenicke, *J. Mol. Catal. A. Chem.* 150 (1999) 287.
10. J. H. Clark, J. Butterworth, S. J. Tavener, A. J. Teasdale, S. J. Barlow, T. W. Bastock, K. Martin, *J. Chem. Tech. Biotechnol.* 68 (1997) 367.
1. E. E. Getty, R. S. Drago, *Inorg. Chem.* 29 (1990) 1186.
2. L. B. Young, US Patent, 4, 301, 317 (1981) to Mobil Oil Corporation.
3. J. A. Kocal, US Patent, 5, 196, 574 (1993) to UOP (Des Plaines, IL).
4. J. F. Knifton, P. R. Anantaneni, P. E. Dai, US Patent, 5, 847, 254 (1998) to Huntsman Petrochemical Corporation (Austin, TX).
5. J. A. Kocal, D. J. Korous, US Patent, 5, 276, 231 (1994) to UOP (Des Plaines, IL).
6. J. F. Knifton, P. R. Anantaneni, US Patent, 5, 777, 187 (1998) to Huntsman Petrochemical Corporation (Austin, TX).
7. D. J. Stewart, D. E. O'Brien, US Patent, 6, 417, 420 (2002) to UOP LLC (Des Plaines, IL)
8. J. F. Knifton, P. R. Anantaneni, M. E. Stockton, US Patent, 5, 770, 782 (1998) to Huntsman Petrochemical Corporation (Austin, TX).

39. J. F. Knifton, P. R. Anantaneni, M. E. Stockton, US Patent, 3, 315, 964 (2001) to Huntsman Petrochemical Corporation (Austin, TX).
40. J. F. Knifton, P. R. Anantaneni, P. E. Dai, M. E. Stockton, *Catal. Lett.* Vol. 75, No. 1-2 (2001) 113.
41. B. Wang, C. W. Lee, T-X. Cai, S-E. Park, *Catal. Lett.* Vol. 76, No. 1-2 (2001) 99.
42. L. L. G. de Almeida, M. Dufaux, Y. B. Taarit, C. Naccache, *Appl. Catal. A Gen.* 114 (1994) 141.
43. P. Meriaudeau, Y. B. Taarit, A. Thangaraj, J. L. G. de Almeida, C. Naccache, *Catal. Today* 38 (1997) 243.
44. M. Han, Z. Cui, C. Xu, W. Chen, Y. Jin, *Appl. Catal. A Gen.* 238 (2003) 99.
45. W. S. Emersion, V. E. Lucas, R. E. Heimsch, *J. Am. Chem. Soc.* 11 (1949) 1742.
46. W. L. Lenneman, R. D. Hites, V. I. Komarewsky, *J. Org. Chem.* 19 (1954) 463.
47. A. C. Olson, *Ind. Eng. Chem.* 52 (1960) 833.
48. R. D. Swisher, E. F. Kaelble, S. K. Liu, *J. Org. Chem.* 26 (1961) 4066.
49. S. H. Patinkin, B. S. Friedman in "Friedel-Crafts and Related Reactions", G. Olah, Ed. Vol. II, Interscience Publishers, Inc., New York, N. Y. (1964) Chapter 14, p. 3
50. G. Russel, *J. Am. Chem. Soc.* 80 (1958) 4987.
51. L. M. Stock, H. C. Brown, *Advan. Phys. Org. Chem.* 1 (1963) 49
52. H. C. Brown, C. J. Kim. E. C. Scheppele, *J. Am. Chem. Soc.* 89 (1967) 376.
53. L. M. Stock, A. Himoe, *Tetrahedron Letters*, 13 (1960) 9.
54. Y. Cao, R. Kessas, C. Naccacha, Y.B. Taarit, *Appl. Catal. A Gen.* 184 (1999) 231.
55. J. W. Ward, R. C. Hansford, *J. Catal.* 13 (1969) 364.
56. M. Muscas, J. F. Dutel, V. Solinas, A. Auroux, Y. B. Tarrit, *J. Mol. Catal. A Chem.* 106 (1996) 169.
57. J. Turkevichy, F. Nozaki, D. Stamirer, in; W. M. H. Sachtler, G. C. A. Schuit, P. Zwietering (Eds), *Proceedings of the Third Congress on Catalysis, Vol.1*, North Holland, Amsterdam (1965) p. 586.
58. M. Weihe, M. Hunger, M. Breuninger, H. G. Karge, J. Weitkamp, *J. Catal.* 198 (2000) 256.
59. M. Hunger, G. Engelhardt, J. Weitkamp, *Micropor. Mater.* 3 (1995) 497.
60. B. Thomas, S. Sugunan, *Micropor. Mesopor. Matr.* (in press).
61. D-S. Shy, S-H. Chen, J. Leivens, S-B. Liu, K-J. Chao, *J. Chem. Soc. Faraday Trans.* 87(17) (1991) 2855.

Chapter 4

2. R. W. Hansford, J. Ward, *Adv. Chem. Ser.* 102 (1971) 354.
3. C. Mirodatos, A. A-Kais, J. C. Verdrine, P. Pichat, D. Barthomeuf, *J. Phys. Chem.* 80 (1976) 2366.
4. E. O' Donoghue, D. Barthomeuf, *Zeolites Vol. 6* (1986) 267.
5. H. R. Alul, *Ind. Eng. Chem. Prod. Res. Dev.* 7 (1968) 7.
6. W. M. Meier, *Z. Kristallogr.* 115 (1961) 439.
7. W. H. Baur, *Am. Mineral.*, 49 (1964) 697.
8. Arumugamangalam, V. Ramaswamy, *Sci. Tech., Chimica & Industria*, (2000) 1.
9. Z. Da, P. Magnoux, M. Guinet, *Catal. Lett.* 61 (1999) 203.
0. W. G. Liang, Y. Jin, Z. Wang, B. Han, M. He, *E. Min, Zeolites*, 17 (1996) 297.
1. B. V. Vora, P. R. Cottrell, *US Patent*, 5, 012, 021, 1991.
2. E. E. Wolf and F. Alfani, *Catal. Rev. Sci. Eng.* 24 (1982) 329.
3. Z. Da, H. Han, P. Magnoux, M. Guisnet, *Appl. Catal. A. Gen.* 219 (2001) 45.
4. S. M. Csicery, *Zeolites* 7 (1989) 202.
5. Z. Da, P. Magnoux, M. Guisnet, *Appl. Catal. A. Gen.* 182 (1999) 407.
6. P. Magnoux, A. Mourran, S. Bernard, M. Guisnet, *Stu. Surf. Sci. Catal.* 108 (1997) 107.
7. M. Guisnet, P. Magnoux, *Appl. Catal. A. Gen.* 54 (1989) 1.
8. B. V. Vora, P. R. Pujado, J. B. Spinner, T. Imai, *Hydrocarbon Proc.* 63 (1984) 86.
9. B. V. Vora, P. R. Pujado, T. Imai, T. R. Fritsch, *Chem. Ind.* 83 (1990) 187.
0. M. Guisnet, P. Magnoux, *Appl. Catal. A. Gen.* 54 (1989) 1.
1. M. Han, Z. Cui, C. Xu, W. Chen, Y. Jin, *Appl. Catal. A. Gen.* 238 (2003) 99.

Chapter 5

Friedel-Crafts Alkylation 2

*"In Nature's infinite book of secrecy
A little can be read"*

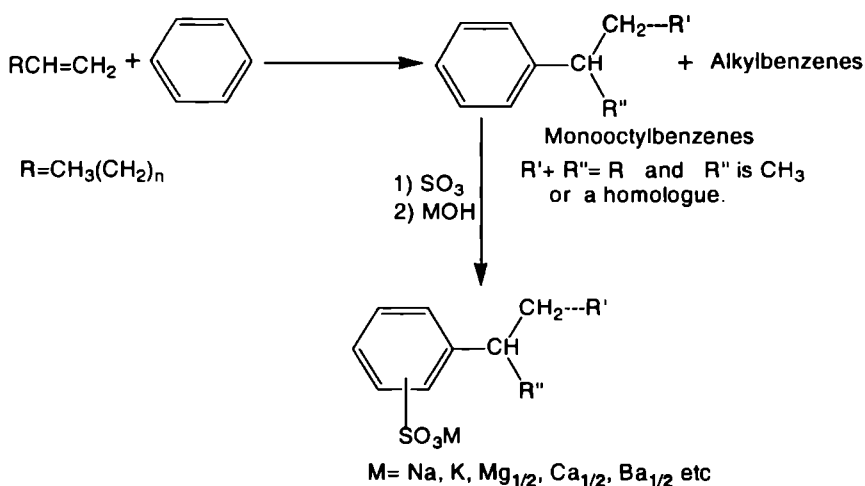
William Shakespeare

Linear alkylbenzene technology has almost completely replaced the old conventional branched alkylbenzene technology for the production of surfactants due to improved biodegradability and cost-effectiveness. The technology of today is the dehydrogenation of n-paraffins to n-olefins followed by benzene alkylation to produce LAB. Traditionally, this Friedel-Crafts alkylation reaction is performed by acid catalyst such as HF acid or $AlCl_3$. The corrosive nature and potential environmental hazards in the case of HF and $AlCl_3$ as well as difficulties in recycling and disposal of the spent catalyst are major downsides of these homogeneous systems. Hence the choice of the acid catalyst is a major issue in these environmentally conscious days. Solid acid catalyst-based systems are slowly replacing HF acid units in order to ensure environmental safety and improve cost effectiveness. Numerous materials have been evaluated as solid acid catalysts for this alkylation process ranging from zeolites, clays, various metal oxides, heteropoly acids, mesoporous materials, and $AlCl_3$ supported on solid acids (heterogenized homogenous catalysts) etc. At present, only UOP DetaTM Technology has been commercialized. In the ongoing studies on reaction mechanism and catalytic activity, significant progress has been made to improve the selectivity, catalyst stability and reusability of these solid acids under commercial operating conditions. In the present section alkylation of benzene with C_{10} and C_{12} alkene is described with special importance to the catalyst stability.

5.1 General introduction

The carbocation alkylation of arenes with detergent range linear olefins catalyzed by protic acids typically produces linear secondary phenyl alkanes (LABs) that are a mix of number of positional isomers, i. e. 2-phenyl, 3-phenyl, 4-phenyl etc.¹⁻⁴ Scheme-5.1 depicts the possible isomer distribution during the alkylation of benzene with higher olefins.

Scheme 5.1. Plausible alkylation pathway leading to the formation of linear alkyl benzene (LABs) and linear alkylbenzene Sulphonates (LAS) or detergents.



Worldwide production of LAB is increasing everyday and the global consumption is predicted to grow at an annual rate of 3.5%.⁵⁻⁶ The practice of its chemistry on a commercial scale is still presenting peculiar challenges such as;

The regioselectivity of an alkylation with long chain olefin is really difficult to control, specifically, in the case of benzene alkylation, where there is now an increasing need to preferentially generate the more desirable 2-phenyl alkylate ($R''-CH_3$ in equation 2 in scheme-1) and to avoid the formation of non-linear alkylbenzene. The 2-phenyl isomer is preferred as

amongst the possible Phenyl Alkane Sulphonates (LAS) isomer derivatives (Scheme-1; equation 2), the 2-phenyl LAS (R"- CH₃) have the most favorable biodegradability, solubility, and emulsification characteristics.

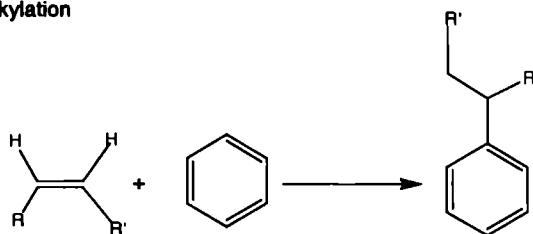
- The use of long chain alkenes may result in the formation of significant quantities of heavy organics such as poly alkylated products, alkyltetralines, polyaromatics such as naphthalene, indane etc⁷, with other carbonaceous deposits.
- The low mutual solubilities of the liquid alkenes with the liquid aromatics may necessitate alternative mixing procedures in order to achieve high yields of the most desired product.
- The low temperature needed to conduct this alkylation (when use HF and AlCl₃) selectively may result in the accumulation of water in the reactor, brought in with the alkylation feed components.

Typically, the alkylated aromatics are manufactured commercially using Friedel-Crafts method. Such methods produce high conversions, but the selectivity to 2-phenyl isomer is only around 20%. So selectively catalyzed alkylations are considered widely in the world. The common acid catalysts used in these commercial processes are hydrofluoric acid and aluminium chloride.⁸⁻¹⁴ High efficiency, superior product quality, and ease of use relative to aluminium chloride lead to the dominance of HF acid in alkylation complexes. However, the selectivity for the 2-phenyl isomer is a major concern. The HF catalysis typically gives 2-phenylalkane selectivity of only 17-18%. The high reactivity of HF acid cause many side reactions ranging from alkylation, dialkylation, isomerization/alkylation and dimerisation/oligomerization (scheme-2). Thus, HF based catalytic alkylation reactions typically will have very high E-factor. This kind of low selectivity is a major concern, when it is well known in the detergent field that the biodegradability of alkylbenzene sulphonic acid-

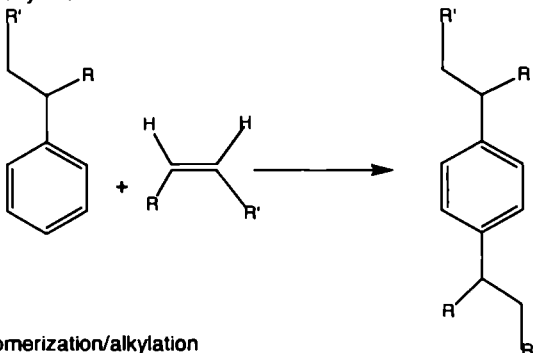
As the average substitution position number of benzene ring on the alkyl chain is reduced, i.e. for example detergent based

Scheme 5. 2. Plausible reaction pathways associated with benzene alkylation with higher olefins over acidic catalysts.

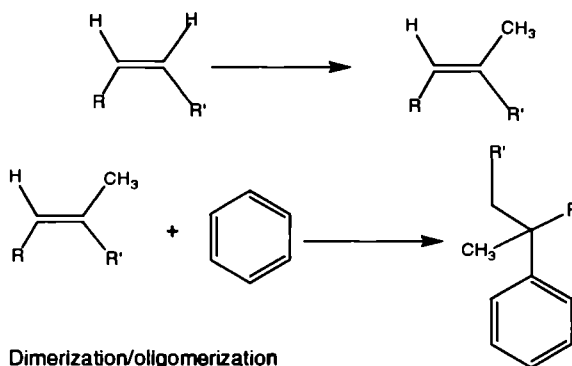
Alkylation



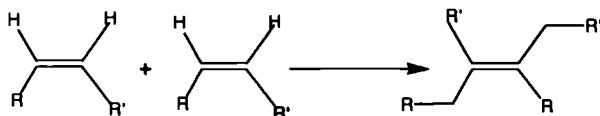
Dialkylation



Isomerization/alkylation



Dimerization/oligomerization



on (2-alkyl)-benzene sulphonic acid is more easily biodegraded than one based on (3-alkyl)-benzene sulphonic acid, the latter in turn more biodegradable than another detergent based on (4-alkyl) benzen sulphonic acid and so forth. Therefore the phenylalkane produced in the reported method could be ultimately utilized to produce detergents which are more easily biodegradable than those produced by current HF acid technique.

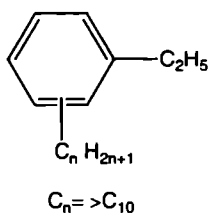
There are many other unfavorable properties for HF acid catalyst. The normal work-up procedure for reactions employing these acid catalysts involves a water quench, which prevents the acid being used again, and subsequent neutralization leads to an aqueous salt waste stream. The corrosive nature and potential environmental hazards in the case of liquid acid catalyst as well as difficulties in recycling and disposal of spent catalyst are some other drawbacks of these homogeneous catalytic systems. Since the catalysts are irreversibly lost, the overall atom efficiency of such catalytic reactions is very low. Added to this, conventional Friedel-Crafts alkylation reactions use greater than stoichiometric amounts of homogeneous catalysts. This is a major concern from the economic point of view. All these add to the potential complexity of such catalytic reaction. Therefore, there is a strong need for procedures that can overcome the above difficulties and lead to benefits in terms of clean technology.¹⁵⁻¹⁸

The introduction of solid acid catalyst has removed the need for quench step, facilitating the catalyst reuse through continuous reactions or by the separation of solid phase on workup. Also, solid acids are much easier and safer to handle. These are much more desirable for environmental reasons, are non-corrosive and offer additional advantages for controlling the selectivity via their shape-selective properties. However, unfortunately they have significantly lower activities than the homogeneous acid catalysts, although give greatly improved reaction selectivity for the desired 2-phenylalkane.

Therefore, while the reaction of benzene with linear alkenes using AlCl_3 or HF acid occur rapidly at room temperature, the corresponding reaction with solid acid catalysts occur only under severe conditions of pressure and temperature.¹⁹ This is, however, not necessarily a disadvantage. Alkylations are usually exothermic reactions. For example, the synthesis of ethylbenzene from benzene and ethylene occur with reaction enthalpy of -113 kJ/mol .²⁰ Operation at high temperature allows much of the heat to be economically recovered, in contrast to low temperature synthesis.

A number of papers and patents have been published describing the near alkylbenzene synthesis using a range of solid acids (sterically constrained) catalysts. They include; metal oxides,²¹⁻²³ sulphides,²⁴⁻²⁶ heteropoly acids,²⁷⁻³¹ cation exchanged resins,³²⁻³⁸ mesoporous materials,³⁹⁻⁴² acidic clays,⁴³⁻⁴⁵ and a variety of acidic zeolites.⁴⁶⁻⁵⁸

At this point we would like to mention the use of some of the important by-products of the alkylation of benzene with higher olefins such as;



dialkylbenzenes containing one short chain (2 to 4 carbon atom in the chain and one long chain linear alkyl group (preferably greater than C_{10} alkyl group) are used as synthetic lubricating oils and additives.¹⁸

2 Alkylation with C_{10} and C_{12} olefins

The alkylation of benzene with higher 1-olefins, typically C_{10} to C_{13} , is performed industrially for the manufacture of the LABs, an intermediate used in the production of biodegradable surfactants; Linear Alkylbenzene Sulphonates (LAS). The reaction proceeds via carbocation mechanism.^{1-4, 14, 20, 59-60} In the present cases we observe 5 (in the case of 1-decene) and 6 (in the case of 1-dodecene) carbocations. However, the carbocation at carbon number one is not stable and

hence 1- phenylalkane is not observed. Detailed mechanism of alkylation reaction and possible side reactions associated with it are described in previous chapter (refer scheme-4.2, chapter 4). The percentage conversion and selectivity were also calculated by the method illustrated in chapter-4 (refer section 4.2, chapter 4).

5.3 Effect of Reaction Variables

The vapour phase reaction runs were performed under constant flow of nitrogen. The process is extremely sensitive to reaction variables and optimization of the reaction conditions is very critical. The effect of reaction temperature, catalyst loading, benzene to olefin molar ratio, flow rate or weight hourly space velocity, and time on stream (TOS) was examined in order to optimize the conversion of olefin and selectivity to the monoalkylated product or more precisely the 2-phenyl isomer formation.

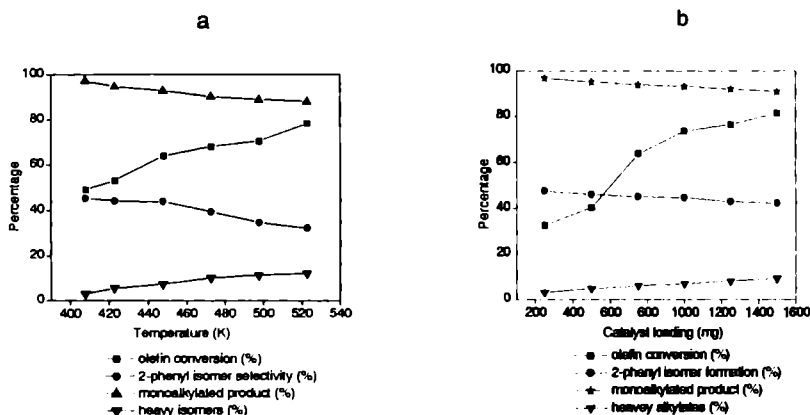
I. Effect of temperature

Figure 5.1.a shows the effect of reaction temperature in the vapor phase alkylation of benzene with 1-dodecene. The reaction temperature was varied from 408 K to 523 K over a representative sample HFAU-Y zeolite. The conversion of 1-dodecene increases with increase in the reaction temperature (49.1% at 408 K. increased to 78.3% at 523 K). However, the increase in conversion is at the cost of selectivity for 2-phenyl isomer. This can be due to the increasing probabilities of catalytic cracking, rapid equilibration of the olefin isomer or easy diffusion of the bulkiest LAB isomer out of the zeolite cavities at higher temperature. By comparing the results, in general, we can say that temperature has a positive influence on alkylation of benzene with higher olefins. The effect of reaction temperature is discussed in section 4.3b in the previous chapter.

Influence of catalyst loading

The total conversion of 1-alkene and selectivity for the monoalkylated product as a function of catalyst loading is displayed in Figure-5.1b. The catalyst amount is varied by taking different amounts of HFAU-Y zeolite and keeping the other variables constant.

Figure 5.1. Influence of reaction variables during the alkylation of benzene with 1-dodecene over HFAU-Y zeolite, (a) effect of reaction temperature, and (b) effect of catalyst loading.



Notes: Catalyst; HFAU-Y, 1-octene to benzene molar ratio; 1:20, catalyst loading; 750 mg weight hourly space velocity; 4.90 h⁻¹, time on stream; 3 h, constant flow of nitrogen (10 mL/h).

Notes: Catalyst; H-Y, reaction temperature; 448 K, 1-octene to benzene molar ratio; 1:20, weight hourly space velocity; 4.90 h⁻¹, time on stream; 3 h, constant flow of nitrogen (10 mL/h).

Notes: Olefin in pure 1-dodecene obtained from Lancaster used without further purification.

Monoalkylated products include 2, 3, 4, 5, and 6-phenyldodecane isomers. Heavies include dodecane dimer, didodecylbenzene, alkyltetralenes, some other polymeric products, and nv etc (nv; not detected by GC).

As the amount of catalyst increases, total conversion of 1-alkene increases. However, at the same time there is slight decrease in the formation of

monoalkylated product. The formation of heavy isomers seems to increase with the amount of catalyst. Hence it might be concluded that the decrease in the monoalkylated product with catalyst amount is at the expense of an increase in heavy isomer formation. With the increment in the catalyst loading, the opportunity for the reaction over external surface acid sites increased and the conversion of alkene is increased and selectivity for the 2-phenylalkane decreased slightly from 47.5 to 42.2%. A detailed discussion is also given in 4.3.1. in chapter 4.

III. Effect of feed rate

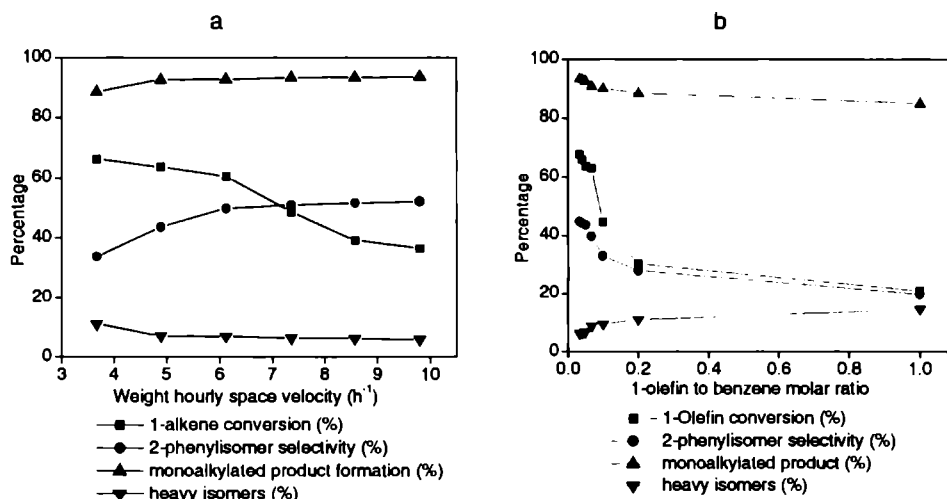
A series of experiments were conducted to study the influence of feed rate or weight hourly space velocity of reactant on the conversion of alkene and the selectivity for the monoalkylated product. A typical profile of the influence of feed rate on the alkylation activity of HFAU-Y zeolite under standard reaction conditions is given in Figure-5.2a. The feed rate has a highly pronounced effect on the conversion of alkene and selectivity for the desired products. The total conversion decreases as the feed rate increases while the selectivity for the monoalkylated product increases. Conversion decreased from 66.5% to 36.6% as the feed rate increased from 3 to 8 mL/h (weight hourly space velocity 3.68 to 9.81 h⁻¹). The feed rate or WHSV alters the contact time (1/WHSV; h) and at high feed rates the reactant spent less time on the catalyst surface resulting in a decrease in the conversion. However, at the same time, as the reactants and products spent time on the catalyst surface, the probabilities of hydride shift to produce the isomeric carbocation decreases. Decrease in the isomeric carbocation formation means a decrease in the formation of other isomers like 3, 4, 5, and 6-phenyldodecane. This explains an increase in the 2-phenyl isomer formation with an increase in the feed rate (2-phenyl isomer formation increased from 33.8% to 52.3% on increasing the feed rate from 3 to 8 mL/h).

This also explains the decrease in the production of heavy isomers at high feed rates. Nevertheless, at the same time other isomers are also detected.

7. Effect of olefin to benzene molar ratio (effect of solvation)

Another set of experiments were carried out to establish the predominant influence of the 1-alkene to benzene molar ratio. The molar ratio of the

figure 5.2. The influence of reaction variables on the benzene alkylation with 1-dodecene over HFAU-Y zeolite, (a) effect of feed rate or weight hour space velocity (h^{-1}), and (b) 1-dodecene to benzene molar ratio.



Notes: Catalyst; HFAU-Y, reaction temperature; 448 K 1- dodecene to benzene molar ratio; 1:20, catalyst loading; 750 mg, time on stream; 3 h, constant flow of nitrogen (10 mL/h).

Notes: Catalyst; HFAU-Y, reaction temperature; 448 K, catalyst loading; 750 mg, weight hourly space velocity; 4.90 h^{-1} , time on stream; 3 h, constant flow of nitrogen (10 mL/h).

Notes: Olefin is pure 1-dodecene obtained from Lancaster used without further purification. Monoalkylated products include 2, 3, 4, 5 and 6-phenyldodecane isomers. Heavies include dodecane dimer, didodecylbenzene, alkyltetralenes, some other polymeric products, and nv etc (nv; not detected by GC).

Reactants of a particular reaction play an important role in deciding the conversion and selectivity of the desired product. Alkene to benzene molar

ratio was varied from 1:1 to 1:25 under constant reaction conditions. The results of the study are represented in Figure; 5.2b.

From the figure it is clear that molar ratio of the reactants has a significant influence on the conversion and selectivity of the alkylation reaction. The conversion increased from 21% to 66.1% on decreasing the alkene to benzene molar ratio from 1 to 0.033. A similar increase in the 2- phenylalkane (also the selectivity of monoalkylated products) formation is observed with a decrease in molar ratio. However, the formation of heavy isomers decreased from 14.9% to 6.4%. The selectivity for the 2-phenyl isomer increased from 19.9 to 44.5% on increasing the molar ratio. As the reversible reaction reaches equilibrium state, the increase in the amount of benzene leads to an increase in the conversion of 1-alkene.

The increase in the 2- phenylalkane selectivity could be explained in terms of solvation effect of benzene in higher molar ratios. In the alkylation of benzene with 1-alkene, the solvation of the reaction intermediates by the solvent molecules apparently reduces the differences in their stabilities, which results in greater formation of 2-phenyldecane. This effect of solvation is practically absent when the molar ratio of benzene and 1-decene is 1:1. Excess benzene acts as solvent. The involvement of solvent in certain reactions is widely reported (the influence of solvation is also discussed in section 4.3.III. in the previous chapter).⁶¹⁻⁶² The solvation of the carbocation formed by solvation of the benzene molecules slows down the rate of isomerization to the internal isomers even though the hydride ion transfers are rapid. This reduces the probability of formation of internal carbocations such as 3, 4, 5, and 6. Hence, the 2-carbocation first formed reacts with the aromatic hydrocarbon before undergoing further rearrangement.^{3, 12} Therefore, it is concluded that the isomerization is fast enough to allow the isomeric ion to attack benzene. If, on the other hand, the rate of alkylation can effectively

compete with the rate of isomerization, the isomer distributions of the product would have been different and the most probable product would be the 6-phenylalkane. Since the 2-phenylalkane formation (obviously monoalkylated product too) is high, the probability of heavy isomer formation is less as the availability of alkene is very low at high molar ratios.

.4 Performance of different zeolite systems

Table-1 show the results of alkylation experiments of different 1-alkenes with binder free K-Y, various rare earth exchanged K-Y zeolites, and K-10 montmorillonite clay. As expected, binder free K-Y is near inefficient as an alkylation catalyst. The alkylation activity of this zeolite seems to be enhanced by exchanging K^+ with rare earth metal ions. As-exchanged LaK-Y has comparatively lower ability to alkylate benzene with 1-olefins than CeNa-Y zeolite. K-10 Mont. converts very small amounts of alkene. Added to this, it produces small amounts of desired product. The difference in the behavior of different catalytic systems seems to be a function of the pore structure. The increased formation of 2-phenyl isomer in the case of rare earth exchanged zeolites might be due to the enhanced diffusional properties upon rare earth exchange. Also, the selectivity for the monoalkylated products and the total 1-olefin conversion increase from 1-decene to 1-dodecene.

Alkylation experiments with different 1-alkenes (C_{10} - C_{12}) are summarized in tables-5.1 to 5.4. Binder free Na-Y zeolite shows very low activity. Exchange of sodium with rare earth metal ions seems to enhance the catalytic activity and selectivity of the desired product considerably (Table-5.2). Because of mild reaction conditions, no skeletal rearrangement takes place in the alkene chain (branched isomers are not detected by careful GC-MS analysis) nor were any oligomers of the olefins detected. The desired linear alkyl benzenes are obtained in good yield. The rare earth exchanged zeolites produce 2-phenyl isomers slightly

Benzene alkylation with C₁₀ and C₁₂ olefins

more selectively than the pure H-Y form. However, H-mordenite is far more superior in its ability to produce the desired isomer.

Table 5. 1. Alkylation of benzene with C₁₀ and C₁₂ olefins over binder-free K-Y, parent H-Y, various as-exchanged rare earth KFAU-Y zeolites, and K-10 montmorillonite clay.

Alkene	Catalyst system	Alkene conversion (%)	2-phenyl alkane (%)	Monoalkylated ¹ (%)	Heavy ² (%)
1-decene	H-Y	79.5	43.3	90.4	9.6
1-dodecene		81.9	39.2	92.8	7.2
1-decene	K-Y	10.2	43.2	95.6	5.4
1-dodecene		10.6	40.5	97.6	2.4
1-decene	CeK-Y	73.6	48.5	93.8	6.2
1-dodecene		73.9	45.1	95.5	4.5
1-decene	LaK-Y	64.7	47.8	94.5	5.5
1-dodecene		66.0	46.5	95.9	4.1
1-decene	REK-Y	66.9	46.1	93.4	6.6
1-dodecene		67.3	44.8	94.7	5.3
1-decene	K-10 Mont. ³	38.9	38.7	93.1	6.9
1-dodecene		39.1	34.0	95.2	4.8

Notes: Reaction temperature: 448 K; amount catalyst: 1500 mg; benzene to 1-decene molar ratio: 20:1; time on stream: 3 h; constant flow of nitrogen: (10 mL/h). ¹ Include 3, 4, 5, and 6 phenylalkane isomers (however, for 1-decene up to 5 isomers). ² Include small amounts decene and dodecene dimers, didecylbenzene and didodecylbenzene, alkyltetralines, skeletal isomerization products (<2%), and some other polymeric products. Also, lower hydrocarbons formed during the reaction through the cracking of 1-decene (occurred to a very limited extent), which reacts with benzene to form lower alkyl benzenes (see scheme showing the reaction mechanism in the previous chapter), ³ K-10 montmorillonite (silica-alumina ratio 2.7) layered aluminosilicate clay with average pore size >1 nm, which is purchased from *Sigma-Aldrich*, USA and used without further modification.

In all the cases besides the desired mono-substituted product (> 90%), small amount of di-substituted products are also formed. The selectivity for the

mono-substituted product increases with increase in the chain length of the 1-alkene. Also, the total conversion of 1-alkene increases from 1-decene to 1-dodecene. This means that the decylation of benzene occur slightly slower compared to dodecylation over zeolite catalysts.

Table 5. 2. Alkylation of benzene with C₁₀ and C₁₂ olefins over binder free Na-Y, parent H-Y, various as-exchanged rare earth NaFAU-Y, and H-mordenite zeolites.

Alkene	Catalyst system	Alkene conversion (%)	2-phenyl alkane (%)	Monoalkylated ¹ (%)	Heavy ² (%)
1-decene	H-Y	79.5	43.3	90.4	9.6
1-dodecene		81.9	39.2	92.8	7.2
1-decene	Na-Y	10.2	40.1	96.1	3.9
1-dodecene		13.4	37.1	97.2	2.8
1-decene	CeNa-Y	74.2	48.8	92.1	7.9
1-dodecene		75.1	46.4	94.3	5.7
1-decene	LaNa-Y	66.3	47.9	92.8	7.2
1-dodecene		67.6	44.6	93.9	6.1
1-decene	RENa-Y	66.7	47.8	92.7	7.3
1-dodecene		66.8	45.6	93.4	6.6
1-decene	SmNa-Y	70.3	49.3	92.5	7.5
1-dodecene		71.7	46.3	94.9	6.1
1-decene	H-MOR ³	84.2	59.1	93.8	6.2
1-dodecene		86.5	54.5	94.1	5.9

Notes: Reaction temperature: 448 K; amount catalyst: 1500 mg; benzene to 1-decene molar ratio: 20:1; time on stream: 3 h; constant flow of nitrogen: (10 mL/h). ¹ Include 3, 4, 5, and 6 phenylalkane isomers (however, for 1-decene up to 5 isomers). ² Include decene and dodecene dimers, didecylbenzene, alkyltetralines, skeletal isomerization products (<2%), and some other polymeric products. Also, lower hydrocarbons formed during the reaction through the cracking of 1-decene or 1-dodecene (occurred to a very limited extent), which reacts with benzene to form lower alkyl benzenes (see scheme showing the reaction mechanism in the previous chapter). ³ H-mordenite used as a model catalyst through out the text is a product from *Zeolyst International* New York, USA with a Si/Al ratio of 19.

Table-5.3 presents the results of alkylation of benzene with 1-alkenes; 1-decene and 1-dodecene over binder free Mg-Y, various rare earth exchanged magnesium Y zeolites, and a common alkylation catalyst silica-alumina. Mg-Y zeolite exhibits good catalytic activity and selectivity for the desired 2-phenyl isomer. The conversion and selectivity towards the desired isomer are 47.5% and 40.8% in the case of 1-decene and 48.1% and 39.7% in the case of 1-dodecene respectively. Hence Mg-Y is very different compared to Na-Y and K-Y, which are almost inefficient as alkylation catalysts (conversion of 1-alkenes are 10.2 and 13.4% with Na-Y and 10.2 and 10.6 over K-Y, Table-5.1 and 5.2). Exchange of magnesium ions with rare earth metal ions further enhances the catalytic activity considerably. 2-Phenylalkane formation also shows an increment. Among the different magnesium zeolites CeMg-Y shows maximum conversion and selectivity for 2-phenylalkane. However, silica-alumina with its very poor acid structure and diffusional properties (silica-alumina does not have a regular pore system) show very low catalytic activity.

Table-5.4 summarizes the experimental results of alkylation of benzene with detergent range of olefins, namely 1-decene and 1-dodecene over pure H-Y, its different rare earth doped derivatives, and a common alkylation catalyst H-mordenite. Among Y zeolites pure H-Y converts maximum olefin. Exchange of H⁺ ions with rare earth metals seem to decrease the 1-alkene conversion considerably. However, with this decrease there is corresponding increase in the selectivity of the 2-phenyl isomer formation (for H-Y it is 43.3% and 39.2% with 1-decene, with CeH-Y 48.5 and 46.8% with 1-dodecene). In this series, highest conversion of 76.3 and 76.5% for the 2-olefins is exhibited by CeH-Y zeolite. H-mordenite as explained in the previous sections shows maximum conversion of 84.2% and 86.5% conversion and selectivity of 59.1 and 54.5% respectively for the two alkenes.

Table 5. 3. Alkylation of benzene with C₁₀ and C₁₂ olefins over binder free Mg-Y, parent H-Y, various as-exchanged rare earth MgFAU-Y zeolites, and silica-alumina.

Alkene	Catalyst system	Alkene conversion (%)	2-phenyl alkane (%)	Monoalkylated ¹ (%)	Heavy ² (%)
1-decene	H-Y	79.5	43.3	90.4	9.6
1-dodecene		81.9	39.2	92.8	7.2
1-decene	Mg-Y	47.5	40.8	94.2	5.8
1-dodecene		48.1	39.7	95.6	4.4
1-decene	CeMg-Y	75.7	49.7	93.1	6.9
1-dodecene		75.9	47.0	94.5	5.5
1-decene	LaMg-Y	67.8	47.3	93.4	6.6
1-dodecene		68.1	45.7	95.5	4.5
1-decene	REMg-Y	67.9	47.9	92.1	8.9
1-dodecene		68.1	46.2	93.8	6.2
1-decene	SiO ₂ - Al ₂ O ₃ ³	27.4	33.1	95.9	4.1
1-dodecene		30.2	30.2	95.3	4.7

Notes: Reaction temperature: 448 K; amount catalyst: 1500 mg; benzene to 1-decene molar ratio: 20:1; time on stream: 3 h; constant flow of nitrogen: (10 mL/h). ¹ Include 3, 4, 5, and 6 phenylalkane isomers (however, for 1-decene up to 5 isomers). ² Include decene and dodecene dimers, didecylbenzene, alkyltetralines, skeletal isomerization products (<2%), and some other polymeric products. Also, lower hydrocarbons formed during the reaction through the cracking of 1-decene (occurred to a very limited extent), which reacts with benzene to form lower alkyl benzenes (see scheme showing the reaction mechanism in the previous chapter). ³ Silica-alumina, which was used as a model alkylation catalyst was synthesized in the laboratory using frequently available chemical methods.⁶³⁻⁶⁴

Table 5. 4. Alkylation of benzene with C₁₀ and C₁₂ olefins over parent H-Y, various as-exchanged rare earth HFAU-Y, and H-MOR zeolites.

Alkene	Catalyst system	Alkene conversion (%)	2-phenyl alkane (%)	Monoalkylated ¹ (%)	Heavy ² (%)
1-decene	H-Y	79.5	43.3	90.4	9.6
1-dodecene		81.9	39.2	92.8	7.2
1-decene	CeH-Y	76.3	48.5	93.3	6.7
1-dodecene		76.5	46.8	94.0	6.0
1-decene	LaH-Y	68.7	47.8	93.8	6.2
1-dodecene		69.2	45.9	94.9	5.1
1-decene	REH-Y	68.9	46.4	92.3	7.7
1-dodecene		69.2	45.4	94.1	5.9

Notes: Reaction temperature: 448 K; amount catalyst: 1500 mg; benzene to 1-alkene molar ratio: 20:1; time on stream: 3 h; constant flow of nitrogen: (10 mL/h). ¹ Include 3, 4, 5, and 6 phenylalkane isomers (however, for 1-decene up to 5 isomers), ² Include decene and dodecene dimers, didecylbenzene, alkyltetralenes and some other polymeric products. Also, lower hydrocarbons formed during the reaction through the cracking of 1-decene (occurred to a very limited extent), which reacts with benzene to form lower alkyl benzenes (see scheme showing the reaction mechanism in the previous chapter).

It is also observed that the 1-dodecene conversion is always greater than the 1-decene conversion and is in expected lines. The effect of alkylating agent on the rate of Friedel-Crafts alkylation reactions is well documented. Isopropylation occurs about 1460 times faster than ethylation. Very similar results have been obtained in the rare earth-Y alkylation of benzene with alkene at 373 K where propylene reacted about 300 times faster than ethylene. These data are in direct agreement with greater ease of protonation of the more substituted alkenes, as indicated by their proton affinities (681, 747, and 803 kJmol⁻¹) for ethylene, propylene and *i*-butene respectively.⁶⁵⁻⁶⁶ Based on these observations, a faster dodecylation compared to decylation is not surprising.

As seen from the tables 5.1 to 5.4, the catalysts exhibit wide difference in alkylation ability and selectivity for the 2-phenylalkane formation. Since we are dealing a similar alkylation type of reactions and same catalysts, the explanations for the difference in the catalytic performance are the same as we have already discussed in the previous chapter (chapter-4, section 4. 4). These discussions also deal with the correlations between acid structural properties and number of active sites per unit area of the catalysts with catalytic performance. In a similar way a very simple correlation could be arrived between the catalytic activity and acid structural properties. We conclude that the improvement in the acid structural properties upon rare earth metal exchange leads to an improvement in the 2-phenylalkane production under the given reaction conditions.

The results of alkylation of benzene with 1-decene and 1-dodecene over series of catalysts are presented in tables 5.1 to 5.4. From the data it is seen that there is much difference in the product distribution for both alkenes. This difference in the product distribution is explained as follows. As explained earlier, the alkylation of benzene with 1-alkenes such as the present ones goes through a carbocation mechanism (see references therein). This carbocation undergoing rapid isomerization in varying degrees and finally attacks benzene in what is considered to be the rate determining step to form the product. The intermediate carbocation ion undergoing a series of fast hydride shifts producing isomeric ions. The hydride transfers, though very rapid, are not instantaneous,⁶⁷⁻³ and therefore, some of the carbocation ion may react with aromatic ring before undergoing rearrangement.⁶⁸ Therefore, it is seen that the isomerization to internal isomers in the carbon chain is fast enough to allow isomeric ions to attain equilibrium before they attack benzene. In the present case this thermodynamic equilibrium is not probably reached. A greater 2-phenyl isomer content in the product mixture suggests a non-attainment of thermodynamic

equilibrium. In other words, it must be stated that under the present reaction conditions the intermediate carbonium ions from 1-decene and 1-dodecene do not come to equilibrium before they attack the aromatic ring or the rate of alkylation step is not sufficiently low to allow isomerization of the intermediate to proceed to the most stable distribution. It must be remembered at this point that the relative stabilities of the carbonium ions increase as the carbon number increases, the least stable being the primary ion (C₁-position). In fact due to its very low stability, the 1-phenylalkane is not at all detected. On the basis of this, one would expect the isomer content to increase with the carbon number (towards the center of the 1-alkene chain). This is possible only if the thermodynamic equilibrium is reached before the carbonium ion attacks benzene. This is found to be so in the case of HF acid in which thermodynamic equilibrium is probably reached.

In all the cases, we observe formation of very small amounts of tertiary alkylbenzene (<2%) indicating the probabilities of skeletal isomerization of the intermediate ions (included as heavies in Tables 1 to 4). Though the rate of skeletal isomerization is much smaller than the rate of alkylation or the rate of hydride shifts which results in the isomerization across the chain. Apparently under the given moderate reaction conditions, mainly high dilution (1-alkene to benzene molar ratio; 1:20) such an isomerization is not as fast as rate of alkylation step. Actually skeletal isomerization of 1-dodecene in presence of acid catalyst has been reported even at 348 K and observation of small amounts of such reaction products in the mixture is not surprising.⁶⁹

On the basis of the present data the possibility of long-range isomerization within the reactive intermediates (carbocation) is not ruled out. The positive ions abstract a hydrogen anion from a carbon atom other than the adjacent one. However, in the present system of alkylation, the reactive intermediates exist as ion pairs and since long range hydride shifts require

greater charge separation and greater energy than 1,2-hydride shifts, these long range isomerizations are not likely to occur to any significant extent. The fact that the rate of attack on benzene has been estimated to be nearly 350 times faster than the abstraction of a hydride ion from an iso-paraffin, which is more reactive than a n-paraffin argues against long range isomerization.⁷⁰

5.5 Deactivation studies

A catalyst is defined as a substance, which accelerates the rate of a chemical reaction without itself getting affected or changed. The definition suggests an infinite life for the catalyst. In practice, this is really not true and all the catalysts deactivate, though at different rates, and have finite life. The deactivation is most often a result of side or parallel reactions.⁷¹⁻⁷² Fouling (one of the five reasons for catalyst deactivation) of a solid acid catalyst takes place when carbonaceous materials also called coke are deposited on the catalyst. This deposition of carbonaceous materials lowers the catalytic activity either by strong adsorption on the active site or by the plugging of the micro and mesopores of the catalyst. The apparent effects of fouling are activity loss (temperature of the reactor is continuously increased to compensate for the loss of activity) and increase in pressure drop across the bed.⁷²

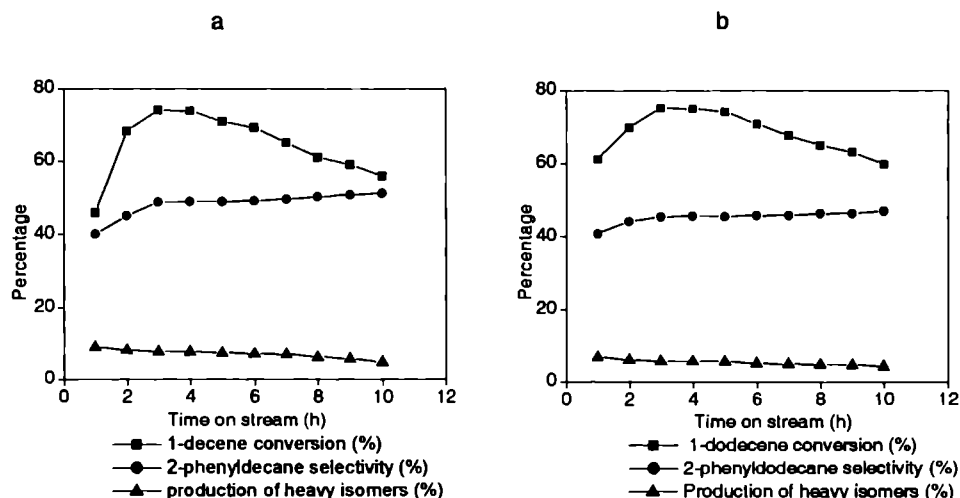
As stated before, fouling is the major cause of deactivation of zeolite type of solid acid catalysts. Once the catalyst has been deactivated to the extent that it is not economical to continue the operation, it has to be regenerated or reactivated. The best method of zeolite regeneration is to burn the coke in presence of oxygen.⁷² However, as the burning process is extremely exothermic and local heat will be generated which raise the temperature and may completely damage the catalyst. In most of the cases the process burn away a lot of useful components also and is to be done under extreme control.^{7, 72}

Zeolites present high initial activity during the alkylation of benzene with higher olefins and are highly selective for the production of desired 2—phenyl isomer. However, they are not really stable towards the drastic reaction conditions. Hence zeolites too are no exception for the phenomenon of catalyst deactivation. In general, zeolite deactivation is due to the formation and trapping of heavy secondary reaction products in the zeolite pores (called as coke for simplicity). In the liquid phase alkylation of toluene with 1-heptene (a model reaction for LAB synthesis) it is shown that the deactivation of different zeolites such as HFAU, HMOR, and HBEA was due to heptyltoluenes blocked inside the zeolite pores.⁷³⁻⁷⁸

Generally, coke removal is carried out through oxidative treatment under air or oxygen flow at high temperatures. This method, which can be easily applied to catalysts operating at high temperatures, is very costly for catalysts working in the liquid phase. However, coke molecules formed at low temperature result mainly from condensation reaction without practically any intervention of hydrogen transfer reaction. Thus, sample treatment under strong nitrogen flow at reaction temperature or slightly above can regenerate catalyst.

Da et al. investigated the deactivation and regeneration of HFAU type of zeolite during the liquid phase alkylation of toluene with 1-dodecene.^{75, 77} Liang et al. reported the mode of deactivation and regeneration of H-Y zeolite during the activation of benzene with 1-dodecene.⁷⁴

Figure 5.3. The influence of time on stream during the alkylation of benzene with (a) decene and (b) dodecene over as-exchanged CeNa-Y zeolite



Notes: Heavies include decene dimers, didecylbenzene (BDB), tridecylbenzene (TDB) alkytetralenes and some other polymeric products.

Notes: Heavies include dodecene dimers, bidodecylbenzene (BDDB), tridodecylbenzene (TDDB) alkytetralenes and some other polymeric products.

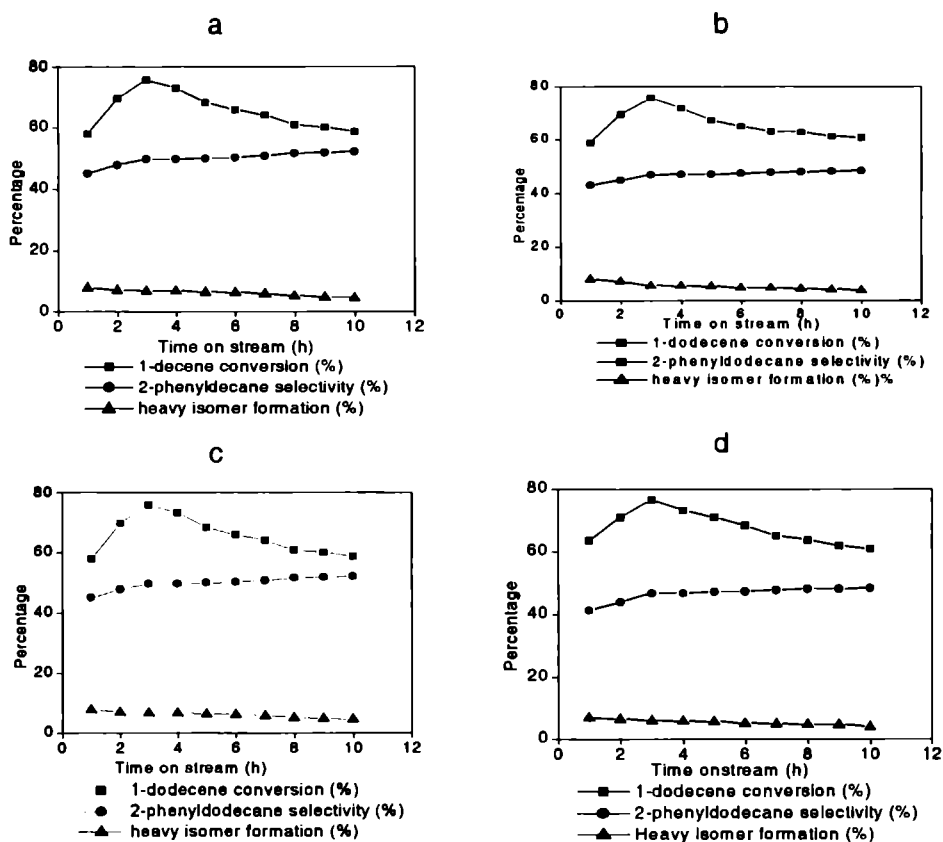
Notes: Reaction temperature: 448 K, amount catalyst: 1500 mg, benzene to 1-decene or 1-dodecene to molar ratio: 20:1, weight hourly space velocity: 2.46 (1-decene) and 2.45 (1-dodecene), constant flow of nitrogen: (10 mL/h).

Due to the low reaction temperature, Wolf et al. considered the carbonaceous compounds formed in the zeolite pores as liquid coke.⁷⁹ It can easily diffuse out of the zeolitic pores under high temperature or constant extraction with a suitable solvent, usually benzene. In the present case, as the reactions are carried out at high temperatures, we adopted an extraction-oxidative treatment method for zeolite regeneration. There are many similar reports in the literature discussing deactivating of zeolite catalysts.⁸⁰⁻⁸¹

Alkylation reaction was carried out for 10 hours continuously over the zeolite catalyst (HFAU-Y, CeNa-Y, LaNa-Y, CeK-Y, CeMg-Y, CeH-Y and H-mordenite) and products were collected at intervals of 1 hour. The deactivated catalyst was taken out from the reactor, extracted continuously with acetone for many times, dried in the oven at 383 K overnight and XRD profile was taken. It was then calcined at different temperatures in the range of 423-773 K and at 773 K for 5 hours with a heating rate of 12 K/ min with constant air blowing over the sample (as described in the experimental section). The XRD patterns of the deactivated, reactivated and fresh catalysts were taken. These profiles show that some of the patterns are missing or their intensities are diminished. This is clearly due to the deposition of coke in the zeolite pores. But upon regeneration of the deactivated sample, all the peaks reappeared with almost same intensity. Carrying out reaction with the regenerated sample we could get a maximum conversion of 81.0% with HFAU-Y zeolite (>95 of the fresh catalyst) after three hours of the reaction, which is very close to the conversion obtained for the fresh catalyst.

The conversion and selectivity as a function of reaction time is shown in Figure-3-3 to 3.7. All the systems show uniform product distribution. The percentage conversion of 1-alkene increases initially from second hour to approximately four hours whereas; the selectivity for 2-phenyloctane increases very slowly from second hour onwards.

Figure 5.4. The influence of time on stream during the alkylation of benzene with 1-decene (a) & (c) and benzene with 1-dodecene (b) & (d) over as-exchanged CeMg-Y and CeH-Y zeolites respectively.



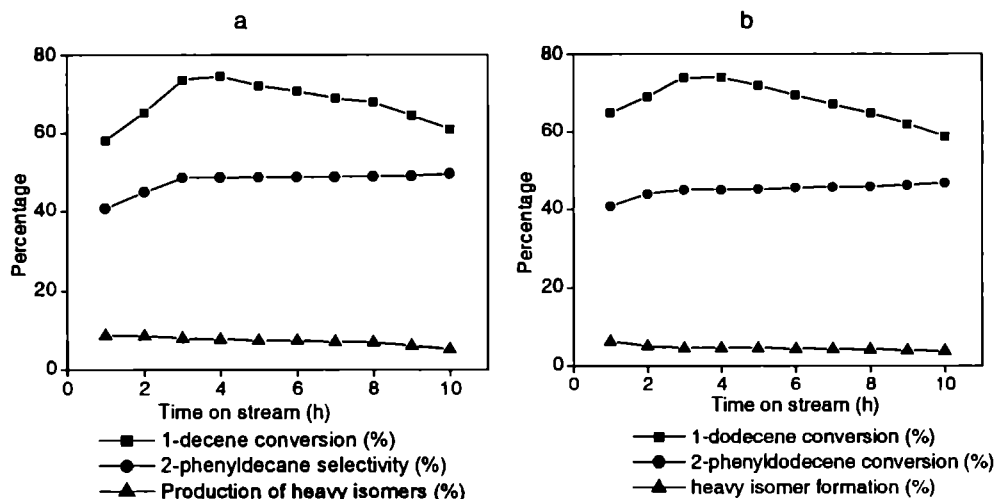
Notes: Heavies include decene dimers, dodecylbenzene (BDB), tridecylbenzene (TDB) alkyltetralenes and some other polymeric products.

Notes: Heavies include dodecene dimers, bidodecylbenzene (BDDB), tridodecylbenzene (TDDB) alkyltetralenes and some other polymeric products.

Notes: Reaction temperature: 448 K; amount catalyst: 1500 mg; benzene to 1-decene or dodecene molar ratio: 20:1; weight hourly space velocity: 2.46 (1-decene) and 2.45 (1-dodecene) constant flow of nitrogen: (10 mL/h).

Benzene alkylation with C₁₀ and C₁₂ olefins

Figure 5.5. Shows the influence of time on stream during the alkylation of benzene with (a) decene and (b) dodecene over as-exchanged CeK-Y zeolite.



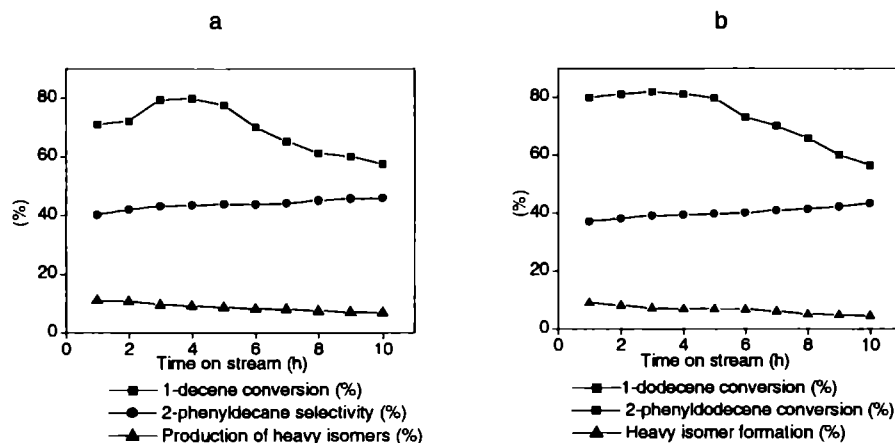
Notes: Heavies include decene dimers, bidodecylbenzene (BDB), tridecylbenzene (TDB) alkyltetralenes and some other polymeric products.

Notes: Heavies include dodecene dimers, bidodecylbenzene (BDDDB), tridodecylbenzene (TDDDB) alkyltetralenes and some other polymeric products.

Notes: Reaction temperature: 448 K; amount catalyst: 1500 mg; benzene to 1-decene or dodecene to molar ratio: 20:1; weight hourly space velocity: 2.46 (1-decene) and 2.45 (1-dodecene) constant flow of nitrogen: (10 mL/h).

(H-Y lost almost 12% activity under same reaction conditions and TOS in 10 hours conversion at fourth hour is 94.9% and at 10th hour 59.4%). At the same time the selectivity for the desired 2-phenyl isomer increases slowly from the very first hour. Also, H-mordenite seems to undergo very fast deactivation with time and it lost as much as 40% activity. As seen from the deactivation studies the as-exchanged zeolites exhibit better stability than pure H-Y or H-mordenite zeolites.

Figure 5.6. Shows the influence of time on stream during the alkylation of benzene with (a) decene and (b) dodecene over as-exchanged H-FAU-Y zeolite



Notes: Heavies include decene dimers, decylbenzene (BDB), tridecylbenzene (TDB) alkyltetralenes and some other polymeric products.

Notes: Heavies include dodecene dimers, bidodecylbenzene (BDDB), tridodecylbenzene (TDDB) alkyltetralenes and some other polymeric products.

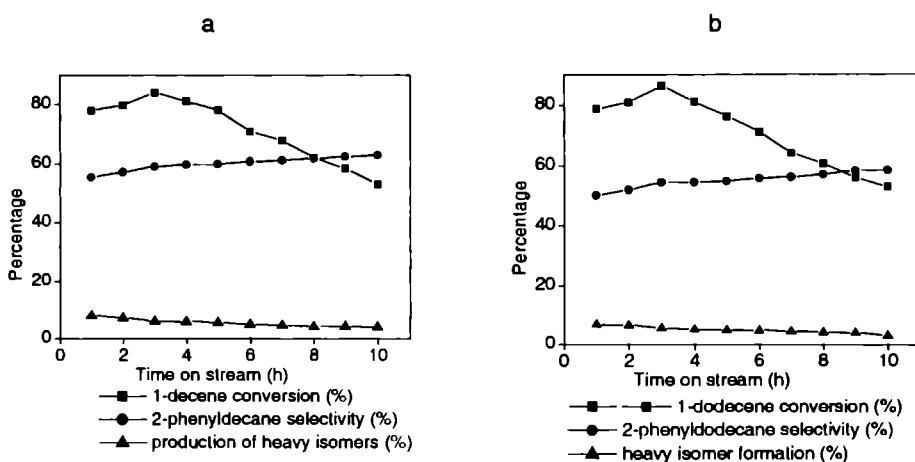
Notes: Reaction temperature: 448 K; amount catalyst: 1500 mg; benzene to 1-decene or 1-dodecene to molar ratio: 20:1; weight hourly space velocity: 2.46 (1-decene) and 2.45 (1-dodecene) constant flow of nitrogen: (10 mL/h).

Whatever be the reaction, pure H-Y, and H-mordenite were far more active for the alkylation of benzene with 1-decene and 1-dodecene. The initial activities of H-Y, and H-MOR were far higher over any rare earth exchanged zeolite. However, deactivation is more pronounced over them. These zeolites, which are very active at initial stages of the reaction decays very rapidly with time than any of the rare earth exchanged zeolites.

Whatever be the reaction and catalyst, the monoalkylated product monodecylbenzene, MDB and monododecylbenzene, MDDB appear rapidly in the liquid phase as the main product of the reaction. The dialkylated products;

bidecylbenzene (BDB) and bidodecylbenzene (BDDDB) appears as secondary products. Trialkylated products; tridecylbenzene (TDB) and tridodecylbenzene (TDDDB) appear in very small amounts in the product mixture.

Figure 5.7. Shows the influence of time on stream during the alkylation of benzene with (a) decene and (b) dodecene over as-exchanged H-MOR zeolite.



Notes: Heavies include decene dimers, bidecylbenzene (BDB), tridecylbenzene (TDB) alkyltetralenes and some other polymeric products.

Notes: Heavies include dodecene dimers, bidodecylbenzene (BDDDB), tridodecylbenzene (TDDDB) alkyltetralenes and some other polymeric products.

Notes: Reaction temperature: 448 K; amount catalyst: 1500 mg; benzene to 1-decene or dodecene to molar ratio: 20:1; weight hourly space velocity: 2.46 (1-decene) and 2.45 (1-dodecene) constant flow of nitrogen: (10 mL/h).

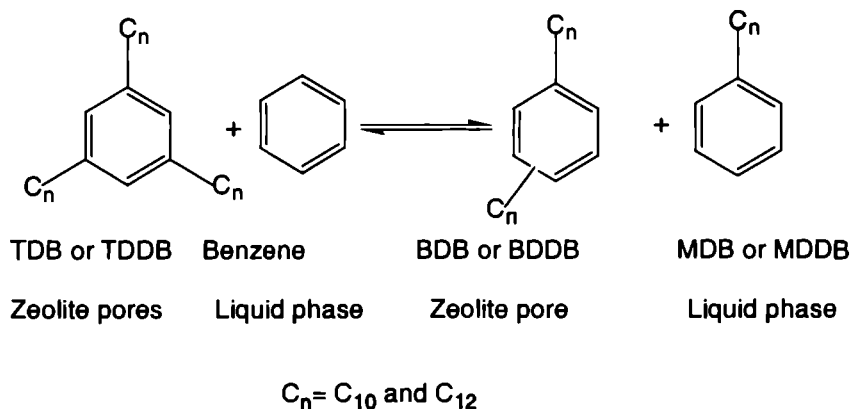
As stated earlier alkenes found to undergo skeletal rearrangement producing branched chain alkylbenzenes. No C₂₀ or C₂₄ heavy alkylbenzene are not observed suggesting against a dimerisation and a subsequent alkylation.

In addition to products observed in the liquid phase, reaction products are also found to be trapped in the zeolite micropores. During the alkylation of benzene with 1-decene and 1-dodecene the non-desorbed products retained in

The zeolite pores are mainly constituted by MDB and BDB in the case of 1-decene and MDDB and BDDB in the case of 1-dodecene. More bulky aromatic compounds such as TDB and TDDB, alkyltetralines, and alkene dimers were also found in very small quantities (as determined by the analysis of coke exactly as in the case of 1-octene in the previous chapter). Da et al. reported in similar lines.⁷⁵⁻⁷⁷

The time on stream (TOS) studies of alkylation reaction show that the composition of monoalkylated product (and hence the formation of 2-phenylalkane) increases with time. However, at the same time we observe a reduction in the heavy alkylate content. Heavy isomers mainly contain BDB and BDDB for 1-decene and 1-dodecene. It also contains small amounts of TDB and TDDB for 1-decene and 1-dodecene respectively, alkyltetralines, and the corresponding alkene dimers. The decrease in the heavy alkylate during deactivation could be explained by considering the probability of transalkylation of bi and tri alkylbenzene with benzene producing monoalkylated product (see Figure 5.3 to 5.7).⁷⁵⁻⁷⁷

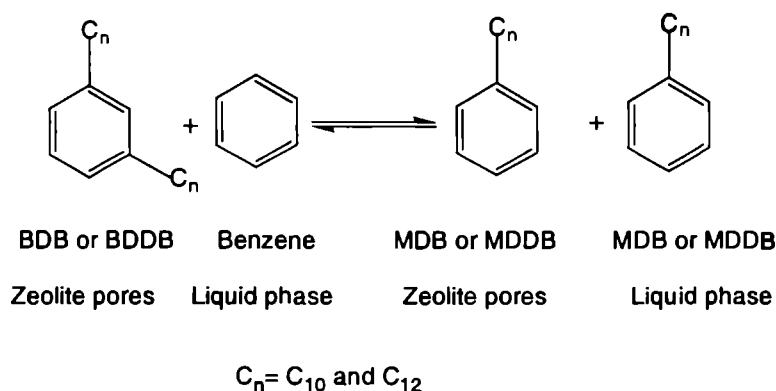
Scheme 5.3. Transalkylation of benzene with trialkylated product during the alkylation of benzene with 1-decene and 1-dodecene.



Benzene alkylation with C₁₀ and C₁₂ olefins

Scheme 5.3. presents the transalkylation of TDB or TDDDB trapped inside the zeolite pores with reactant benzene, producing BDB and BDDDB as dialkylated products and MDB and MDDDB as monoalkylated products for 1-decene and 1-dodecene respectively. Part of BDT or BDDT reacts further with a molecule of benzene producing two molecules of MDB and MDDDB, one in liquid phase and other retained inside the zeolite pores (see scheme-4).

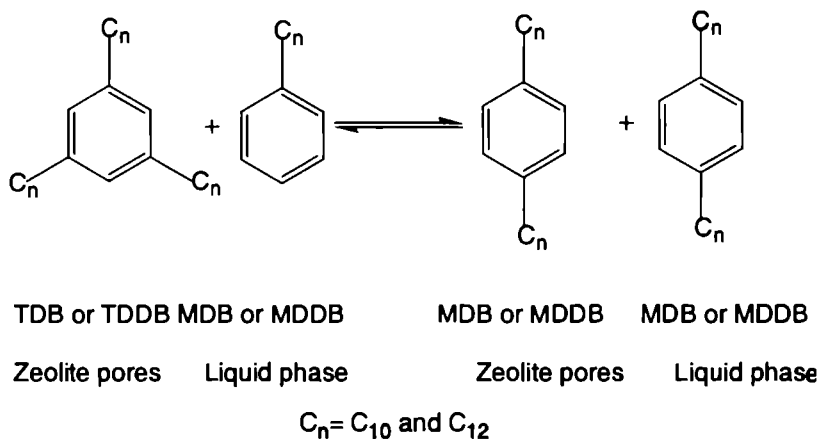
Scheme 5. 4. Transalkylation of benzene with bialkylated product during the alkylation of benzene with 1-decene and 1-dodecene.



Now the increase in the BDB or BDDDB content can also be a result of the transalkylation of TDB or TDDDB with MDB or MDDDB producing 2 molecules of BDB or BDDDB; one diffused into liquid phase and the other retained inside the zeolite pores (scheme-5).

Due to heavy deposition of coke, the access to the pores of the zeolites are very much limited and the transalkylation step occur at the pore mouth. At the pore mouth, molecules occluded inside pores react with molecules in the liquid phase or gas phase to produce the products. G. Colon et al. reported in similar lines for explaining isopropylation of naphthalene over large pore zeolites and skeletal isomerization of n-butane over H-FER zeolite.⁸²⁻⁸³

cheme5. 5. Transalkylation of monoalkylated product with trialkylated product using the alkylation of benzene with 1-decene and 1-dodecene.



6 Conclusions

Friedel-Crafts alkylation of benzene with higher olefins such as 1-decene and 1-dodecene were carried out over a series of rare earth exchanged zeolites and their activities have been compared with some common alkylation catalysts such as K-10 Mont. clay, H-MOR zeolite, and silica-alumina. Based on the results from various studies, we arrived at following conclusions.

Taken together, the present studies clearly shows that the rare earth exchanged zeolites could be efficient catalysts in the intermolecular coupling of the aromatic nucleus with activated compounds like long chain 1-olefins under relatively mild reaction conditions in a continuous down-flow type of reactor. For both the model reactions (one with 1-decene and another with 1-dodecene), which were carried out using benzene as the aryl substrate resulted in excellent yields of coupled products; mainly the 2-phenylalkane. In contrast the conventional series of catalysts such as $AlCl_3$, BF_3 , HF acid and concentrated H_2SO_4 acid catalyzed Friedel-Crafts alkylation reaction, the extent of formation of undesired products from side

reactions such as transalkylation, skeletal isomerization etc was minimal with the use of zeolites. The ability to recover and reuse the catalyst from the reaction mixture, minimal generation of environmentally unfriendly waste, high specificity of reactions and low cost are the important advantages of zeolite catalyst over the conventional Friedel-Craft catalysts.

2. Pure HFAU-Y zeolite exhibits the maximum conversion of 1-alkene. However, the selectivity for the desired product (2-phenylalkane) is very low. Also, binder free Na-Y and K-Y are almost inefficient as alkylation catalyst predominately due to their weak acid structural properties. Sodium and potassium ions are reported to have poisoning effect on the Brønsted acid sites. However, binder free Mg-Y zeolite exhibits comparatively better activity towards the reaction which is explained as an effect of its high polarisability.
3. According to the data from Table-1-4, the catalytic activity depends on the nature of residual cation and it decrease in the order H > Mg > Na > K. As shown in this study, the nature of residual cations (H⁺, Na⁺, K⁺, and Mg²⁺) in rare earth exchanged zeolite can exert a pronounced influence on the catalytic activity of these materials.
4. Deactivation studies were performed with CeNa-Y, CeK-Y, CeMg-Y, CeH-Y, HFAU-Y, and H-MOR zeolites with both 1-decene and 1-dodecene. A model alkylation catalyst H-MOR undergoes very fast deactivation with time. It lost almost 40% of its initial activity in 10 hours of reaction time. HFAU-Y is more stable in comparison with HMOR and it lost only 25% activity with same time on stream. However, all rare earth exchanged zeolites exhibit far better stability towards reaction conditions. On an average they lost almost 15% of their initial activity in 10 hours on stream. However, in all the cases, the 2-phenylalkane formation increases with time.

The deactivation of the catalyst is caused by the squeezing of bulkier molecules, namely monodecylbenzene (MDB), dodecylbenzene (BDB), and tridecylbenzene (TDB) with 1-decene and monododecylbenzene (MDDDB), bidodecylbenzene (BDDDB), and tridodecylbenzene (TDDDB) in the case of 1-dodecene. Also, there are alkyltetralines and branched chain alkylbenzenes. These are all too bulky to diffuse quickly from the intracrystalline pores of zeolites, so they deposit first in these intracrystalline pores and then gradually in the larger pores.

The deactivated catalyst can be regenerated by continuous extraction with acetone followed by high temperature (773 K) oxidative treatment in constant flow of oxygen.

In addition, the solvent extracted zeolite regenerated completely by calcining at high temperature, retain >95% of their initial activity. Regenerated zeolites show identical product distribution as that of the fresh catalyst.

Thus, for the alkylation of benzene with long chain olefins; 1-decene and 1-dodecene, parent H-Y and various rare earth exchanged zeolites not only as the advantage of high 2-phenylalkane selectivity and no corrosive and environmental problem, but also can be regenerated repeatedly. All these materials make very promising catalysts for industrial application.

References

1. S. H. Patinkin, B. S. Friedman, in "Friedel-Crafts and Related Reactions"; (G. A. Olah, Ed.), Vol. II, Cha. 14, Int. Publishers, New York (1964) p. 3
2. A. C. Olson, *Ind. Eng. Chem.* 52 (1960) 833.
3. P. B. Venuto, L. A. Hamilton, P. S. Landis, *J. Catal.* 5 (1960) 21.
4. R. D. Swisher, E. F. Kaelble, S. K. Liu, *J. Org. Chem.* 26 (1961) 4066.
5. J. A. Kocal, B. V. Vora, T. Imai, *Appl. Catal. A Gen.* 221 (2001) 295.
6. "Encyclopedia of Chemical Technology", Vol. 2, Wiley, New York, p. 58.
7. H. Han, Z. Cui, C. Xu, W. Chen, Y. Jin, *Appl. Catal. A Gen.* 238 (2003) 99.
8. J. F. Roth, A. R. Schaefer, US Patent, 3, 356, 757 to Huntsman Corporation New York.
9. P. R. Pujado, "Linear Alkylbenzene Manufacture"; *Handbook of Petroleum Refining Processes* (1997) p. 1.53.
10. B. V. Vora, P. R. Pujado, J. B. Spinner, T. Imai, *Hydrocarb. Proc.* 63 (1984) 86.
11. B. V. Vora, P. R. Pujado, T. Imai, T. R. Fritsch, *Chem. Ind.* 19 (1990) 187.
12. H. R. Alul, G. J. McEwan, *J. Org. Chem.* 32 (1967) 3365.
13. E. Renk, J. D. Roberts, *J. Am. Chem. Soc.* 83 (1961) 878.
14. G. A. Olah, "Friedel-Crafts and Related Reactions" Vol. I, Wiley-Interscience, New York, 1963.
15. J. H. Clark, *Green Chem.* 1 (1999) 1.
16. R. A. Sheldon, R. S. Downing, *Appl. Catal. A Gen.* 189 (1999) 163.
17. G. D. Yadav, A. A. Pujari, *Green Chem.* 1 (1999) 69.
18. K. Smith, G. M. Pollaud, I. Matthews, *Green Chem.* 1 (1999) 75.
19. J. L. G. de Almeida, M. Dufaux, Y. B. Tarrit, C. Naccache, *J. Am. Oil Chem. Soc.* 71, 7 (1994) 675.
20. J. S. Beck, W. O. Haag 'Alkylation of Aromatics'- G. Ertl, H. Knozinger, J. Weitkamp, "Handbook of Heterogeneous Catalysis" Vol. 5, Wiley VCH, 1997, p. 2123.
21. C. Hu, Y. Zhang, L. Xu, G. Peng, *Appl. Catal. A Gen.* 177 (1999) 237
22. T. Okhara, N. Mizuno, M. Misono, *Adv. Catal.* 41 (1996) 113.
23. Y. Izumi, N. Natsume, H. Tamamine, K. Urabc, *Bull. Chem. Soc. Jpn.* 62 (1989) 2159.

Chapter 5

4. J. H. Clark, G. L. Monks, D. J. Nightinggale, P. M. Price, J. F. White, *J. Catal.* 193 (2000) 348.
5. P. M. Price, J. H. Clark, K. Martin, D. J. Macquarrie, T. W. Bastock, *Org. Process. Res. Dev.* 2 (1998) 221.
6. K. Tanabe, W. F. Holderich, *Appl. Catal. A. Gen.* 181 (1999) 399.
7. R. T. Sebulsky, A.M. Henke, *Ind. Eng. Chem. Process. Des. Develop.* Vol. 10, No. 2 (1971) 272.
8. C. Hu, Y. Zhang, L. Xu, G. Peng, *Appl. Catal. A. Gen.* 177 (1999) 237.
9. T. Okhara, N. Mizuno, M. Misono, *Adv. Catal.* 41 (1996) 113.
0. Y. Izumi, N. Natsume, H. Tamamine, K. Urabc, *Bull. Chem. Soc. Jpn.* 62 (1989) 2159.
1. A. Corma, *Chem. Rev.* 95 (1995) 559.
2. E. R. Lachter, R. A. da S. S. Gil, D. Tabak, V. G. Costa, C. P. S. Chaves, J. A. dos Santos, *React. Funct. Polym.* 44 (2000) 1.
3. J. Klein, H. Widdeeke, *Chem. Ing. Tech.* 51 (1979) 560.
4. C. Buttersack, H. Widdeeke, J. Klein, *J. Mol. Catal. A. Chem.* 35 (1986) 77.
5. C. Buttersack, H. Widdeeke, J. Klein, *J. Mol. Catal. A. Chem.* 35 (1986) 365.
6. C. Buttersack, J. Klein, H. Widdeeke, *React. Polym.* 5 (1987) 181.
7. A. Chakrabarti, M. M. Sharma, *React. Polym.* 20 (1993) 1.
8. A. B. Dixit, G. D. Yadav, *React. Funct. Polym.* 31 (1996) 237.
9. X. Hu, M. L. Foo, G. K. Chuah, S. Jaenicke, *J. Catal.* 195 (2000) 412.
0. X. Lin, G. K. Chuah, S. Jaenicke, *J. Mol. Catal. A. Chem.* 150 (1999) 287.
1. J. H. Clark, J. Butterworth, S. J. Tavener, A. J. Teasdale, S. J. Barlow, T. W. Bastock, K. Martin, *J. Chem. Tech. Biotechnol.* 68 (1997) 367.
2. E. E. Getty, R. S. Drago, *Inorg. Chem.* 29 (1990) 1186.
3. H. M. Yuan, L. Zhonghui, M. Enze, *Catal. Today.* 2 (1988) 321.
4. S. Shivashanker, A. Thangaraj, *J. Catal.* 138 (1992) 386.
5. L. Huisheng, W. Ying, "International Report of Research Institute of Petroleum processing", 1985.
6. L. B. Young, US Patent, 4, 301, 317 (1981) to Mobil Oil Corporation.
7. J. A. Kocal, US Patent, 5, 196, 574 (1993) to UOP (Des Plaines, IL).

Benzene alkylation with C₁₀ and C₁₂ olefins

48. J. F. Knifton, P. R. Anantaneni, P. E. Dai, US Patent, 5, 847, 254 (1998) to Huntsman Petrochemical Corporation (Austin, TX).
49. J. A. Kocal, D. J. Korous, US Patent, 5, 276, 231 (1994) to UOP (Des Plaines, IL).
50. J. F. Knifton, P. R. Anantaneni, US Patent, 5, 777, 187 (1998) to Huntsman Petrochemical Corporation (Austin, TX).
51. D. J. Stewart, D. E. O'Brien, US Patent, 6, 417, 420 (2002) to UOP LLC (Des Plaines, IL)
52. J. F. Knifton, P. R. Anantaneni, M. E. Stockton, US Patent, 5, 770, 782 (1998) to Huntsman Petrochemical Corporation (Austin, TX).
53. J. F. Knifton, P. R. Anantaneni, M. E. Stockton, US Patent, 3, 315, 964 (2001) to Huntsman Petrochemical Corporation (Austin, TX).
54. J. F. Knifton, P. R. Anantaneni, P. E. Dai, M. E. Stockton, Catal. Lett. Vol. 75, No. 1-2 (2001) 113.
55. B. Wang, C. W. Lee, T-X. Cai, S-E. Park, Catal. Lett. Vol. 76, No. 1-2 (2001) 99.
56. L. L. G. de Almeida, M. Dufaux, Y. B. Taarit, C. Naccache, Appl. Catal. A. Gen. 114 (1994) 141.
57. P. Meriaudeau, Y. B. Taarit, A. Thangaraj, J. L. G. de Almeida, C. Naccache, Catal. Today 38 (1997) 243.
58. W. Liang, Z. Yu, Y. Lin, Z. Wang, Y. Wang, M. He, E. Min, J. Chem. Tech. Biotechnol. 62 (1995) 98.
59. P. B. Venuto, L. A. Hamilton, P. S. Landis, J. J. Wise, J. Catal. 5 (1966) 81.
60. P. B. Venuto, Micropor. Mater. 2 (1994) 297.
61. G. Russel, J. Am. Chem. Soc. 80 (1958) 4987.
62. H. C. Brown, C. J. Kim. E. C. Scheppele, J. Am. Chem. Soc. 89 (1967) 376.
63. N. N. Greenwood, A. Earnshaw, "Chemistry of the Elements", Second Edition, Butterworth-Heinemann, Oxford, (1997) p. 345.
64. F. A. Cotton, G. Wilkinson, C. A. Murillo, M. Bochmann, "Advanced Inorganic Chemistry" Sixth Edition, John Wiley and Sons Inc., New York, (1999) p.178.
65. J. E. Szulejko, T. B. Macmahon, J. Am. Chem. Soc. 81 (1993) 7839.
66. R. H. Allen, L. D. Yats, J. Am. Chem. Soc. 83 (1961) 2799.
67. M. Sounders, P. Von, R. Schleyer, G. A. Olah, *ibid*, 86 (1964) 5680.
68. C. D. Nenitzescue, Rev. Roumaine Chim. 9 (1964) 5.
69. A. H. Peterson, B. L. Phillips, J. T. Kelly, Ind. Eng. Chem. 4 (1965) 261.

Chapter 5

3. F. E. Condon, M. P. Matuszak, *J. Am. Chem. Soc.* 70 (1948) 2534.
1. D. L. Trimm in "Handbook of Heterogeneous Catalysis", vol. 3 (Eds G. Ertl, H. Knozinger, J. Weitkamp), VCH, Weinheim (1997) p. 1263.
2. S. Sivasanker, "Catalyst Deactivation" (Ed.,) B. Viswanathan, S. Sivasanker, A. V. Ramaswamy, "Catalysis Principles and applications", Narosa Publishing House, New Delhi (2002) p. 253.
3. P. Magnoux, M. Mourran, S. Bernard, M. Guisnet, *Stu. Surf. Sci. Catal.* 108 (1997) 107.
4. W. Liang, Y. Lin, Z. Yu, Z. Wang, B. Hau, M. He, E. Man, *Zeolites* 17 (1996) 297.
5. Z. Da, P. Magnoux, M. Guisnet, *Appl. Catal. A Gen.* 182 (1999) 407.
6. Z. Da, H. Han, P. Magnoux, M. Guisnet, *Appl. Catal. A Gen.* 219 (2001) 45.
7. Z. Da, P. Magnoux, M. Guisnet, *Catal. Lett.* 61 (1999) 203.
8. M. Guisnet, P. Magnoux, *Appl. Catal. A Gen.* 54 (1989) 1.
9. E. E. Wolf, F. Alfani, *Catal. Rev. Sci. Eng.* 35 (1982) 329.
0. B. V. Vora, R. P. Cottrell, US Patent 5, 012, 021 (1991) to UOP.
1. "Petrochemical Processes", *Hydrocarbon Proc.* 74 (1995) 89.
2. G. Colon, I. Ferino, E. Rombi, P. Magnoux, M. Gusinet, *React. Kinet. Catal. Lett.* 63 (1998) 3.
3. P. Andy, N. S. Gnep, M. Guisnet, E. Benazzi, C. Travers, *J. Catal.* 173 (1998) 322.

Chapter 6

Summary and Conclusions

"Truth is ever to be found in the simplicity, and not in the multiplicity and confusion of things"

-Sir Issac Newton

Increasingly stringent environmental regulations and political pressure demand that many traditional chemical processes be conducted in a cleaner manner. Alkylation of aromatics with higher olefins are of considerable interest for the production of LABs, but in this field, the traditional catalysts are notorious, suffering from a number disadvantages such as low selectivity towards a desired product and requirement of large amounts of mineral or Lewis acid catalysts and plant corrosion and generation huge amounts of waste. Major efforts are therefore needed to reduce these problems. The area of current interest towards investigating the use of binder free and rare earth exchanged-Y zeolites to gain much needed selectivity enhancement for the Friedel-Crafts alkylation of benzene with higher 1-alkenes in the synthesis of linear alkylbenzenes. Here we review some of our progress already discussed in detail in the preceding chapters.

When we talk about solid acid catalysts, the foremost among them are the zeolites, which are microporous, highly crystalline aluminosilicates, many of them are classified into small, medium, and large pore zeolites, the largest pore being 0.74 nm in faujasite (zeolite X and Y). They possess both Brønsted acid sites (BAS) and Lewis acid sites (LAS). However, the acidic nature is a function of temperature at which they use. The phenomenon of shape selectivity has its origin in well defined pore structure. Both these properties could be manipulated through appropriate modifications to zeolites. Faujasite-Y zeolite is one of the most common starting materials because of its favourable properties of high framework stability, ion exchange capacity and easy availability. The structural and textural properties can be improved by proper treatment before use. Cation exchange using rare earth metal ions is one of the best methods to enhance the surface properties of zeolite Y.

6.1 Summary of the work

The present work envisaged the rare earth modification of different metal FAU-Y zeolites. Sodium, potassium, magnesium and hydrogen-Y zeolites were prepared using available literature. The metal-Y zeolites were further ion exchanged with rare earth metal ions. The prepared zeolites were studied using various spectroscopic techniques. The up-gradation in the acid structural properties upon rare earth modification was followed by independent techniques. The prepared systems were effectively employed for the vapour phase alkylation of benzene with higher olefins for the synthesis of linear alkylbenzenes. We summarize the results;

Chapter 1 covers a brief literature review on different zeolites. The structure of zeolite-Y, properties of rare earth exchanged-Y zeolite, mechanism of acidity generation, creation of Brønsted acidity in rare earth zeolites is also demonstrated. The chapter also provides an update on the current linear

alkylbenzene technology. *Green* aspects of the solid acid catalyst technology are reviewed.

Chapter 2 is devoted to a complete discussion of the materials used in the present work, their preparation, and diverse experimental techniques employed for the catalyst characterization.

Chapter 3 describes the physicochemical characteristics of the prepared zeolite systems. Catalytic systems were characterized by surface area and pore volume measurements, EDX, SEM, IR spectroscopy, UV-vis DRS, different MAS NMR spectral studies, and ^1H - ^{27}Al dipolar decoupling MAS NMR studies for rare earth exchanged H-Y zeolites. Acid structural properties were determined by NH_3 -TPD and cumene cracking test reaction.

Chapter 4 discusses the application of the prepared catalytic systems for the vapour phase of alkylation of benzene with 1-octene. Special significance was given to the dependence of improved structural and textural properties on 2-phenyloctane selectivity. The effect of time on stream (deactivation) on the activity was studied in detail. The nature of carbonaceous compounds trapped inside the zeolite pores during the alkylation was also determined by careful analysis. The reusability of the catalytic systems were checked. A plausible mechanism has been suggested after critical analysis of various products formed during reaction.

Chapter 5 describes the application of the prepared zeolites for the vapour phase Friedel-Crafts alkylation of benzene with two higher 1-olefins namely, 1-decene and 1-dodecene for the synthesis of linear alkylbenzenes. The influence of various experimental parameters have been discussed in detail. Here also, we tried to correlate the enhanced formation of 2-phenyl isomer upon rare earth modification to the improvement in the total zeolite characteristics. The catalytic activity of rare earth exchanged-Y zeolites has

been compared with some common alkylation catalysts such as H- mordenite zeolite, K-10 montmorillonite clay, silica-alumina etc. Deactivation of the catalytic systems with time on stream is explained in detail.

Chapter 6 outlines the summary and potential conclusions of the present work. Future perspective and scope of the study is given at the end of the chapter.

6.2 Future perspectives and conclusions

There has been growing demand for selected solid acid catalysts carrying out organic transformations. Zeolite-Y is good example of solid acid catalyst which has been chemically treated (ion-exchange with rare earth cations) to enhance the textural and structural properties. These chemically treated zeolites have been extensively studied as a solid acid catalyst for the vapour phase alkylation of benzene with higher 1-olefins. These materials are particularly effective catalysts for the reaction. The thesis discussed the preparation and extensive physicochemical characterization of a series of rare earth zeolites. Recent advances in process development technology for linear alkylbenzene production and their driving forces, including economics, and other relevant variables are also discussed. Alkylation of benzene with 1-alkenes (C_8 , C_{10} , C_{12} olefins) is performed over a series of solid acid catalysts such as pure H-Y zeolite, binder free Na-Y, K-Y and Mg-Y, and their corresponding rare earth exchanged forms, H-mordenite, K-10 montmorillonite, and silica-alumina. All materials except Na-Y and K-Y are found to be highly active for the reaction. The near inefficiency of Na-Y, K-Y zeolites could be explained by considering their poisoning effect on the Brønsted acid sites. A model alkylation catalyst H-mordenite exhibits maximum conversion and produces the maximum amount of 2-phenylalkane owing to an effective uni-directional pore system. Other common alkylation catalyst such as K-10 montmorillonite and silica-alumina are far inferior in converting 1-alkenes or in producing the desired product. The

enhancement in the 2-phenyl isomer formation upon rare earth exchange is correlated to the enhancement in the Brønsted acidic nature as studied by cumene cracking test reaction. Binder free Mg-Y zeolite and its rare earth derivatives are far more active than K-Y or Na-Y zeolites. The very specific influence of magnesium cation, which improves significantly the catalytic performance by introducing a high acid strength, is most likely due to its very high polarizing power compared to K^+ or Na^+ , which influences the OH bond strength through the lattice.

It is apparent that crystalline rare earth exchanged-Y zeolites actively catalyse the alkylation reaction, with considerable variation in the reaction conditions. Nevertheless, for efficient use of these highly acidic zeolites some guidelines have emerged. With higher 1-alkenes as alkylating agents, moderate to higher olefin to benzene molar ratios may be employed to minimize unfavourable interaction of the reactive alkylating agent with catalysts and to favour monoalkylation. Temperatures in the range 423-623 K are generally required for efficient alkylation of benzene with C_8 , C_{10} , and C_{12} olefins.

A strong diffusion limitations for the desorption of bulky mono, bi, and trialkylated benzenes was observed for all zeolites. These bulky compounds formed owing to the low diffusion of alkylation products block or limit the desorption of the reaction products and the reactants from the micropores of zeolites. This is responsible for catalyst deactivation. Pure H-Y and H-mordenite undergoes comparatively faster deactivation than rare earth exchanged Y zeolites. Thus, we conclude that rare earth exchange invariably enhances catalyst life. Deactivated catalysts can be regenerated by dichloromethane washing followed by oxidative treatment at high temperatures.

The potentials of rare earth zeolites and other molecular sieves for minimizing the environmental impact should become increasingly apparent to

chemical industry in the future. The major advantages include ease of separation of products, recovery and recyclability, enhanced stability, much safer handling compared to H_2SO_4 , HF, H_3PO_4 or solid Lewis acids, catalytic rather than stoichiometric reaction, catalyzing multi-step reaction in a single catalyst bed and of course most importantly minimization or elimination of large amounts waste; inorganic salts. The scope of current economic analysis has now expanded to include much important environmental factors such as recycle, disposal, remediation etc., with emphases on preventing pollution at the source of manufacture. With this in mind, it would be worthwhile to reassess the economics of many chemical processes where zeolites as catalysts had not been considered before. Increased attention to integration of zeolite chemistry and catalysis with creative chemical engineering techniques should also be highly productive.

The drive towards *green chemistry* or the so called *clean technology* in the chemical industry and the emergence of *green chemistry* related issues in chemical research and academic education are unlikely to be a short term fashions. In the coming future, synthetic organic chemists need to be concerned about *atom efficiency* as the synthetic route and the process chemist will need to be concerned about the waste produced as the product made. Now, the enormous number of reactions and the rapidly growing number of new catalysts will definitely require the use of rapid screening methods and the use of highly innovative engineering to fully exploit the new and emerging chemistry. Synthetic chemists must be more prepared to work more closely with catalysts chemists and process engineers. For every challenge offered by the green chemistry revolution there is also an exiting opportunity.

enhancement in the 2-phenyl isomer formation upon rare earth exchange is correlated to the enhancement in the Brønsted acidic nature as studied by cumene cracking test reaction. Binder free Mg-Y zeolite and its rare earth derivatives are far more active than K-Y or Na-Y zeolites. The very specific influence of magnesium cation, which improves significantly the catalytic performance by introducing a high acid strength, is most likely due to its very high polarizing power compared to K^+ or Na^+ , which influences the OH bond strength through the lattice.

It is apparent that crystalline rare earth exchanged-Y zeolites actively catalyse the alkylation reaction, with considerable variation in the reaction conditions. Nevertheless, for efficient use of these highly acidic zeolites some guidelines have emerged. With higher 1-alkenes as alkylating agents, moderate to higher olefin to benzene molar ratios may be employed to minimize unfavourable interaction of the reactive alkylating agent with catalysts and to favour monoalkylation. Temperatures in the range 423-623 K are generally required for efficient alkylation of benzene with C_6 , C_{10} , and C_{12} olefins.

A strong diffusion limitations for the desorption of bulky mono, bi, and trialkylated benzenes was observed for all zeolites. These bulky compounds formed owing to the low diffusion of alkylation products block or limit the desorption of the reaction products and the reactants from the micropores of zeolites. This is responsible for catalyst deactivation. Pure H-Y and H-mordenite undergoes comparatively faster deactivation than rare earth exchanged Y zeolites. Thus, we conclude that rare earth exchange invariably enhances catalyst life. Deactivated catalysts can be regenerated by dichloromethane washing followed by oxidative treatment at high temperatures.

The potentials of rare earth zeolites and other molecular sieves for minimizing the environmental impact should become increasingly apparent to